final report

CRYOGENIC THERMAL DIODE HEAT PIPES

GRUMMAN AEROSPACE CORPORATION

CRYOGENIC THERMAL DIODE HEAT PIPES

final report
NASA CR-152,268

prepared for
NASA/AMES Research Center
Moffett Field, California 95035
Contract: NAS 2-7492 (Mods 8 through 12)

by
Grumman Aerospace Corporation
Bethpage, New York 11714

Prepared by: J. Alario
Approved by: R. Haslett
February 1979

CONTENTS

ILLUSTRATIONS

ILLUSTRATIONS (contd)

TABLES

FOREWORD

This report was prepared by Grumman Aerospace Corporation for the Ames Research Center of the National Aeronautics and Space Administration. The work was done under Contract NAS 2-7492 (Modifications 8 through 12), from September 1976 to February 1979. Dr. C. McCreight was the NASA technical monitor. Grumman personnel were Mr. R. Haslett, program manager, and Mr. J. Alario, project engineer.

We wish to acknowledge Dr. C. McCreight for nurturing development of cryogenic diode heat pipe technology, particularly the artery liquid blockage and liquid trap concepts where the challenges are sometimes as great as the potential rewards. In addition, we are particularly indebted to Dr. R. Kosson and Mr. F. Edelstein for their invaluable technical assistance. Dr. Kosson was responsible for the entire analytical study of the artery priming phenomenon, including the writeup in Section 6.1 of this report. Mr. Edelstein supervised the final assembly of the in-situ test chamber and the experimental investigation of the wetting characteristics of ethane. He also wrote Section 6.2 of this report. Finally, Messrs. W. Combs and E. Leszak are acknowledged for their expertise in the fabrication and assembly of the heat pipe hardware.

Section 1

SUMMARY

The primary objective of this multitask program was to continue the development of spiral artery cryogenic thermal diode heat pipes. Ethane was the working fluid and stainless steel the heat pipe material in all cases. The major tasks included: (1) building a liquid blockage (blocking orifice) thermal diode suitable for the HEPP space flight experiment; (2) building a liquid trap thermal diode engineering model; (3) retesting the original liquid blockage engineering model, and (4) investigating the startup dynamics of artery cryogenic thermal diodes.

The liquid blockage diode for HEPP was U-shaped and had a two diameter stainless steel envelope (6.35 mm, evaporator and 9.525 mm, transport/condenser). An electrically heated copper block was bolted to the evaporator and a flanged aluminum saddle was brazed to the condenser so that a radiator surface could be attached to it. Qualification test results were near predictions except for one shortcoming. Start up attempts directly from a room temperature cooldown or from an adiabatic condition after a hard thermal dry-out were erratic although a few successes were achieved. Successful priming could only be effected by first entering a reverse mode (i.e., flooding the evaporator section), which both pressure primed the artery and wetted the evaporator surfaces, followed by a gradual condenser cooldown ($\sim 1°$ C/Min). A summary of the measured performance for all of the heat pipe diodes built under this contract follows.

	Liquid Blockage		Liquid Trap,
	Eng Model	HEPP Model	Eng Model
• $(QL)_{max}$, W-M	11.2	24	12
• Forward Conductance, W/° C	4.5	5	6
• Reverse Conductance, W/° C	0.005	0.005	0.037
• Shutdown Energy, W-hr	0.02 to 0.10	0.10	0.32

Since the startup difficulty could only be overcome by undergoing a preconditioning sequence, this might limit the possible application of artery thermal diodes. An investigation was therefore undertaken to study and possibly resolve the problem. Two reasons were suspected: artery priming difficulties and/or surface wetting problems. An analytical

investigation of artery priming determined that artery permeability is the important criterion for how easily an artery primes. For a given capillary pore size, the higher the wick permeability the larger the evaporator heat load at which full artery priming will occur.

An experimental investigation was also conducted into the wetting characteristics of ethane/stainless steel systems using a specially constructed chamber that permitted insitu observations. Results were qualitative but revealed that there are no wetting problems with the ethane/stainless steel system. Ethane exhibited the same predictable wetting behavior as Freon 113 and Acetone which were used as comparison standards.

Section 2

INTRODUCTION

The application of heat pipe thermal diodes to the cryogenic temperature range would greatly expand the mission capabilities of the ever-increasing number of spacecraft that require low temperature cooling for their payloads. Instead of relying upon solid cryogens or refrigerated helium loops, which are either heavy or unreliable, the thermal diode would permit the use of a passive space radiator system for almost any vehicle orientation. When the radiator surface becomes cold enough to serve as an acceptable heat sink (e.g., views deep space), the diode heat pipe would operate as a high thermal conductance link between the radiator and the heat source. This allows the payload to be cooled by radiation. If the radiator surface becomes warmer than the heat source, as when illuminated by sunlight, the diode action would break the thermal connection thereby isolating the payload. During this time, the payload would either remain cold due to its own thermal inertia or it could be coupled to an alternate heat sink such as a solid cryogen. In any event, the benefits of a viable heat pipe diode thermal control system are obvious - less overall system weight and/or longer mission life.

The thermal diode concepts that are considered the most practical for hardware implementation because they result in the fastest, most positive shutoff, are the liquid trap and liquid blockage configurations.

In the liquid trap design, a non-communicating reservoir is located at the evaporator end of the heat pipe and also is in thermal contact with the heat source. During normal mode operation, when the evaporator and reservoir are warmer than the condenser section, the reservoir is empty because any fluid in it has vaporized. The fluid cannot return since there is no wick communication with the evaporator. When the thermal gradient reverses (condenser warmer than evaporator) heat pipe operation is terminated because all of the working fluid eventually condenses and stays trapped in the reservoir. Thus, the heat pipe wick becomes starved of fluid and cannot operate. Because the liquid trap diode mechanism relies on complete removal of all working fluid, the shutoff time is directly related to fluid inventory. It is usually better suited to those heat pipe wicking systems that require less fluid (i.e., axially grooved heat pipes as opposed to arteries), since the shutoff energy requirements are lower and shutoff time quicker.

The liquid blockage concept also uses a non-communicating fluid reservoir but with two important differences. The reservoir is located at the condenser end of the heat pipe and it is completely filled with excess fluid during the normal operating mode. Shutoff is effected when, due to the reversed temperature gradient, the excess fluid evaporates from the reservoir and condenses in the vapor space of the evaporator section. The reservoir is sized so that it holds enough fluid to completely choke the evaporator vapor space, which interrupts the heat pipe action.

The conventional liquid blockage design needs a vapor space small enough to self-prime during 1-g testing. But this restriction also results in decreased transport capacity during normal operation due to excessive vapor pressure losses. A unique concept which permits blockage without requiring a restricted vapor space is the blocking orifice design (References 1 and 2). In this concept, a solid plate with one small opening (orifice) adjacent to the wall, is located inside the heat pipe at or before the entrance to the evaporator section. During normal operation, a small vapor pressure drop is experienced at the orifice. During the reverse mode blockage is established by the creation of a liquid meniscus across the orifice, which retains (without draining) all of the excess liquid which has condensed in the vapor space of the evaporator.

As previously mentioned, a very common aerospace application of thermal diodes involves heat rejection from a source package to a radiator during normal operation, with shutoff when the radiator is exposed to a hot environment. The conventional liquid blockage diode concept or liquid blockage using an internal orifice are attractive shutoff techniques in this case for the following reasons:

- The liquid reservor can be easily heated by the hot environment to expell liquid in the shutoff mode and it can be cooled by radiation to a cold environment to promote liquid retention in the normal mode
- Generally, the evaporator is short compared with the condenser and total pipe length, minimizing blocking fluid requirements
- The liquid reservoir volume may be substantially reduced or eliminated by the extent to which the blocked length liquid requirement is satisfied by expansion of the normal fluid inventory during the hotter reverse mode condition.

The liquid trap concept for blockage in this case is less attractive because of packaging considerations. For reverse-mode operation, the reservoir to collect the normal inventory of working fluid must become an integral part of the heat source package. Thus, not only must there be a thermal interface between the heat pipe evaporator and source but also between the source and the heat pipe reservoir, which complicates the source package assembly.

This report describes four major tasks which were aimed at advancing the development of spiral-artery heat pipe thermal diodes.

1. Build and test a liquid blockage (blocking orifice) cryogenic thermal diode for the HEPP experiment
2. Fabricate a liquid trap cryogenic thermal diode engineering model for testing at NASA-ARC
3. Thermal vacuum test the original liquid blockage (orifice) cryogenic thermal diode, engineering model
4. Investigate (by analysis and experiment) the start-up dynamics of spiral artery cryogenic thermal diode heat pipes.

Section 3

FABRICATION AND TESTING OF A LIQUID BLOCKAGE (BLOCKING ORIFICE) CRYOGENIC THERMAL DIODE FOR THE HEPP SPACEFLIGHT EXPERIMENT (MODS 8 AND 10)

3.1 THE EXPERIMENT

The main objective of the HEPP spaceflight experiment is to measure long term zero-g operation of selective cryogenic heat pipes. The experiment incorporates two types of heat pipes: a conventional axially grooved (rectangular groove profile) aluminum isothermalizer, and a stainless steel thermal diode. Both heat pipes use ethane as the cryogenic working fluid and have a nominal operating temperature around 200 K (-100° F).

The basic experiment shown in Figure 3-1, is mounted in a tray and consists of a shielded space radiator, the two heat pipes, and a phase change material (PCM) canister which contains heptane (melt point = 182 K). For packaging purposes the heat pipes are bent in a U-shape, the condenser sections are mounted to the radiator and the evaporators are positioned inboard and attached to heater blocks. The PCM canister, which has a nominal 30 watt-hour capacity, is also mounted to the radiator and serves as the heat sink for the high power tests, since the dump capability of the radiator is small ($\approx$3 watts) and suited only for the long duration, low power tests. The radiator also serves to resolidify the heptane so that it can be used again.

Two kinds of thermal diode concepts were considered: a liquid trap design (made with axially grooved forged stainless steel tubing), and a liquid blockage design which used a spiral artery wick and the blocking orifice technique. This section describes the development of the liquid blockage thermal diode concept.

3.2 DESIGN AND FABRICATION

Three candidate envelope configurations were considered for the cryodiode heat pipe: (1) the 1/4 inch (6.35 mm) OD tube used for the engineering model (see Section 5), (2) a larger 3/8 inch (0.53 mm) OD tube, and (3) a hybrid two-diameter design that has a 1/4 inch (6.35 mm) OD evaporator/blocked-transport section and a 3/8 (9.53 mm) inch OD condenser/unblocked-transport section. The baselined diode concept for each one was the blocking orifice-liquid blockage technique using ethane as the working fluid, which was successfully demonstrated in the engineering model.

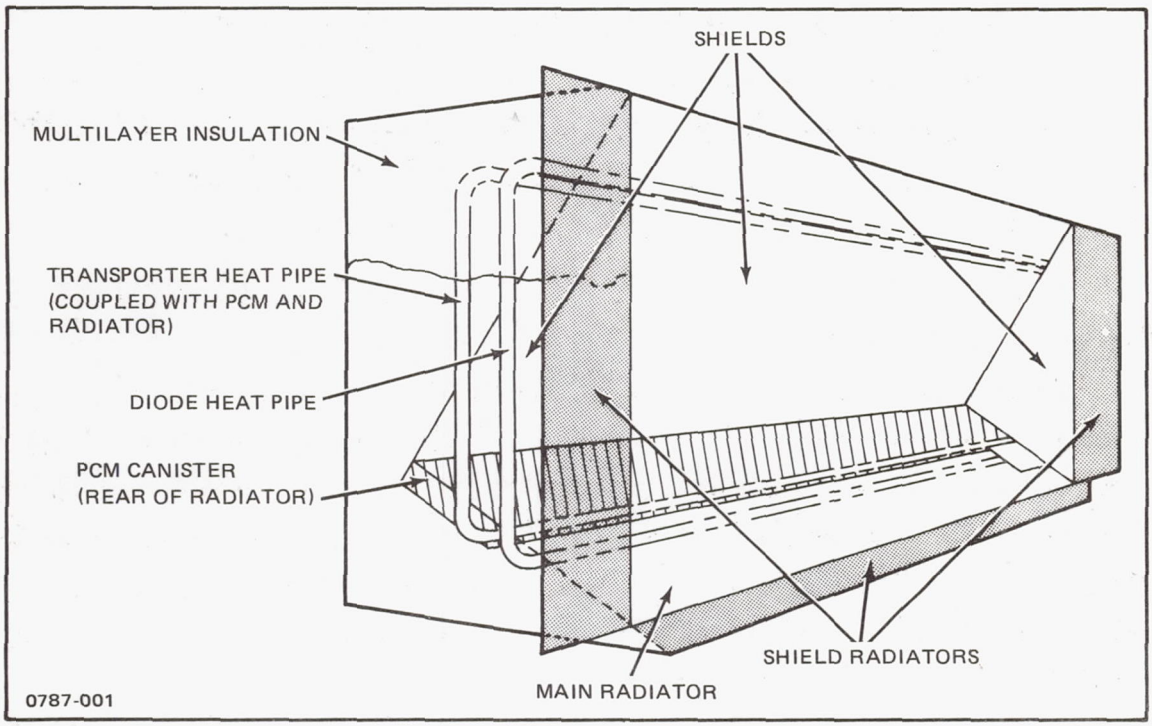

Fig. 3-1 HEPP Cryogenic Heat Pipe Experiment

After running various parametric analyses which altered the artery diameter, it was decided that the most predictable design would be one that used the same artery developed for the engineering model. In this way existing tooling and proven fabrication techniques could be directly utilized. Performance predictions were made for each candidate configuration using the same 0.117 inch (2.97 mm) OD artery. Calculated throughput for the 3/8 (9.53 mm) OD tube and the hybrid 2-diameter designs were nearly equal (9.5 watts @ 190 K, o-g) and about 10% higher than the 1/4 inch (6.35 mm) OD configuration.

However, besides throughput other things must be considered. A prime disadvantage of the uniform 1/4 inch (6.35 mm) OD design is the relatively narrow vapor annulus (0.0385 inch (.978 mm)) that is kept throughout the unblocked transport section and the condenser, when it is only needed in the evaporator section. The narrow vapor space in the evaporator is required since it permits testing in one-g and also minimizes the excess liquid and reservoir volume requirements. In addition to creating assembly problems, maintaining a narrow vapor space in the condenser increases the likelihood that the vapor annulus will self-prime and interfere with normal forward mode performance.

Using the larger 3/8 inch (9.53 mm) OD tube eliminates the self-priming problem but introduces another disadvantage. It requires a larger fluid reservoir (3.9 times larger) to hold the excess fluid needed to block the evaporator vapor space during the reverse mode.

The hybrid two-diameter configuration offers a reasonable compromise. It has a slightly higher throughput over the constant 1/4 inch (6.35 mm) OD envelope, while maintaining the relatively small reservoir size and also providing the advantage of a larger vapor space through the condenser. A comparison of the three concepts with respect to reverse mode considerations (reservoir size, shut-down losses) is presented below for a 190 K evaporator and a 210 K condenser/reservoir.

Reverse Mode Comparison (Ethane Fluid)

Design Concept	HP Charge (grams)	Charge (grams)	Reservoir Volume (in^3)	(1) Length (in.)	Shut down Energy (2) during 1 hour (watt - hr)
1) 1/4 OD (6.35 mm)	3.78	1.13	0.127 (2.08 cc)	2.0 (50.8 mm)	0.19
2) 3/8 OD (9.53 mm)	5.3	4.42	0.496 (8.13 cc)	7.6 (193.0 mm)	0.65
3) 1/4-3/8 OD (6.35-9.53 mm)	5.0	1.13	0.127 (2.08 cc)	2.0 (50.8 mm)	0.19

(1) Reflects engineering model-type design (6.25 in. OD) (158.75 mm)

(2) Includes conduction and transition energy losses.

In addition to the above, the pipe pressure at storage conditions (120° F) (322 K) is much lower for the hybrid design than the others; 886 psia vs. 1449 psia (6108 KPa vs 9989 KPa) for 1/4 OD and 1036 psia (7142 KPa) for 3/8 OD.

Since the hybrid 1/4-3/8 OD design offers the best combination of forward mode and reverse mode performance, it was selected as the baseline configuration for the liquid blockage diode heat pipe. An overall layout of the basic cryodiode configuration is shown in Figure 3-2. Performance predictions as a function of operating temperature are given in Figure 3-3.

Early in the program several hardware samples were fabricated to verify proposed assembly techniques.

- A sample artery was made and tested by performing lift tests before and after several bending cycles. The lift tests verified no degradiation in pore size due to bending
- 3/8 to 3/8 (9.53 mm to 9.53 mm) OD butt weld samples made with an orbital welder showed good weld penetration and negligible drop-through
- Swaging and spinning operations for the transition sections were also successfully demonstrated. Samples were made which join 1/4 inch (6.35 mm) OD (evaporator) to 3/8 (9.53 mm) OD (condenser) tubes and 5/8 (15.88 mm) OD (reservoir) to 3/8 (9.53 mm) OD (condenser) tubes. Both samples were butt-welded (orbital) together with good results

3.3 RESERVOIR DESIGN CONSIDERATIONS

A non-communicating reservoir is usually preferable to one that can communicate with the main artery. Although the latter has the advantage of being able to replenish the main artery in the event of a fluid deficiency, it also has other counterbalancing disadvantages.

- If the artery wick is allowed to extend beyond the end of the condenser, it causes a backpull on the condenser meniscus which decreases the net available capillary head and results in a lower transport capacity. Since cryogenic heat pipes are typically low capacity pipes to begin with, this further decrease in capability is undesirable.

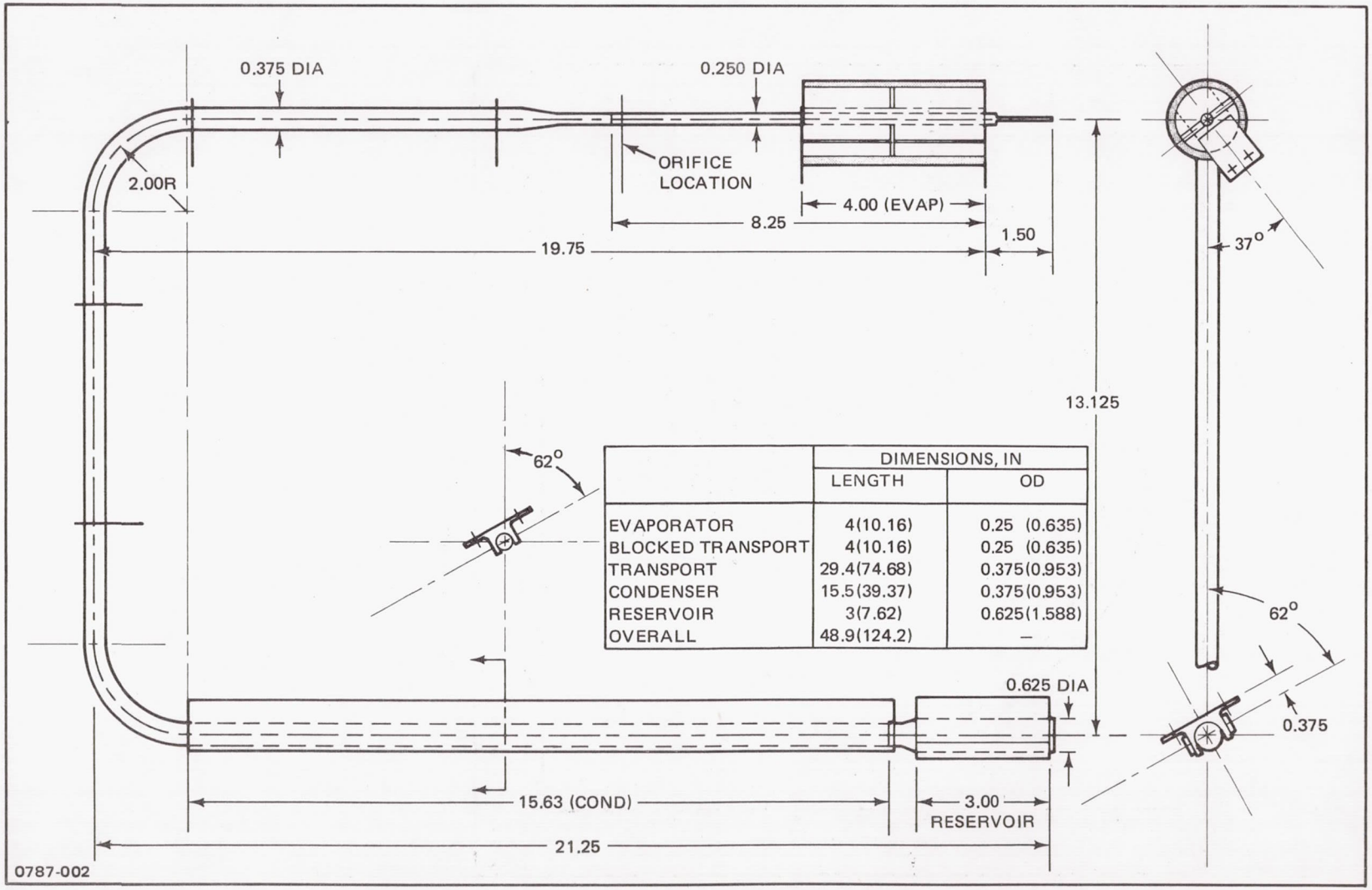

	DIMENSIONS, IN	
	LENGTH	OD
EVAPORATOR	4(10.16)	0.25 (0.635)
BLOCKED TRANSPORT	4(10.16)	0.25 (0.635)
TRANSPORT	29.4(74.68)	0.375(0.953)
CONDENSER	15.5(39.37)	0.375(0.953)
RESERVOIR	3(7.62)	0.625(1.588)
OVERALL	48.9(124.2)	–

Fig. 3-2 Overall Design Layout for HEPP Liquid Blockage Cryodiode Heat Pipe

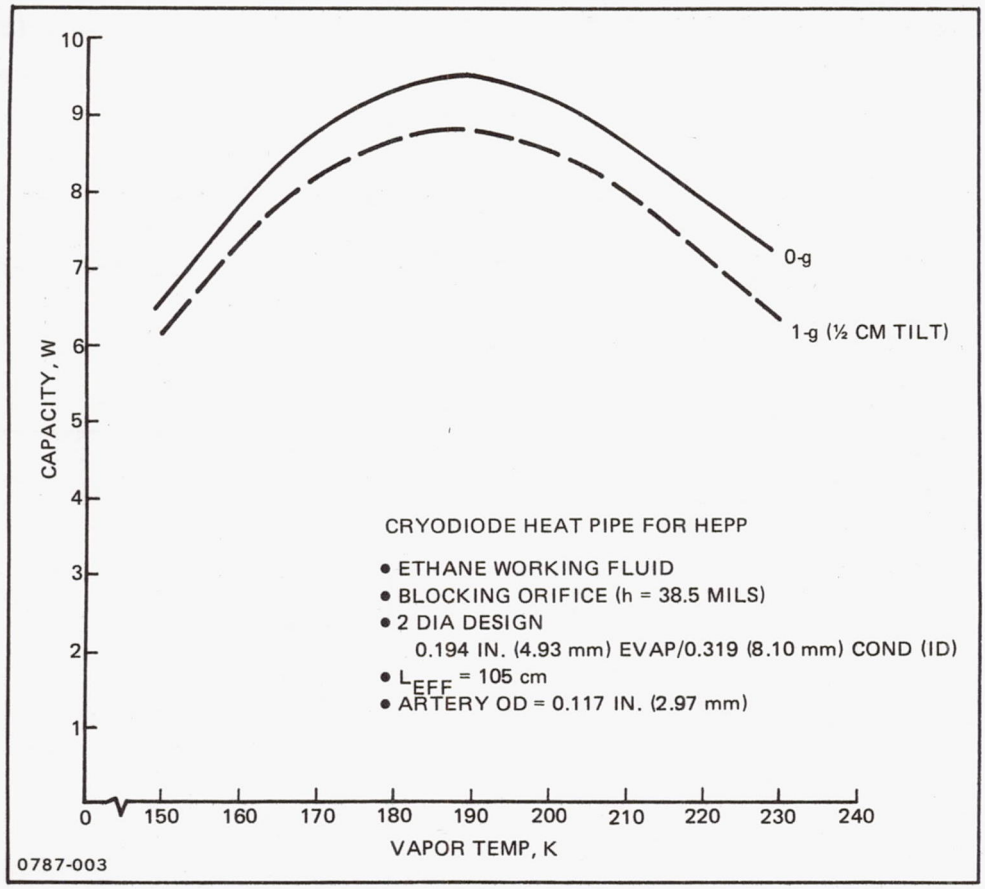

Fig. 3-3 Cryodiode Forward Mode Predictions

- A communicating reservoir requires extra wicking which in turn occupies volume that must be compensated for by increasing the reservoir size significantly. This is especially true with our reservoir design that has individually separated capillary channels and a highly conductive aluminum matrix to accelerate evaporation in the reverse mode.
- The extra wicking in a communicating reservoir increases the required fluid charge, which in turn increases the storage pressure.

Temperature control requirements for the reservoir of a liquid blockage diode are relatively simple: the reservoir should run slightly (a fraction of a degree K) below vapor temperature in the normal mode of operation, and slightly above vapor temperature in the reverse mode of operation. Both requirements can be met by thermally coupling the reservoir to the condenser boundary conditions.

As an example for illustrative purposes, consider a spacecraft application in which a diode couples a detector to a radiator which is subject to a varying space environment. The diode condenser is attached to the radiator. The excess liquid reservoir is at the condenser end of the diode, and has a small portion of the radiator surface dedicated for reservoir thermal control. During normal mode operation, the reservoir will tend to reject heat from the dedicated radiator surface. The axial solid conductance between the condenser and reservoir is relatively small. The reservoir can, however, obtain heat by condensation if only partially filled with liquid. When the reservoir internal passages are filled with liquid, and a thin liquid layer covers the exposed face of the reservoir internal aluminum block, the thermal resistance between the vapor and the reservoir will receive only a small amount of heat by condensation, and the reservoir temperature will fall below the main radiator temperature, to a value approaching the adiabatic surface temperature.

The preceding discussion involved three assemptions:

1) negligible heat leakage from the spacecraft to the reservoir
2) equal absorbed heat flux on the reservoir radiator and main radiator
3) negligible variation in diode boundary conditions during normal mode operation.

Heat leakage must be minimized between spacecraft and diode and spacecraft and radiator for any reasonable cryogenic temperature. Insulation requirements between reservoir and spacecraft will be similar to those for other parts of the diode and radiator, and well within the capabilities of multilayer insulation blankets. Equality of absorbed heat flux

should occur naturally, since both radiators will usually be sharing the same surface. The rate of variation in diode boundary conditions is a function of orbit and surface orientation.

Considering the same example under reverse mode operation, when the absorbed flux drives both radiator surfaces above diode vapor temperature, evaporation occurs in both the reservoir and condenser regions and condensation occurs at the detector end of the pipe (evaporator). Excess liquid obtained from the reservoir will accumulate at the detector end of the diode, effectively shutting off the diode. As the diode shuts off, the temperature of the vapor, condenser, and reservoir all rise. To keep the reservoir above vapor temperature, the inequality:

$$\left(\frac{Q_{abs}}{MC_p} \right)_{res} > \left(\frac{Q_{abs}}{MC_p} \right)_{cond}$$

must be satisfied. Reservoir temperature will then rise faster than condenser temperature, but will stay close to vapor temperature so long as liquid is available in the reservoir for evaporation.

For applications in which the radiator environmental flux varies rapidly, the transient cool down of the reservoir following a shutdown must be at least as fast as the condenser to permit the reservoir to fill with liquid when the diode is ready to turn on. This implies

$$\left(\frac{\epsilon A_R}{MC_p} \right)_{res} > \left(\frac{\epsilon A_{RAD}}{MC_p} \right)_{cond}$$

Where A_R for the reservoir is that portion of the radiator which is segmented and dedicated to reservoir cooling, and A_{RAD} for the condenser is the main radiator area. The MC_p product includes the entire mass which must be cooled by heat rejection to space (i.e. for the reservoir - the reservoir case and internal metal, attachment saddles, and reservoir radiator; for the condenser - the condenser including wick and fluid, the attachment saddles and the main radiator).

It may be noted that the temperature control requirements for a liquid blockage diode are relatively easily achieved compared with those for the gas reservoir variable conductance heat pipe (VCHP). The gas reservoir (or gas reservoir cold trap) must in general be maintained at a temperature significantly below condenser temperature to permit gas storage at a reasonable gas partial pressure in the reservoir. Hence VCHP's are subject to changes in set point as a result of coating degradation or anticipated thermal leakage. The liquid

reservoir, by contrast, runs close to condenser temperature. Thermal isolation of the reservoir from the spacecraft can be handled together with the rest of the diode and radiator, since requirements are similar, and the coating degradation constraint is no more severe for the liquid reservoir radiator then it is for the main radiator.

The ability of the reservoir to function properly with small temperature differences has been confirmed experimentally. A 1/4 in. (6.35 mm) liquid blockage diode with ethane working fluid was operated continuously for 5 hours at 10 watts evaporator power at 1 cm adverse tilt and a temperature of -100° F (200 K) with the reservoir at a temperature only 0.02 to 0.04° F below vapor temperature.

3.4 ORIFICE ORIENTATION

The orientation of the orifice has an effect on the blocking capability of a given size opening under 1-g test conditions. Two orifice orientations are of interest: 12 o'clock and 6 o'clock. The maximum tilt position at which complete blockage can still be realized is obtained by equating the orifice capillary pressure to the hydrostatic head that it must support.

3.4.1 12 O'Clock Orifice

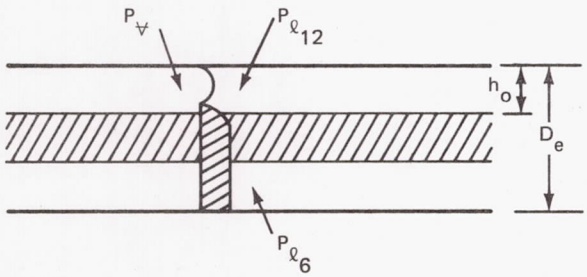

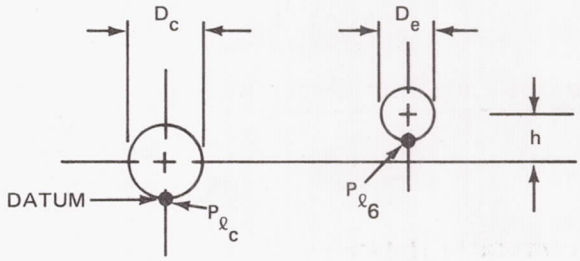

P_{l_c} = Pressure at lowest point in condenser liquid (maximum pressure point, flat menescus)

$P_{\forall}$ = Vapor pressure

$P_{l_c} \sim P_{\forall}$

Orifice Capillary Pressure

$$\Delta P = \frac{\sigma}{\frac{ho}{2}} = \frac{2\sigma}{ho} = (P_{\forall} - P_{l_{12}})$$

Hydrostatic Balance

$$P_{l_{12}} = P_{l_6} - \rho D_e$$

$$P_{l_6} = P_{l_c} - \rho h - \rho \left(\frac{D_c}{2} - \frac{D_e}{2} \right)$$

By manipulating these equations, the orifice pressure equality for the 12 o'clock position can be expressed as:

$$\frac{2\sigma}{h_o} = \rho \left[h + \frac{D_c + D_e}{2} \right]$$

3.4.2 6 O'Clock Position

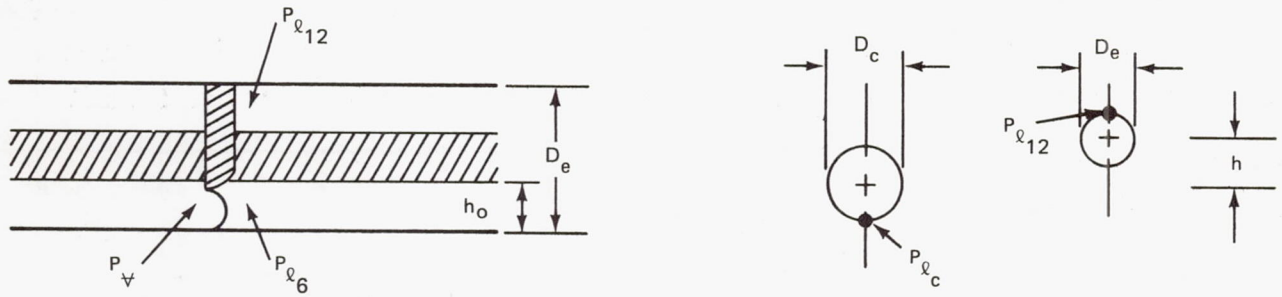

Orifice Capillary Pressure

$$\Delta P = \frac{2\sigma}{h_o} = \left(P_\forall - P_{l_6} \right)$$

Hydrostatic Balance

$$P_{l_{12}} = P_{l_c} - \rho h - \rho \frac{\left(D_c + D_e \right)}{2}$$

$$P_{l_6} = P_{l_{12}} + \rho D_e - \rho h_o$$

In a similar manner, the orifice pressure equality for the 6 o'clock position becomes:

$$\frac{2\sigma}{h_o} = \rho \left[h + h_o + \frac{\left(D_c - D_e \right)}{2} \right]$$

These results have been plotted in Figure 3-4 as a function of both heat pipe temperature and adverse tilt. As seen, the analysis predicts a more tilt sensitive orifice at the 12 o'clock position, which is not intuitively obvious since it is at the top of the pipe. However, this paradox can be explained by studying the hydrostatic balances developed and realizing that the blocking meniscus must sustain a larger vapor-liquid ΔP at the 12 o'clock position since the liquid pressure is lower than the 6 o'clock point, while the vapor pressure remains the same. For adverse tilts, complete blocking (up to the orifice plate) at the 12 o'clock position can only occur at the colder temperatures ($\sim$150 K). However, blocking throughout the 4-inch (101.6 mm) evaporator section only, will take place over the entire temperature range from 150 K to 210 K. The 6 o'clock position can sustain complete blocking up to the orifice over the entire temperature range for adverse tilts below about .10 inches (2.54 mm).

Although the preceding discussion was based on the analytical predictions, test data have been observed that support the results. An evaluation of the test data which was observed during the checkout runs follows.

- At the 12 o'clock orifice position and .10 inch (2.54 mm) adverse tilt only the 4-inch (101.6 mm) evaporator section was successfully blocked at an evaporator temperature of 200 K
- At the 6 o'clock position, complete blocking (up to the orifice plate) was observed for level, .05 (1.27 mm) and .10 inch (2.54 mm) adverse tilts at a 200 K evaporator
- With the orifice still at 6 o'clock, when the tilt was further increased to .15 inches, (3.81 mm) blocking at the orifice could not be achieved. Evaporator temperature was also 200 K.

3.5 THERMAL MODEL

The simplified thermal nodal model of the liquid blockage diode heat pipe experiment which was developed is presented in Appendix A, including the AGTAP subroutine code for the diode mechanism. In addition to altering forward and reverse mode parameters in accordance with the calculated temperature gradients, the program logic includes a PCM routine which models the phase change phenomenon. It also has generalized inputs to permit rapid modification and evaluation of radiator dimensions and location relative to diode attachment points. Two options exist for controlling the inputs to the PCM and reservoir heaters. One uses an on/off duty cycle routine which permits separate changes in both heater wattage and duty cycle. The other heater control option uses a fixed temperature set-point and tolerance band. When the control temperature is above the set point, the heater is off; when it is below it, the heater is turned on.

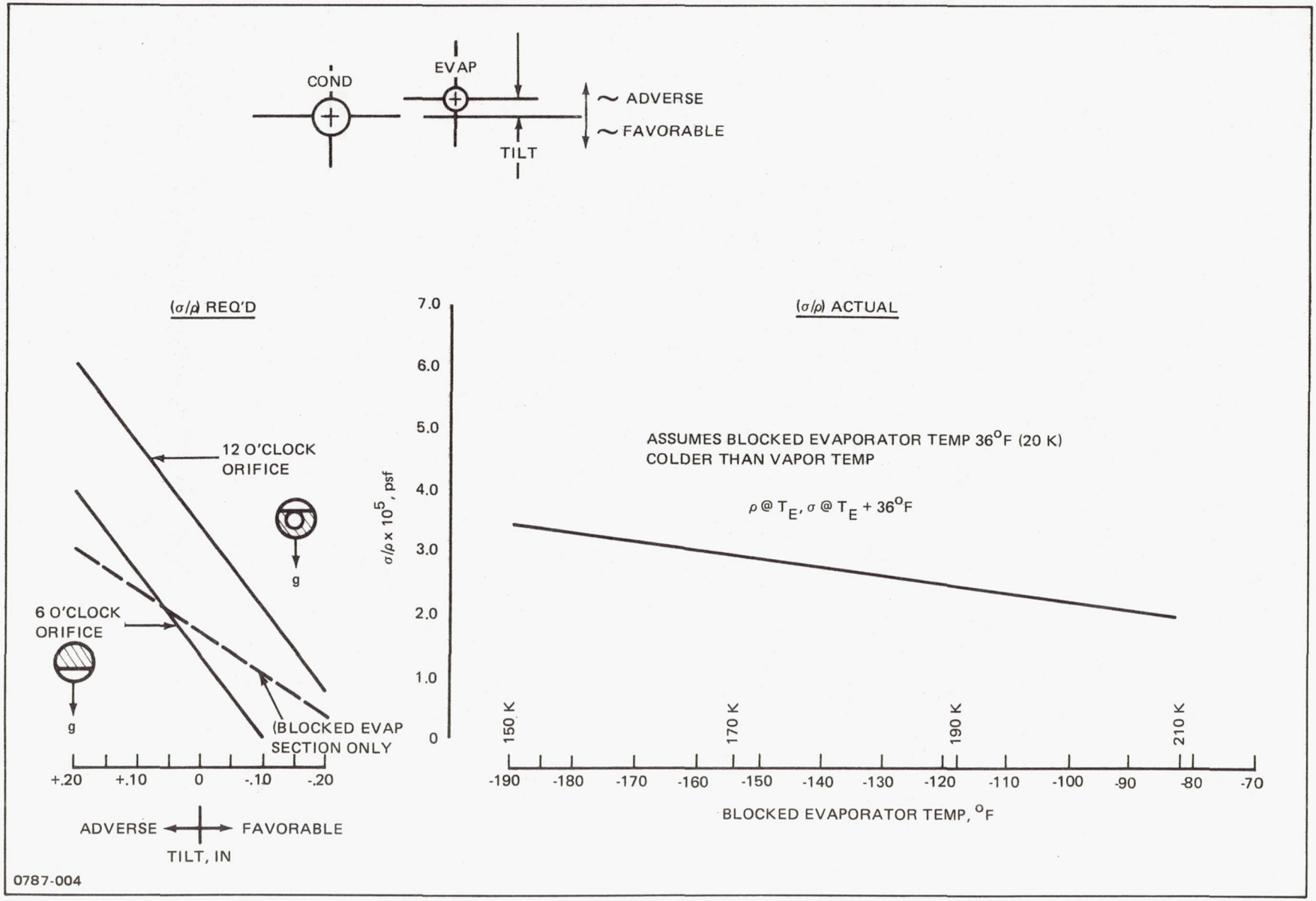

Fig. 3-4 Ground Test Blocking Requirements - HEPP - Cryodiode

Computer runs were made which verified that during the forward mode the reservoir temperature will always be lower than the condenser (and vapor) temperatures by about 1 K, thereby ensuring a filled reservoir and clear condenser vapor space. The predicted thermal profile after 4 hours with an evaporator input of 10 watts is given in Table 3-1. Runs were also made to demonstrate successful reverse mode transition and temperature separation between condenser and reservoir during the following cooldown. Results are given in Figure 3-5 for the case of a 40 watt PCM input (40% duty cycle) and a steady 2 watt reservoir input.

The effect of reservoir heat input on blocking response was also investigated at two extreme PCM heat inputs (5.6 and 40 watts). The results are given in Table 3-2 and indicate a minimum reservoir heater requirement of at least 2 watts to achieve complete blockage in a reasonable time (~10 minutes).

3.6 HARDWARE DESCRIPTION

The HEPP diode heat pipe utilizes the blocking orifice technique to effect liquid blockage of the evaporator vapor space during reverse mode operation. It is made from stainless steel tubing (28 mil wall) and has a 1/4 inch (6.35 mm) OD evaporator/blocked transport section, a 3/8 inch (9.53 mm) OD condenser/transport section, and a 5/8 inch (15.88 mm) OD excess fluid reservoir. The different sections are joined together by swaging the appropriate tubes to achieve a uniform interface OD and then butt welding. The pipe contains a spiral artery wicking system similar to that used in the engineering model (see Section 5) and uses purified ethane as its working fluid.

As shown in Figure 3-2, the diode is bent into a U-shape. One leg of the U contains the evaporator, which is attached to a cylindrical copper heater block; the opposite leg contains a brazed aluminum saddle which is attached to a radiator surface. The excess fluid reservoir is located at the end of the condenser and also contains a brazed aluminum saddle to which a 9 in^2 (58 cm^2) radiator surface is attached. The overall dimensions of the U-shape are approximately 14 inches (0.36 m) across the base and 22 inches (0.56) along each leg. A detailed weight breakdown is contained in Table 3.3.

The finished diode heat pipe assembly is shown in Figure 3-6 after the saddles were brazed to the condenser and reservoir, and the mounting tabs welded onto the transport section. A closeup view of the reservoir assembly which shows the clips for attaching the PRT sensors is shown in Figure 3-7. Closeups of the brazed condenser assembly and the transport-to-evaporator transition section are shown in Figures 3-8 and 3-9. Note the

Table 3-1 Normal Mode Experiment Temperature at 4 hours, Q_{EVAP} = 10 Watts

NODE		TEMP (K)
1	EVAPORATOR BLOCK	193.6
2	EVAPORATOR WALL	192.7
3	HP VAPOR	192.0
4	CONDENSER WALL	191.9
5	RESERVOIR	191.1
6	RESERVOIR RADIATOR	190.9
7	MAIN RADIATOR (W/PCM)	183.3
8	MAIN RADIATOR	191.6
9	PCM CANISTER	182.6

0787-035

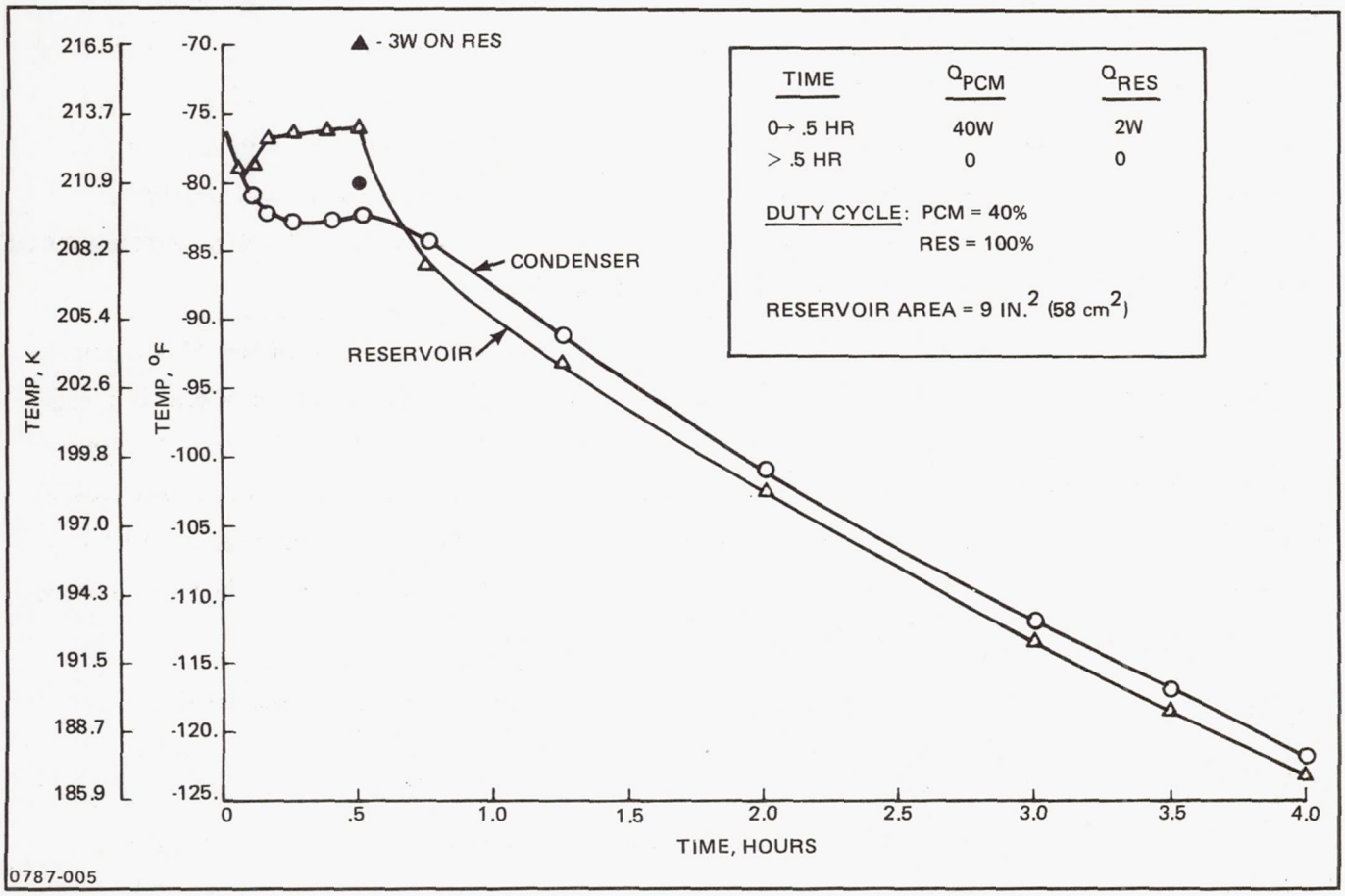

Fig. 3-5 Reverse Mode and Cool Down Predictions for HEPP (Cryodiode)

Table 3-2 Reverse Mode Performance Predictions

INITIAL PCM TEMPERATURE	HEAT INPUT TO RESERVOIR (WATTS)	HEAT INPUT TO PCM (WATTS)	TIME FOR BLOCKAGE TO OCCUR (MIN)	BLOCKED LENGTH (INCHES)
-100	1.0	5.6	15.6	8.77
-100	2.0	5.6	6.2	8.80
-100	5.0	5.6	2.4	8.85
-100	1.0	40.0	4.6 (PARTIAL BLOCKAGE)	1.04
-100	2.0	40.0	9.8	8.88
-100	5.0	40.0	2.6	8.86
-162	1.0	40.0	31.7 (PARTIAL BLOCKAGE)	4.00
-162	2.0	40.0	8.9	8.18
-162	5.0	40.0	2.6	8.16

0787-036

Table 3-3 Detailed Weight Breakdown, HEPP Liquid Blockage Cryodiode

COMPONENT	MATERIAL	WEIGHT (GRAMS)
1) HP TUBE ENVELOPE	304 STAINLESS STEEL	86.7
2) SPIRAL ARTERY	304 STAINLESS STEEL	32.
3) RESERVOIR INSERT	ALUMINUM-6061	25.4
4) WORKING FLUID	ETHANE	10.2
5) EVAPORATOR BLOCK	COPPER 102	998.8
6) SADDLE ASSY	ALUMINUM-6061	272.4
7) RESERVOIR RADIATOR	ALUMINUM-6061	45.4
8) INSULATOR SHIM	KAPTON	5.

0787-037

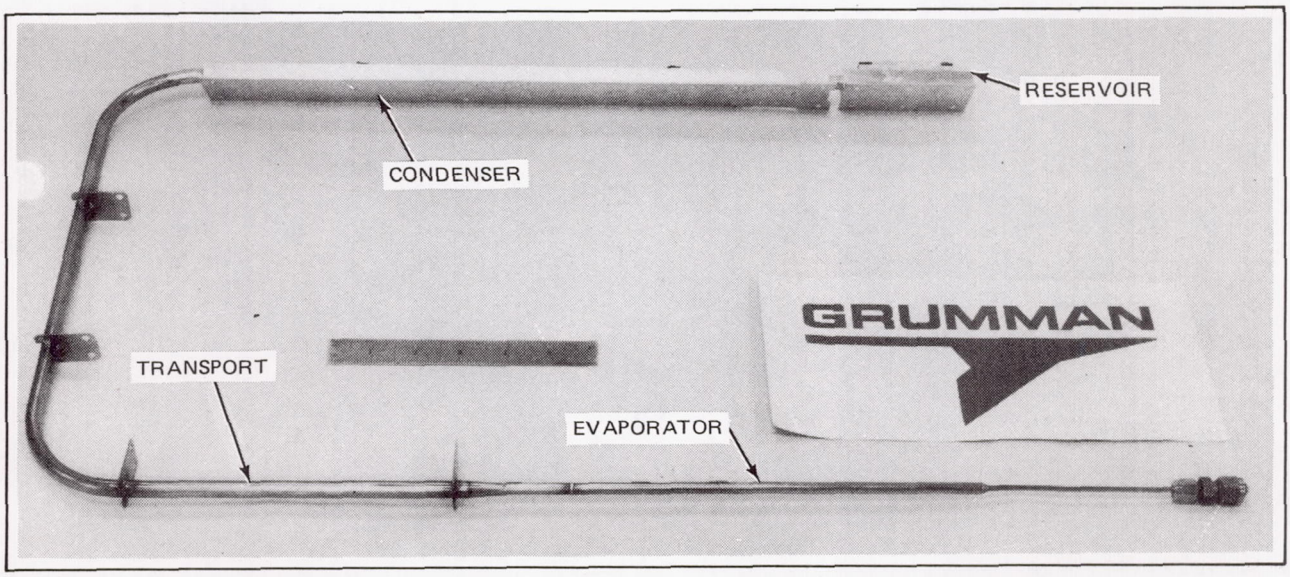

0787-006

Fig. 3-6 Spiral Artery Liquid Blockage Cryogenic Thermal Diode for HEPP

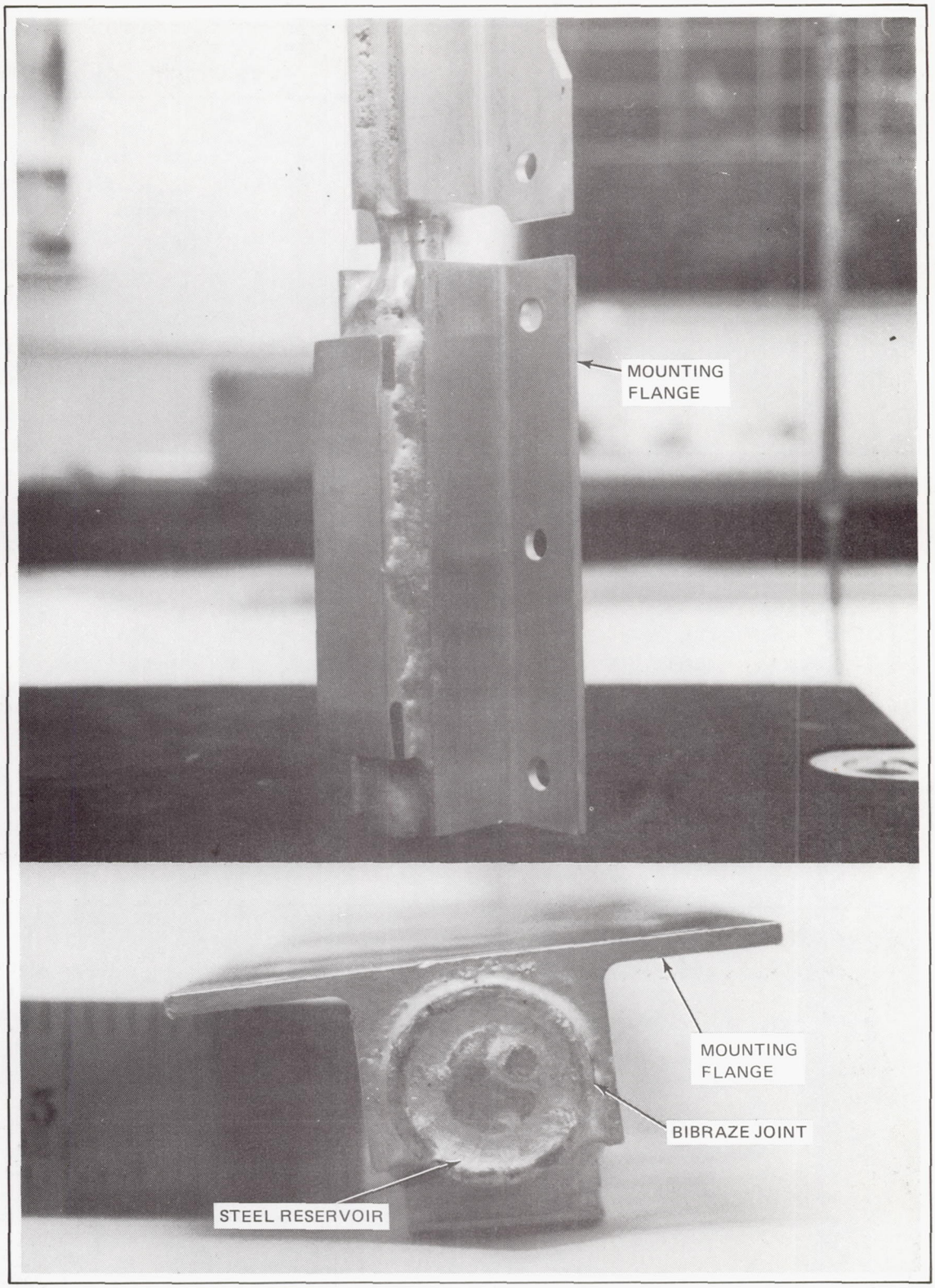

0787-007

Fig. 3-7 Reservoir Assembly

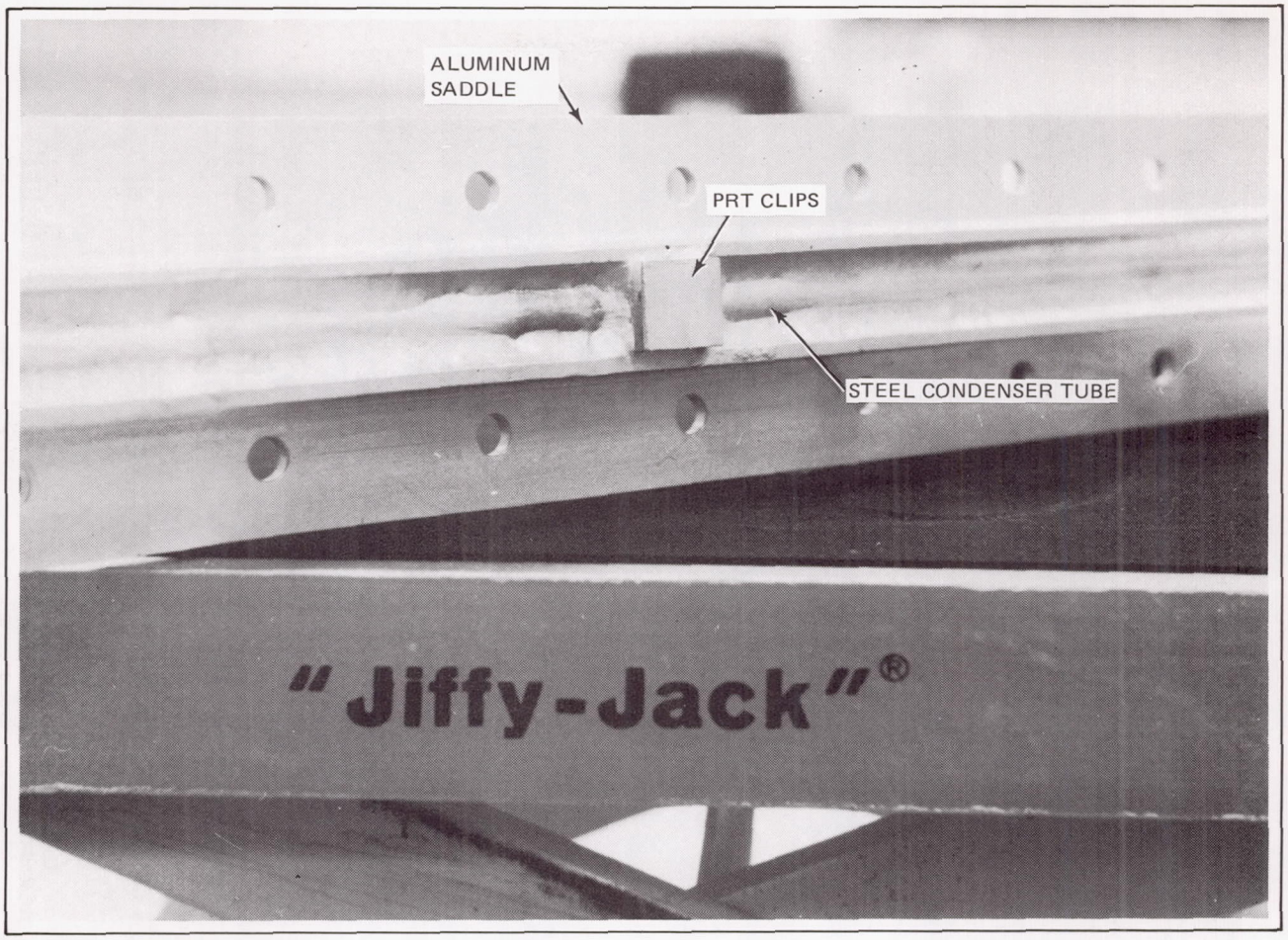

0787-009

Fig. 3-8 Brazed Condenser Assembly

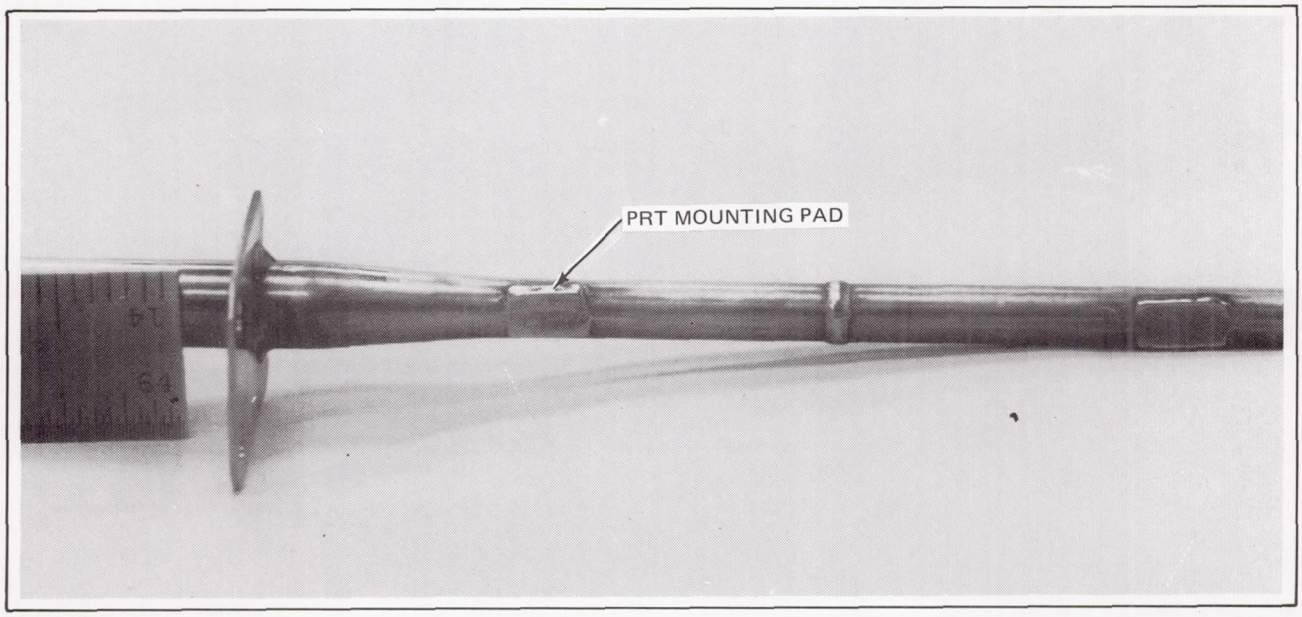

0787-008

Fig. 3-9 Two Diameter Transition Section

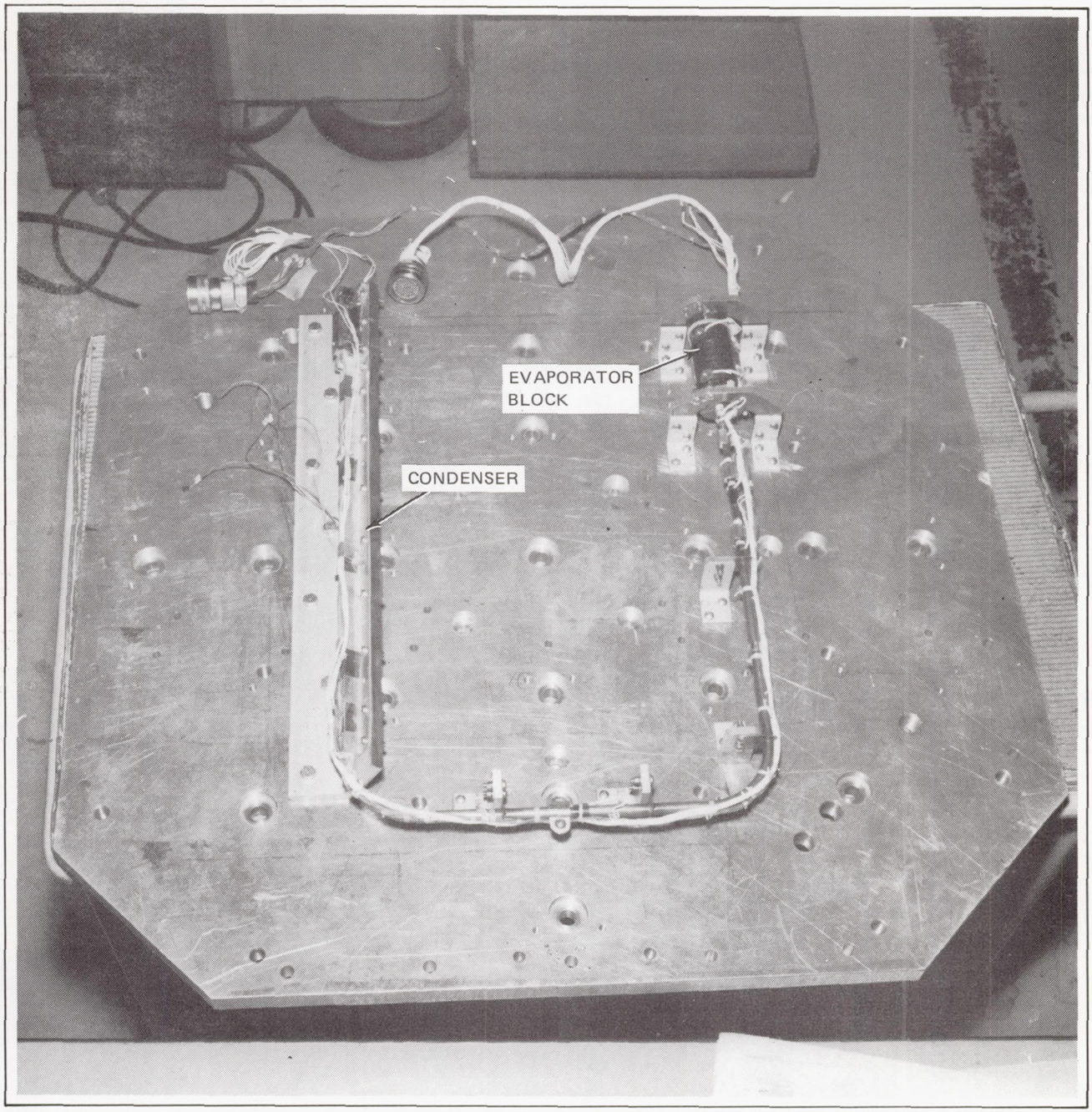

0787-010

Fig. 3-10 Diode HP Assembly Mounted to Vibration Test Fixture

PRT clip and mounting pads. Figure 3-10 shows the final diode heat pipe assembly mounted to its vibration test platform. At this point, it had been charged with ethane, welded closed and thermal vacuum tested.

3.7 QUALIFICATION TESTING

Objective. The main objective of the qualification test was to demonstrate a diode heat pipe that could be effectively used as part of the HEPP experiment. Consistent with this objective, the pipe requirements were: a minimum forward mode throughput of 750 watt-cm (0-g equivalent) and good thermal conductance, at least 5 watts/° C. It should also show a rapid transition to the shut-off operating mode in response to heat inputs at the condenser and reservoir and quick recovery to forward mode operation.

As a secondary objective the effect of orifice orientation on 1-g performance in both the forward and reverse operating modes was also evaluated. Two orifice orientations were considered, (a) orifice opening at the top of the pipe (12 o'clock position) and (b) orifice opening at the bottom (6 o'clock position). As shown in Section 3.4, the 12 o'clock orientation is the more conservative one as far as maintaining a blocked evaporator, since it must sustain a larger delta-P. But even the 6 o'clock orientation imposes a greater demand than the actual zero-g flight requirement. As far as influencing the reverse-to-forward mode transition time, the 6 o'clock position would be most like the zero-g situation since the favorable draining effect would be less than that experience with a 12 o'clock orifice opening.

Test Set-up

The cryodiode heat pipe qualification unit was tested in a 2 ft (0.61 m) diameter x 4 ft (1.22 m) long thermal vacuum chamber located in Grumman's Thermal Laboratory. A cross-section of the installation is shown in Figure 3-11. The U-shaped heat pipe was attached to a rigid mounting platform through low-k thermal isolators, and the entire set-up was isolated from the room ambient by an LN_2 cold wall and a 10^{-5} torr vacuum.

Heat was supplied to the pipe through a 1.5 inch (38.1 m) diameter copper heater block attached to the evaporator section. At the condenser, heat was removed through an aluminum radiator fin (2.6 ft^2) (0.24 m^2) which was bolted to the condenser saddle. The radiator fin contained a tube through which LN_2 could flow to accelerate the system cooldown from room temperature. Once near the desired operating temperature, the LN_2 flow was stopped and the pure radiation coupling to the cold wall used to reject the heat. Strip heaters, attached to the back of the radiator fin and insulated with MLI, were used to adjust the heat pipe vapor temperature as required.

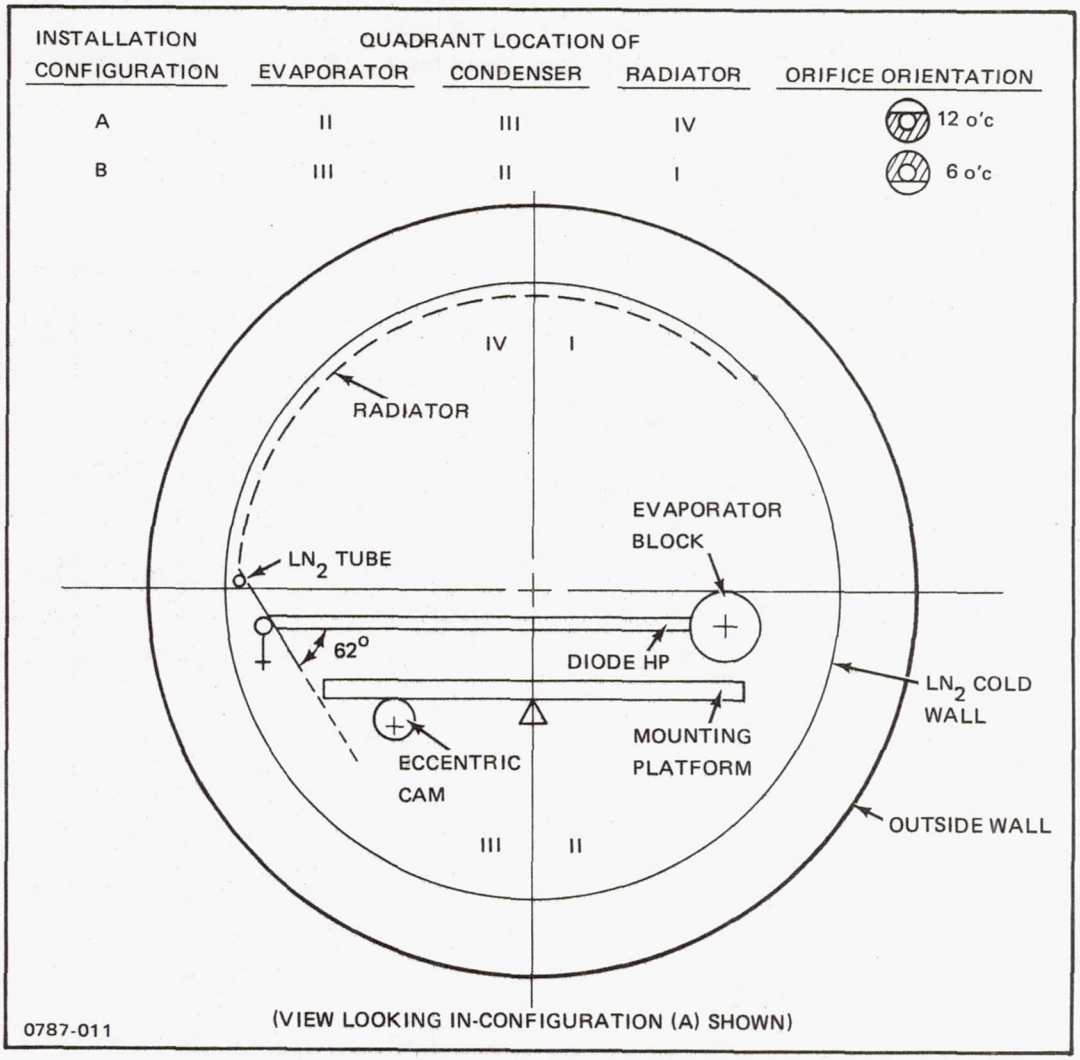

Fig. 3-11 Cryodiode T/V Test Installation (Qualification Unit)

The entire mounting platform was balanced between a center support, which ran the length of the platform, and an eccentric cam which was positioned off-center near the chamber and door. The cam was attached to a rotary feedthru so that it could be adjusted under test. The amount of angular rotation of the plate was measured by a calibrated scale which was hard mounted to the plate and which could be sited through the chamber door viewing port by using a surveyor's transit.

Since the heat pipe was tested with two different orifice orientations (12 o'clock and 6 o'clock) it was necessary to flip the heat pipe 180 degrees and remount it to the base plate. When this was done, the radiator fin was also reinstalled on the condenser flange to conform to the cold wall shape.

Instrumentation

The qualification unit was instrumented with the 11 platinum resistence thermometers baselined for the HEPP experiment and 18 additional copper-constantan thermocouples. The thermocouples were used to check the calibration of the PRTs and provide more detailed thermal profiles. The PRTs were mechanically fastened to the pipe by suitable designed clamps whereas the thermocouples were spot welded to the steel tubing whenever possible. Detailed instrumentation information is given in Figure 3-12. After instrumentation, the entire heat pipe except for the condenser and reservoir radiator interfaces, was insulated with 25 layers of aluminized mylar (MLI).

Before starting the formal test procedure, some preliminary test points were run to determine if the heat pipe contained the proper charge of working fluid. For these preliminary tests, the charge valve was removed from the pipe by pinching off and welding the secondary charge tube, which separated the primary charge tube and the charge valve. After the preliminary test data had verified a properly filled pipe, the primary charge tube was pinched off and welded closed.

Test Results

The test program consisted of a detailed performance evaluation before vibration testing, followed by selective forward and reverse mode spot checks afterward. The majority of the tests were run with the orifice at the 12 o'clock position; only during the pre-vibration sequence were a few tests run with the orifice at 6 o'clock.

The forward mode, steady state tests determined the maximum heat pipe throughput for a combination of four nominal pipe temperatures (150, 170, 190, and 210 K) and four adverse tilt settings (0.25, 1.0, 2.0 and 4.0 cm). The transient tests, which were run at

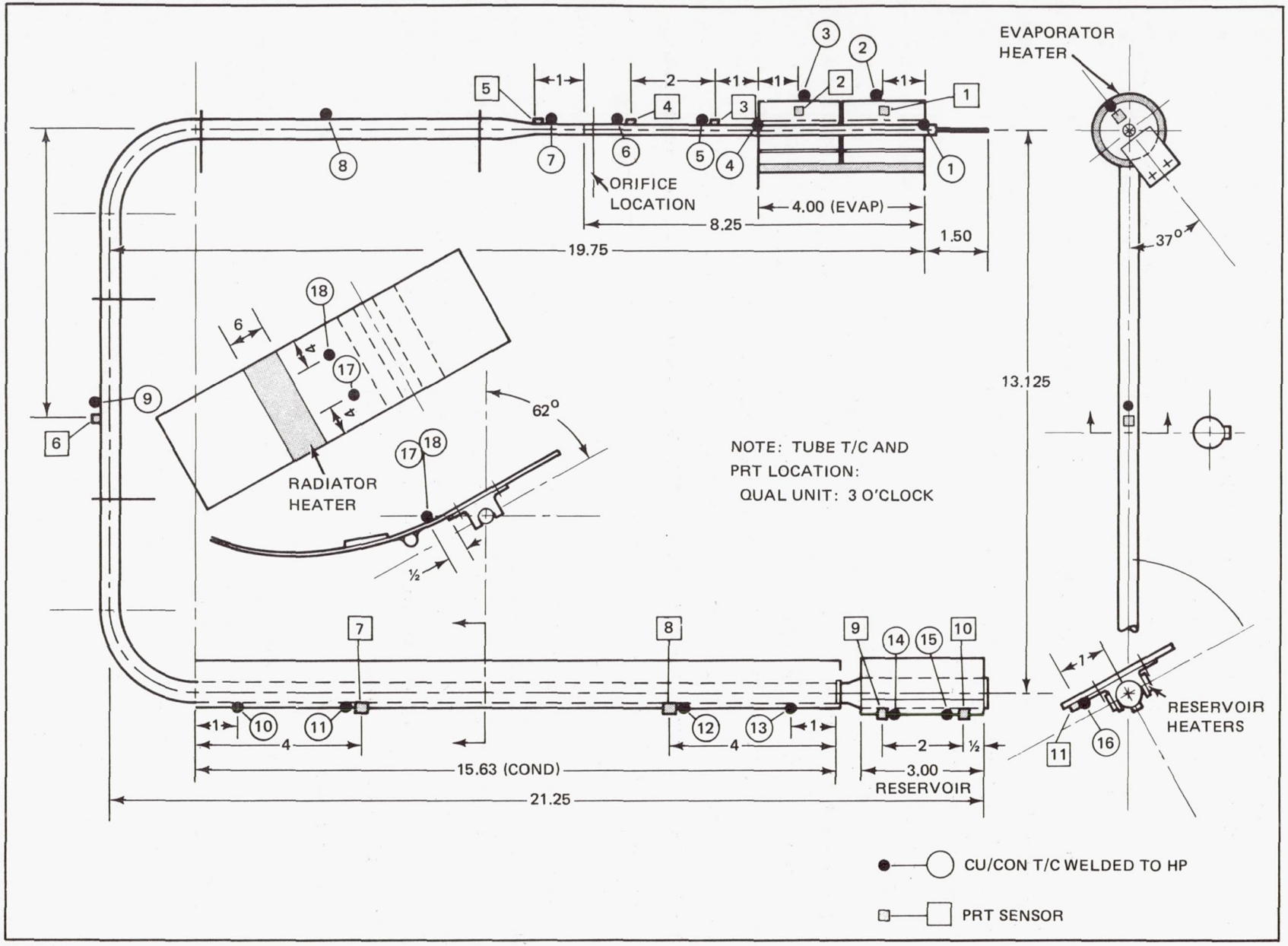

0787-012

Fig. 3-12 Instrumentation Drawing, HEPP Cryodiode Heat Pipe

the lowest (0.25 cm) tilt, monitored the reverse mode response for selective reservoir heat inputs (1, 2 and 3 watts) at the two extreme temperature conditions (150 and 210 K).

Forward Mode

During the forward mode (steady-state) tests the maximum heat load was limited by the dump capability of the condenser radiator. The radiator capacity calculated for the various test temperatures is given below:

Test Temp (K)	Radiator Capacity (Watts)
150	4.9
170	8.5
190	12.4
210	18.5

At all of the test temperatures, the evaporator heat load could be increased to the capacity limit of the radiator, beyond that the heat pipe temperature would increase to accommodate the load. Even at adverse tilts up to 4 cm (the limit of the test setup), the dryout limits could not be reached. A summary of the steady state performance, in the form of evaporator heat load versus adverse tilt, is presented in Figure 3-13. At the maximum tilt (4 cm) the measured heat loads were: 4 watts at 150 K, 7.2 watts at 170 K, 10.5 watts at 190 K and 17.3 watts at 210 K. Using a static wicking height of 12 cm (corresponding to lift test data) a maximum zero tilt heat load of 25 watts was estimated at 210 K. Temperature profiles for representative test points are shown in Figure 3-14. Data are presented for both orifice positions, for pre-and post-vibration test points, and for adverse tilt extremes. As seen by comparing TP154 and TP104, the orifice position has no effect on the forward mode performance. The post-vibration thermal test data (TP101V, TP104V) also show little change. The average value of forward mode thermal conductance is 7.4 watts/°C at the 200 K level, and 2.4 watts/°C at the 150 K level.

Reverse Mode

Temperature profiles at the beginning and end of reverse mode tests for the 6 o'clock and 12 o'clock orifice positions are shown in Figure 3-15. These fully established profiles are shown after 15 and 13 minutes respectively; however, the actual time at which blockage was first established was about half that shown. This data is significant because it verifies the different temperature profiles predicted for the two orifice locations. The 12 o'clock orifice was previously shown to be more sensitive for sustaining a fully blocked vapor space up to the orifice location. This is seen in the TP205 data since the blocked section extends

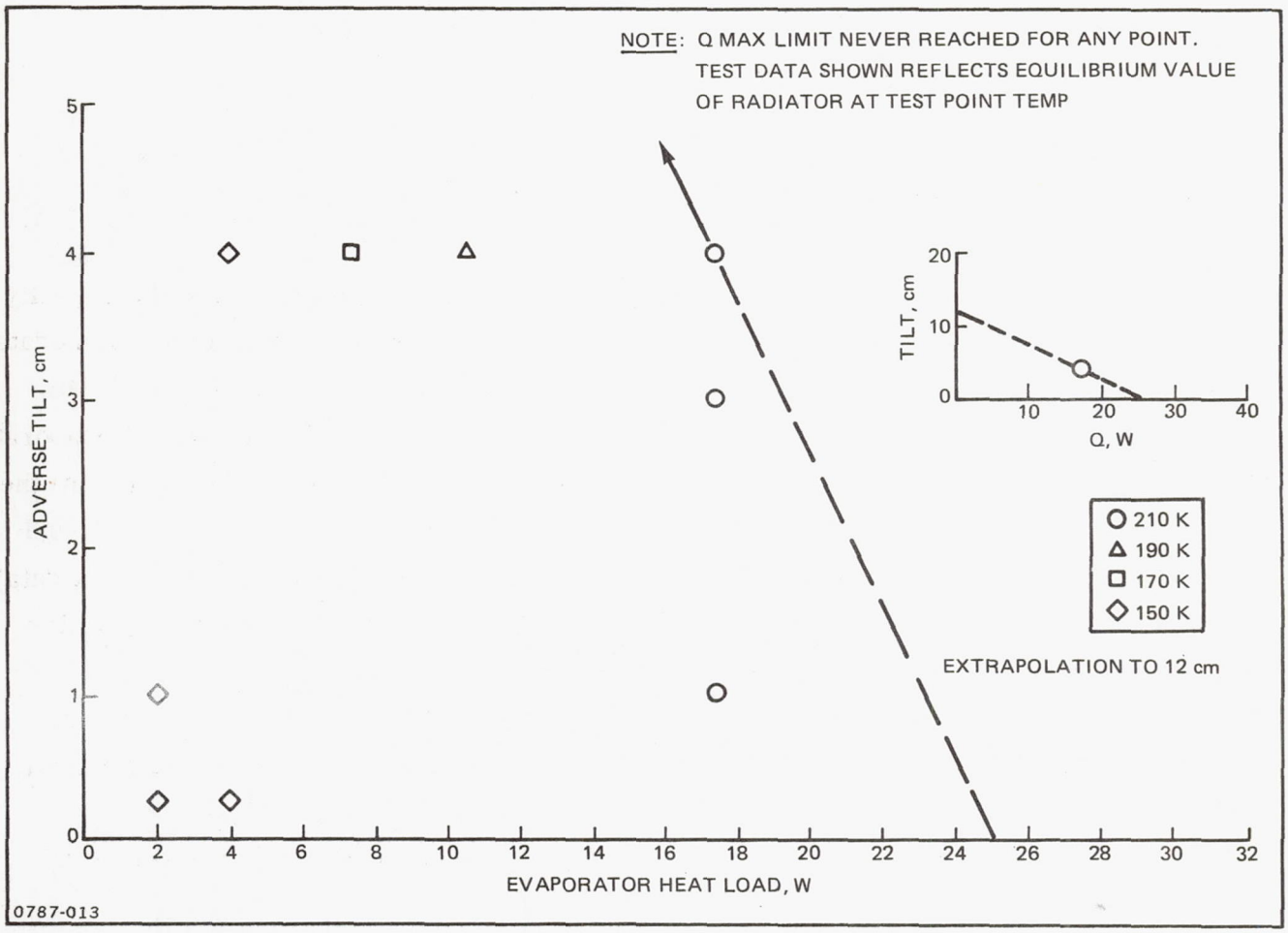

Fig. 3-13 HEPP Liquid Blockage Cryodiode Qual Test Data (Q vs Tilt) $L_{EFF} \approx 100$ cm

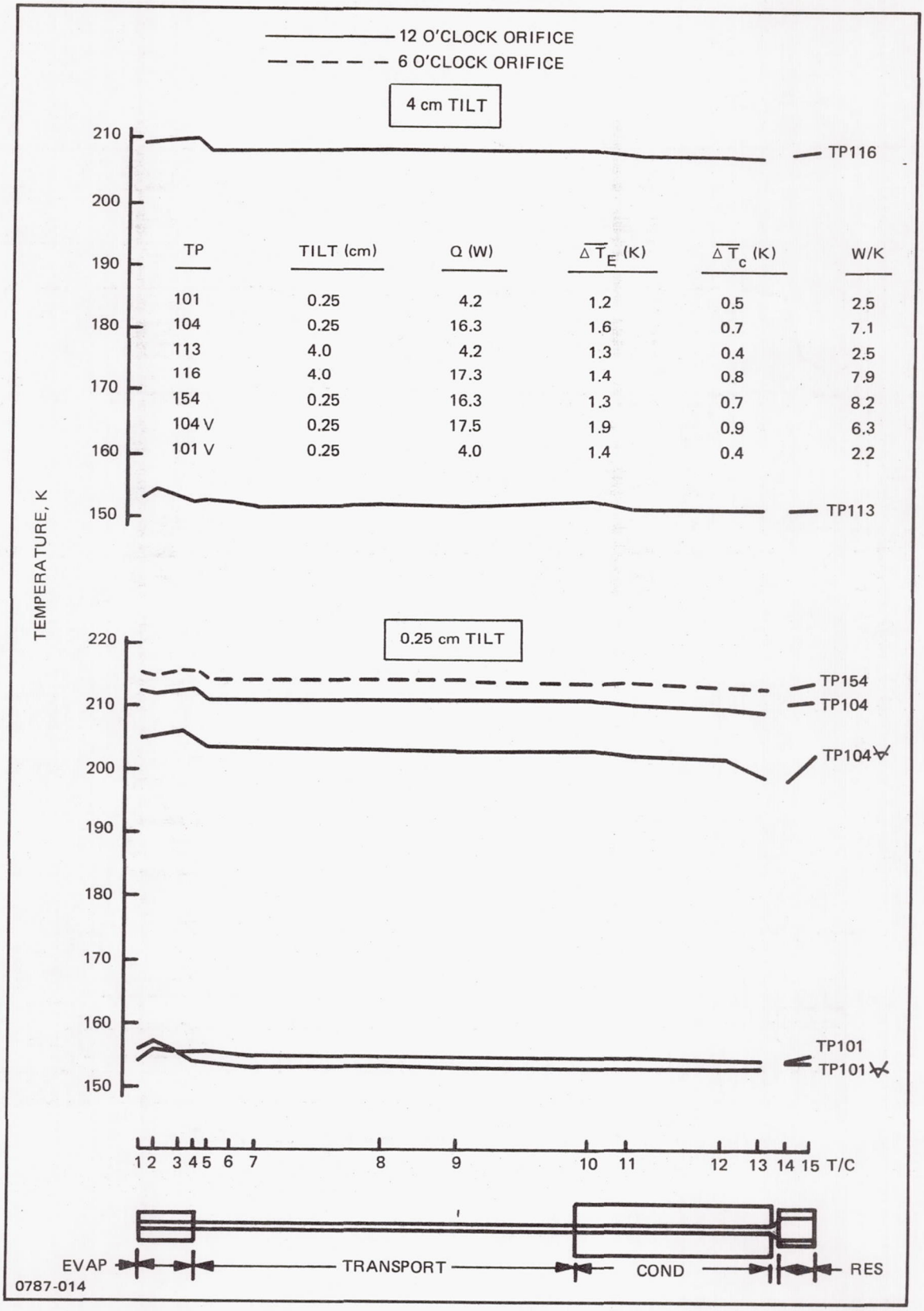

Fig. 3-14 HEPP Cryodiode Temperature Profiles, Qualification Test

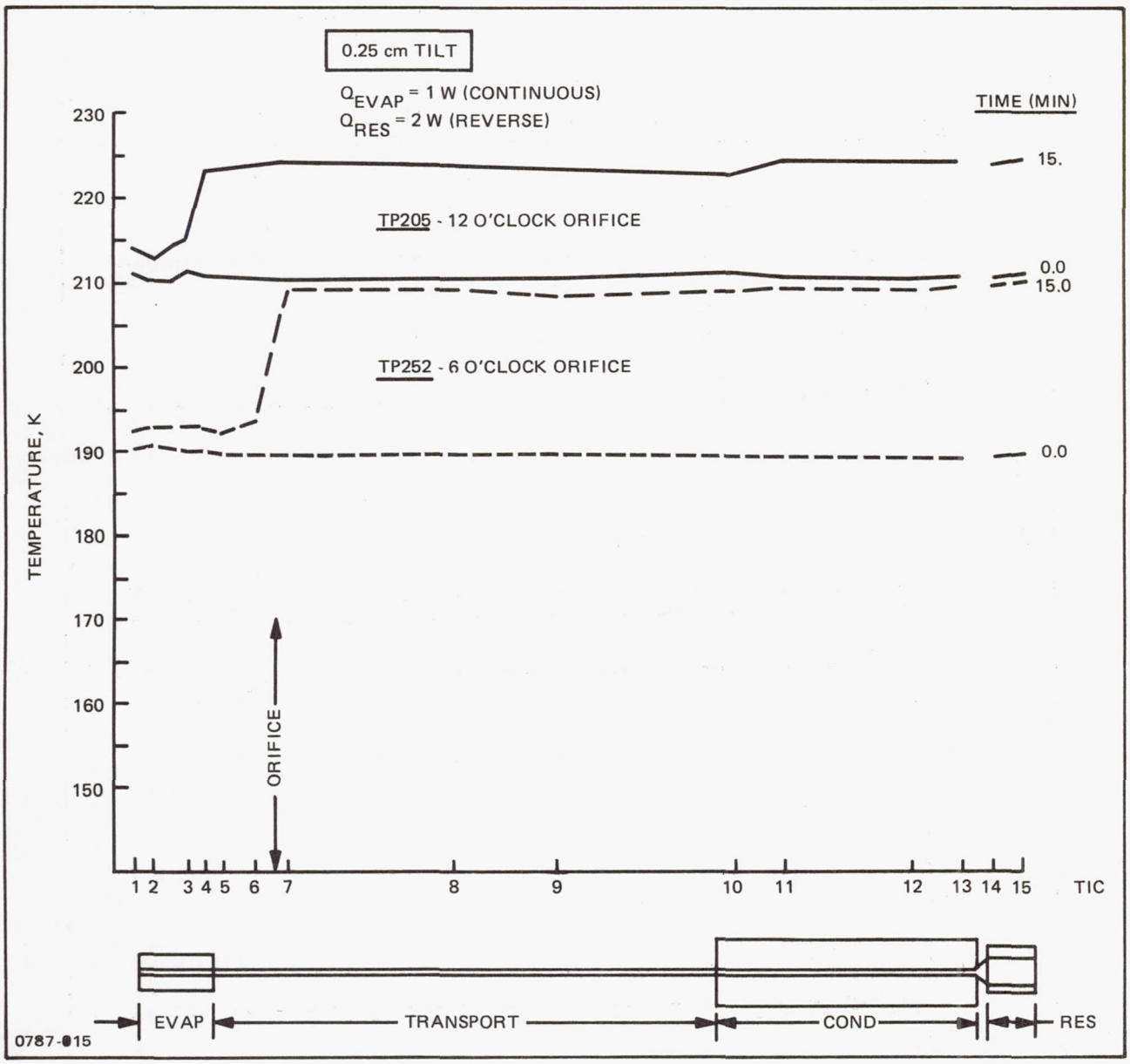

Fig. 3-15 HEPP Liquid Block Cryodiode, Reverse Mode Test Results

only through the evaporator section (about 10 cm). However, at the 6 o'clock position (TP252) the blocked section extends up to the orifice (about 20 cm) and the evaporator is more effectively insulated from the unblocked vapor space, which is filled with warmer vapor.

Shutdown energy was estimated by using the method of Reference 4. The shutdown time is taken as the interval from the moment the reservoir begins to rise in temperature above the transport section to the time the blocked transport section rate of temperature increase drops sharply. The energy absorbed (shutdown energy) during transition is defined as

$$Q = (mc_p)(T_f - T_i) - Q_e\tau$$

where: mc_p = thermal mass capacitance of the diode evaporator and detector block

T_f = temperature of the detector block at complete shutdown

T_i = temperature of the detector block at the start of reversal

Q_e = detector block heater power

τ = shutdown time

This relationship is a conservative estimate since it includes the energy absorbed by the evaporator block due to the surrounding ambient.

Being conservative and using the data shown (Figure 3-15) for TP252, the shutdown energy is calculated to be 0.098 W-hr at the maximum.

The comparison between the platinum resistance thermometers (PRTs) and the corresponding copper-constantan thermocouples is shown in Figure 3-16. The PRT calibration curve is given in Figure 3-17. As seen, the agreement between the measurements is poor ranging from 0.1 to 5° C difference depending upon the sensors. The thermocouple measurements are considered the more accurate, since they were spot welded to the heat pipe tube. The PRT measurements on the other hand are influenced by the uncertainty associated with the interface thermal resistence between the sensor and the tube. They use mechanical clips and an interface grease.

System Testing

Thermal vacuum testing of the integrated HEPP cryogenic heat pipe experiment was conducted at the Johns Hopkins Applied Physics Laboratory (APL) under the direct supervision of ITE, Inc., the system integrator. Two thermal tests were run: one before and

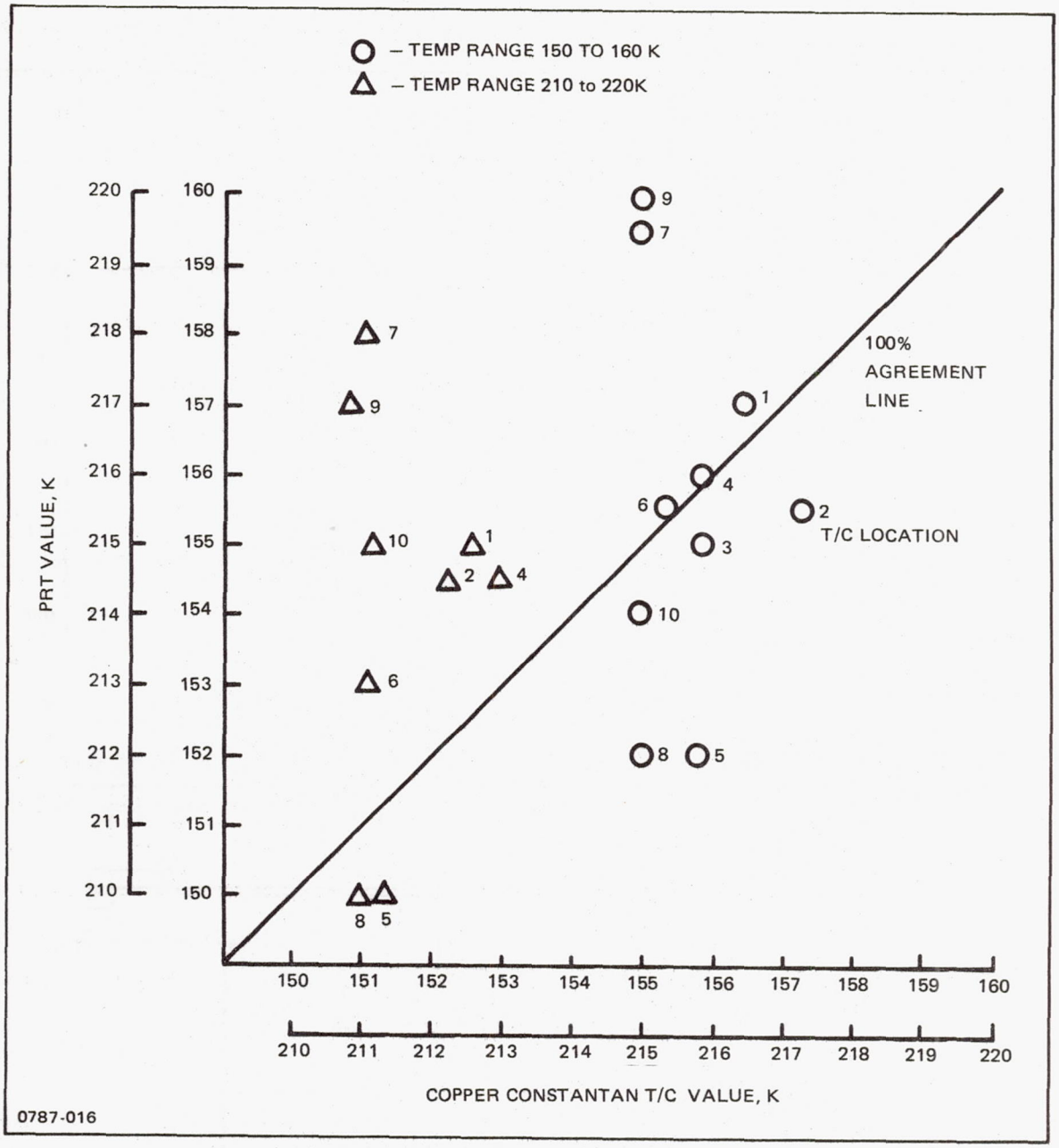

Fig. 3-16 Temperature Comparison PRT vs Copper Constantan Thermocouples

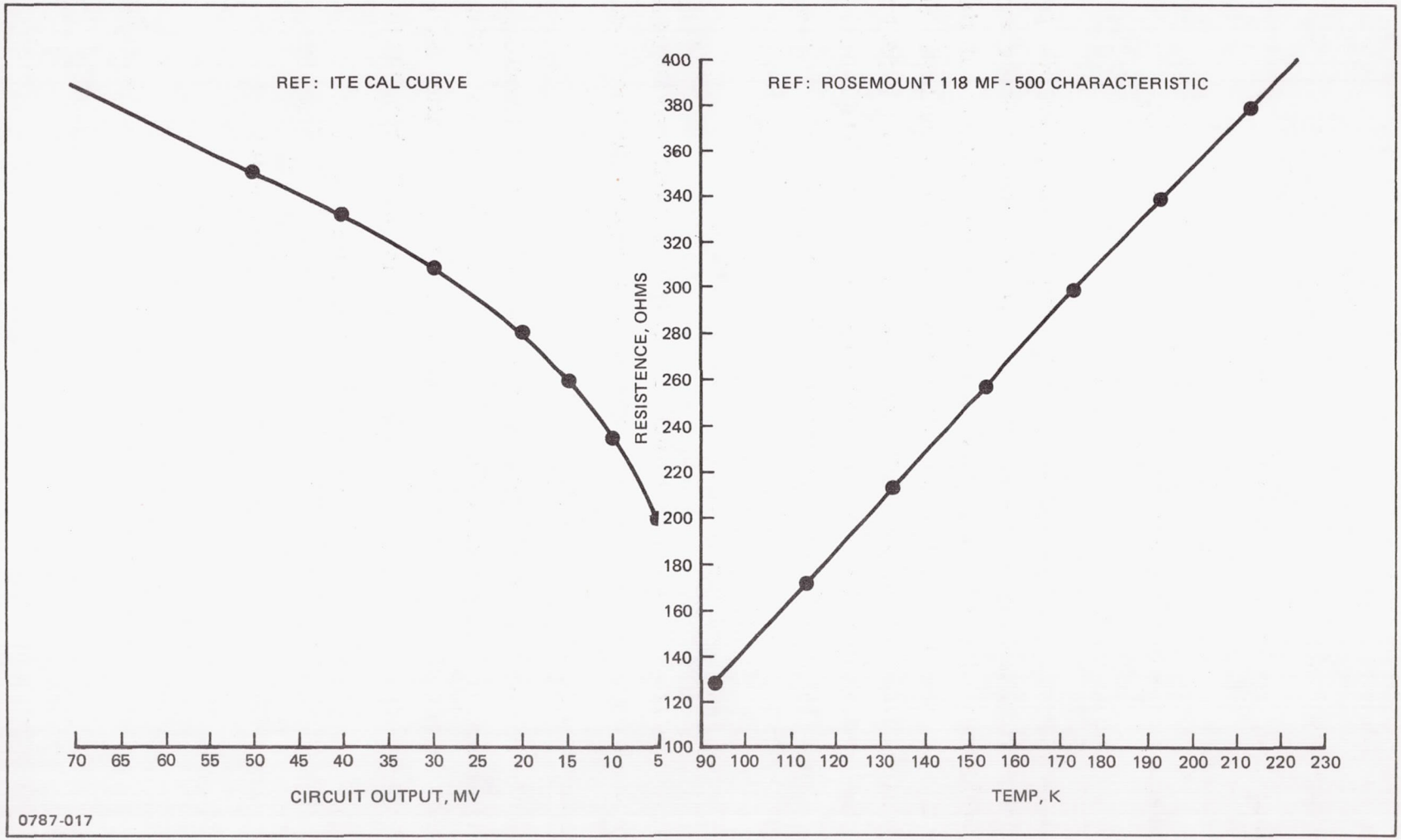

Fig. 3-17 Calibration Curve - PRT Conditioning Circuit

one after vibration testing the entire assembly. During each sequence, the diode was tested to determine the following:

- Startup from ambient
- Long term, low load forward mode performance
- Maximum heat transport capacity
- Reverse (shut-off) mode behavior.

Start Up From Ambient

Initial start up from ambient was successfully demonstrated during both pre- and post-vibration thermal tests by the convergence of evaporator and condenser temperatures during the prolonged cooldown. A low evaporator heat load was applied at all times; 0.5 watt during the pre-vibration test and 1.0 watt during the post-vibration test. Figure 3-18 shows the startup data for the post-vibration test sequence. Initially, a large temperature difference developed between the evaporator and condenser, but the heat pipe eventually recovered. This is indicated by the convergence of the evaporator and condenser temperatures at -40° C (233 K).

Long-Term, Low Load Performance

The cryodiode heat pipe was successfully operated at a 2 watt load for several hours. Figure 3-19 shows a typical temperature profile taken during pre-vibration tests.

Maximum Heat Transport Capacity

The maximum heat transport capacity tests were run at the PCM melting point (182 K) by incrementing the evaporator heat load until a dryout was recorded, as evidenced by a runaway evaporator temperature. The maximum heat transport capacities recorded during the tests are summarized below and reflect operating temperatures from 190 to 200 K.

Summary of Maximum Measured Transport Capacity

Test	Adverse Tilt cm (in.)	Operational Q_{max}, Watts
Pre-Vibration	.19 (.075)	20
Post-Vibration	.19 (0.75)	24
	.51 (.20)	22

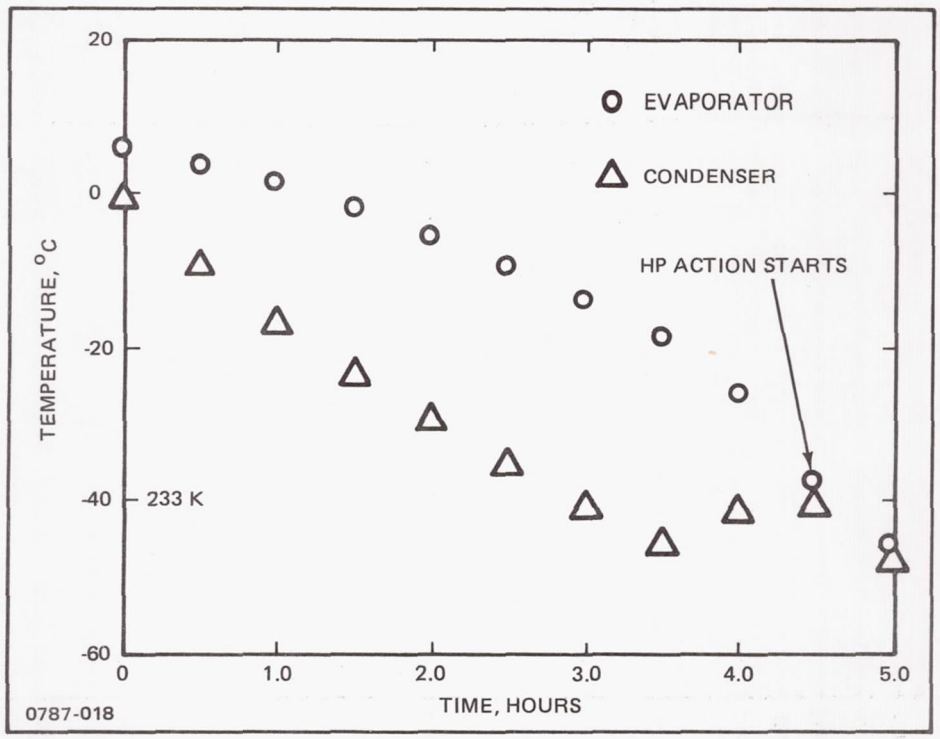

Fig. 3-18 Diode Start-up Behavior During Post-Vibration Testing (1 W on Evaporator)

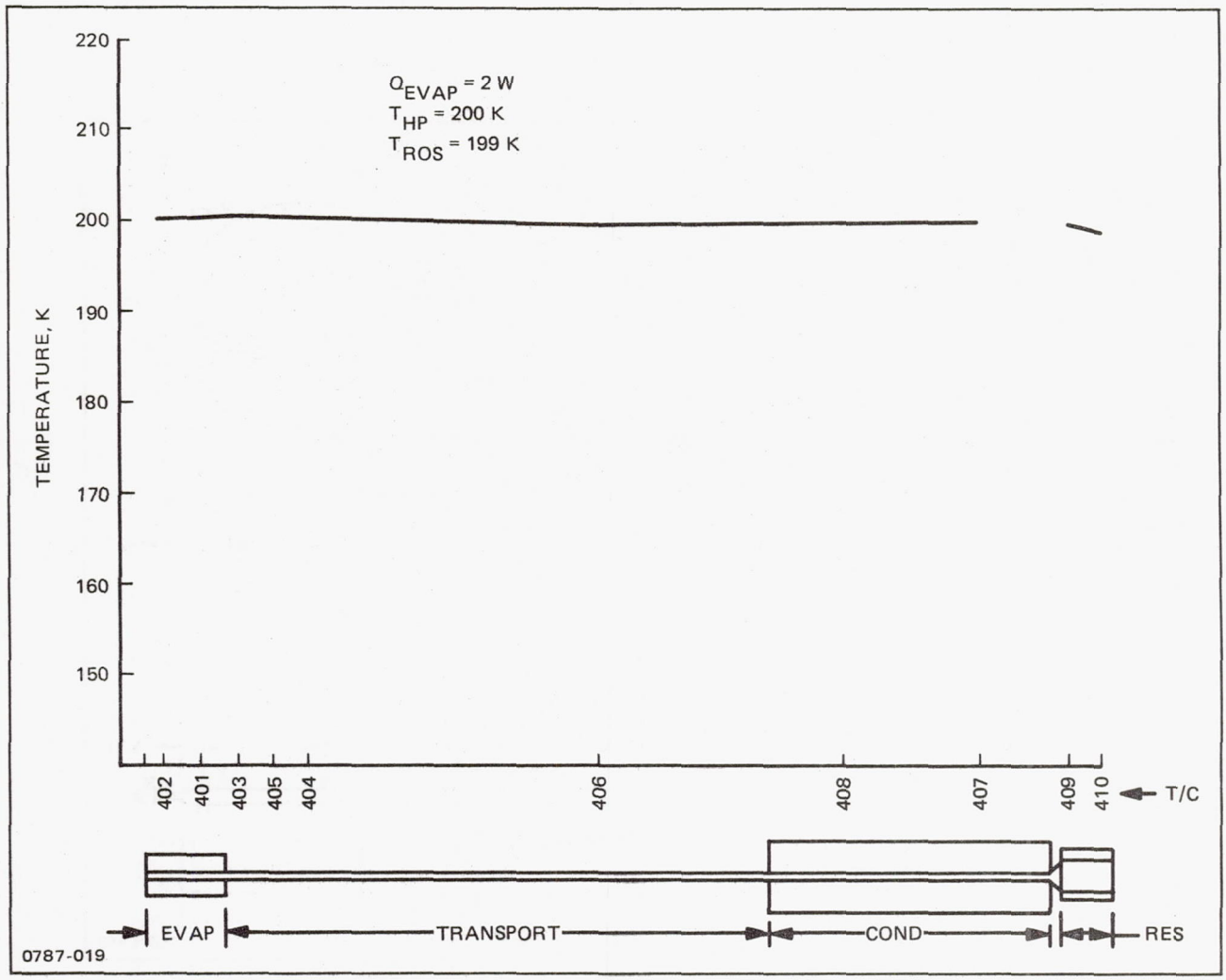

Fig. 3-19 Long Term, Low Load Test Data

These data indicate that there was no performance degradation due to vibration and that the artery diode heat pipe is very insensitive to adverse tilt. A typical temperature profile is shown in Figure 3-20. By comparison, it is of interest to note that the forward mode throughput measured for the axially grooved transport heat pipe degraded from 22 watts to 10 watts when the adverse tilt was increased from 0.19 cm to 0.51 cm, during post-vibration tests.

After experiencing a "hard" dryout, the heat pipe did not always recover when the load was sharply decreased (up to a factor of ten). As in the qualification testing, re-starting the heat pipe after a dryout could always be accomplished by first entering a reverse mode, followed by a controlled condenser cooldown ($\approx 1°$ C/Min).

Reverse Mode Performance

Rapid transition from a low load forward mode to a fully blocked reverse mode was always readily accomplished by appropriate increases in radiator and reservoir heat inputs. All reverse mode tests were run with a melted PCM (>182 K). After a uniform forward mode profile was established, a heat load of 40 watts was applied to the main radiator and a 4 watt load to the reservoir. The measured response of the evaporator, condenser and reservoir temperatures during reversal are shown in Figure 3-21. Both the reservoir and condenser temperatures increased in response to the applied loads and after about 2 minutes, they both exceeded the evaporator temperature and the evaporator started to accumulate fluid. In 4 minutes, the diode was blocked up to the orifice position. The condenser and reservoir were emptied of fluid after 6 minutes, as evidenced by sharply increasing temperatures. The evaporator temperature remained constant throughout the test while the temperatures of the condenser and reservoir increased by 18° C and 26° C, respectively over an 18 minute interval. The corresponding temperature rise on the blocked side of the orifice was 4° C.

Transition back to a forward mode was effected by allowing the condenser and reservoir to cool and applying a low (2 to 6 watt) evaporator heat load.

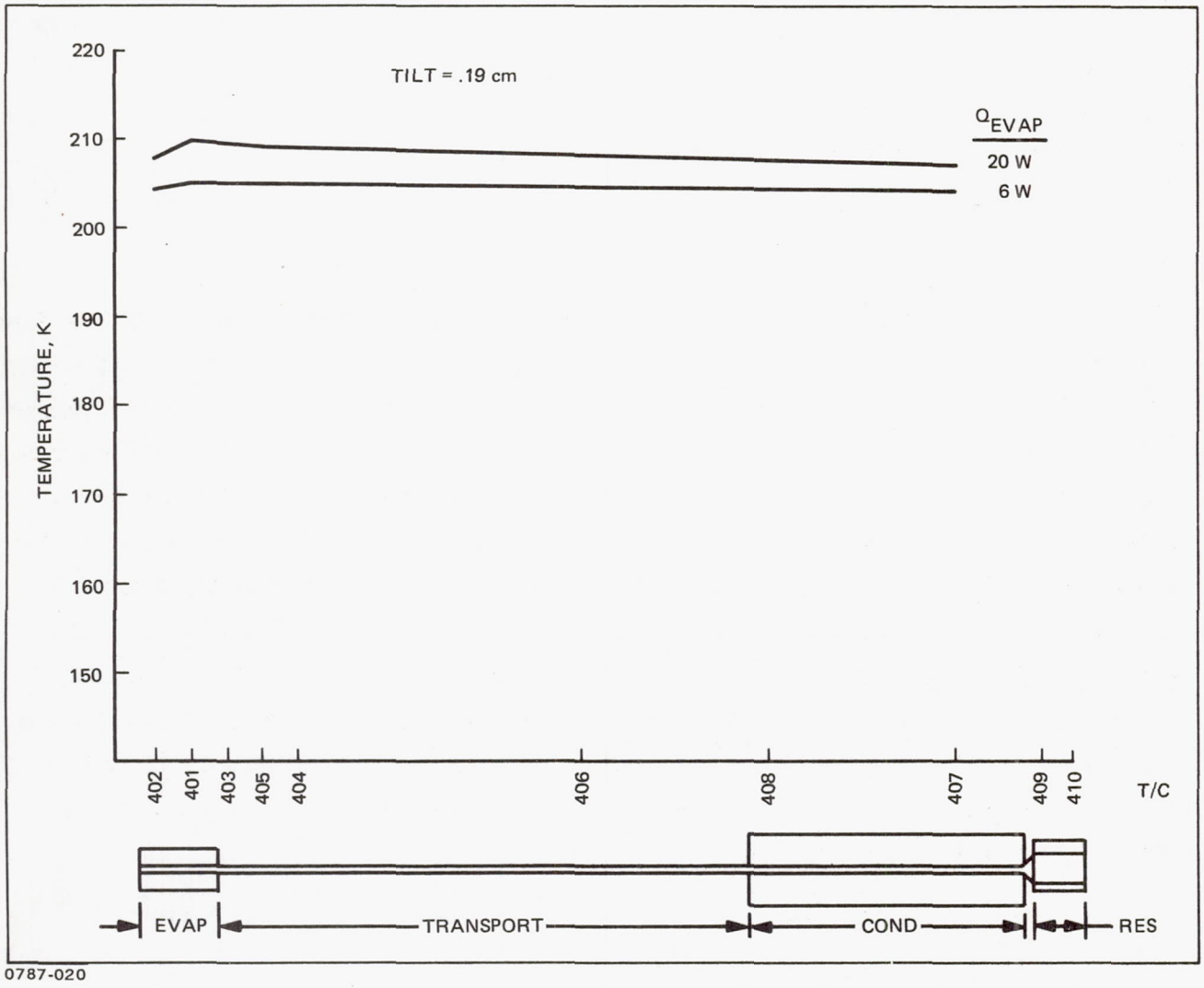

Fig. 3-20 Forward Mode Temperature Profile, Previbration

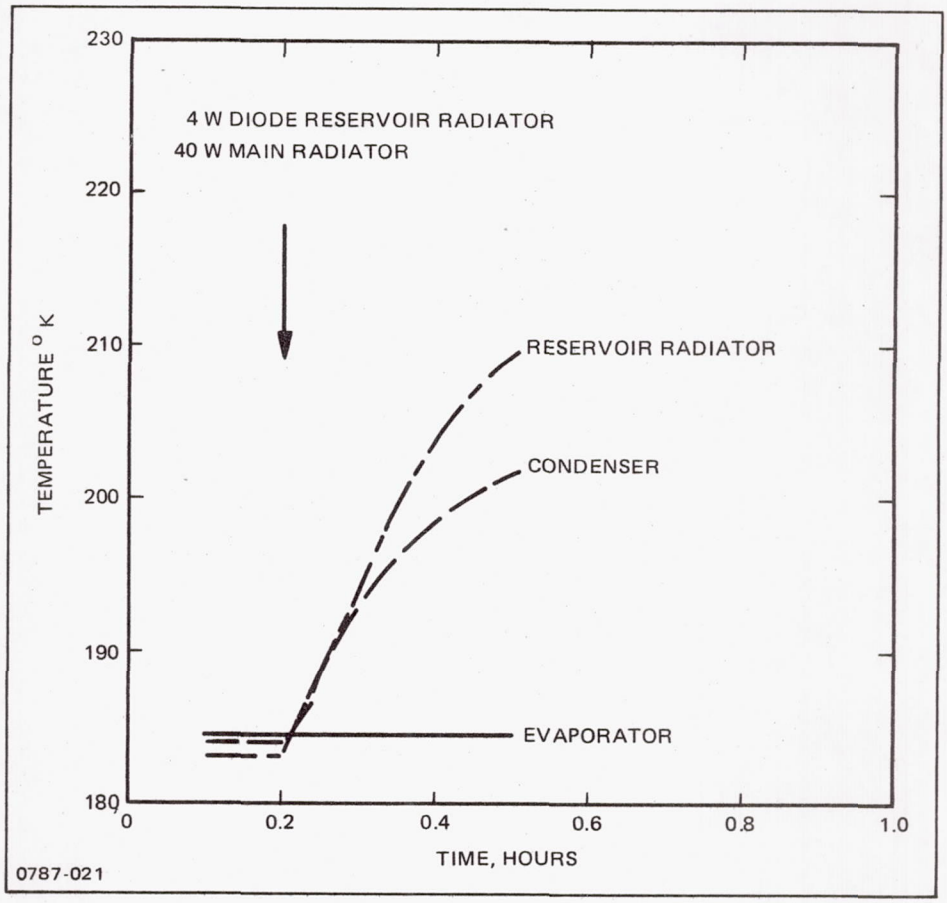

Fig. 3-21 HEPP Diode Reverse Mode Response (Post-Vibration)

Section 4

FABRICATION OF A LIQUID TRAP CRYOGENIC THERMAL DIODE HEAT PIPE, ENGINEERING MODEL (MOD 9)

An engineering model of a spiral artery liquid trap diode heat pipe was fabricated at Grumman and tested at NASA-ARC. Complete details are presented in Reference 3, but the major results are summarized in this section.

The diode heat pipe consisted of four main parts: an evaporator, a transport section, a condenser, and the liquid trap reservoir. The wick was a spiral artery formed by wrapping 250-mesh stainless steel screen and 0.04-cm-diam spacers on a central mandrel. The reservoir had a larger diameter (1.588 cm) than the 0.635 cm OD heat pipe portion and was connected to it by a conical transition section and a butt-welded joint. The internal core of the reservoir consisted of laminated aluminum channels having a total internal void volume of 6.42 cc. There was no capillary connection between the reservoir laminates and the artery wick. Liquid communication between artery and pipe wall was achieved with three scroll-type webs of 250-mesh screen equally spaced in the condenser and evaporator only. Circumferential grooves (63/cm) were used in the evaporator and condenser sections and standoffs were provided on the artery for support in the unblocked transport section.

An overall layout of the liquid trap diode is shown in Figure 4-1 and additional construction details are given in Table 4-1.

Tests were run in a thermal vacuum chamber with varying charges of ethane fluid (see Reference 3). The optimum charge was found to be 2.67 grams. The maximum measured transport capacity was 12 w-m at 200K with a forward conductance of 6 watts/° C. The shutdown energy was estimated as 0.32 watt-hours and the reverse mode thermal conductance was calculated as 0.037 W/° C.

Although the heat pipe demonstrated good transport capacity and reasonable shutoff times, it could not be reliably primed either after a thermay dryout or after a cooldown from ambient. Reliable startup was only initiated when preceded by a diode reversal followed by condenser cooling at a rate less than about 1° C/Min.

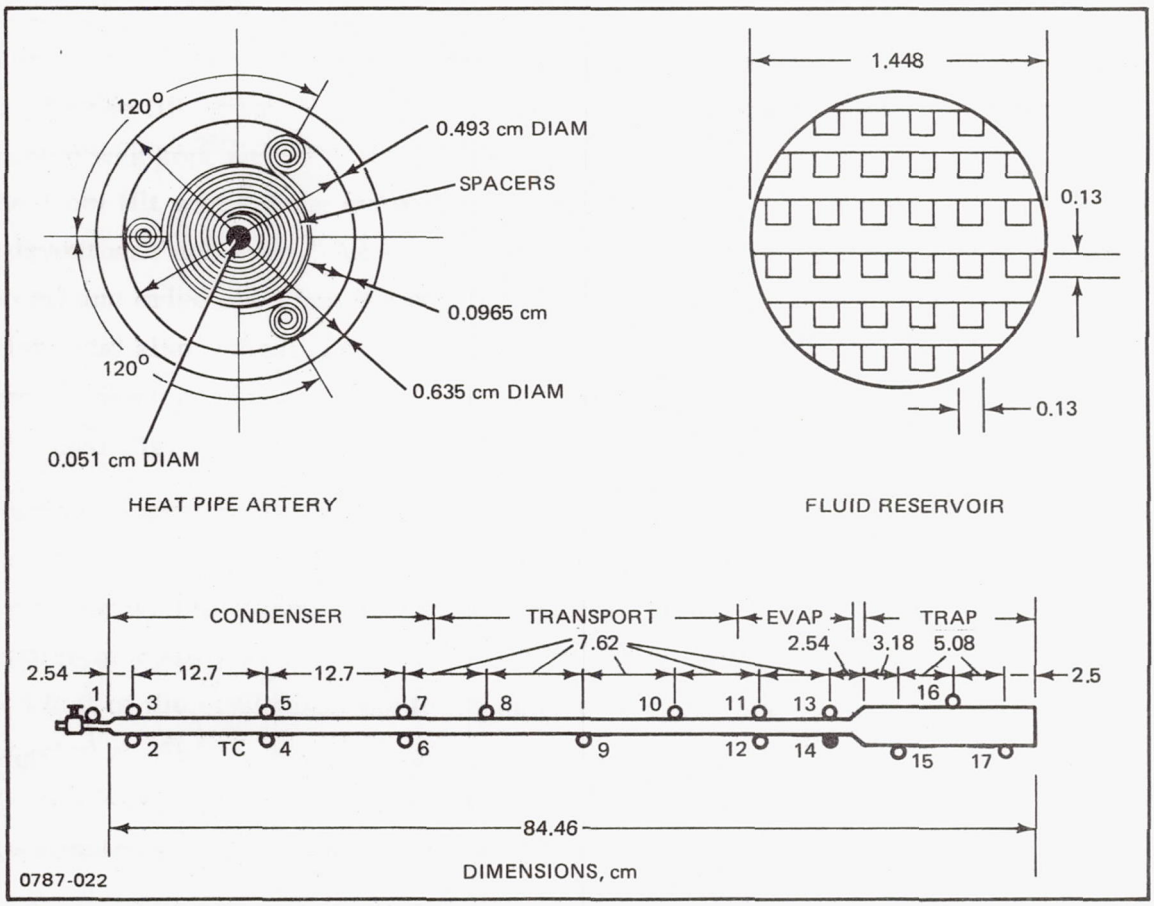

Fig. 4-1 Liquid Trap Diode Heat Pipe Configuration

Table 4-1 Liquid Trap Diode Heat Pipe Design Data

LENGTH, CM	
EVAPORATOR	10.160
TRANSPORT	28.257
CONDENSER	30.48
RESERVOIR	15.56
TRANSITION	1.524
CHARGE TUBE	4.445
INACTIVE SECTIONS	2.540
EFFECTIVE	48.57
DIAMETER, CM	
PIPE OD	0.635
PIPE ID	0.493
ARTERY OD	0.300
SOLID TUNNEL OD	0.051
RESERVOIR OD	1.588
CHARGE TUBE OD	0.318

OTHER PERTINENT DESIGN INFORMATION INCLUDES:

PIPE:	304 – 1/8 HD STAINLESS STEEL
SCREENING:	250–MESH 304 STAINLESS STEEL
CIRCUMFERENTIAL GROOVES:	63/CM (160/IN)
RESERVOIR:	6061 ALUMINUM LAMINATES 0.239 CM THICK WITH 0.127 CM DEEP AXIAL MACHINED GROOVES. CORE MACHINED TO 1.448 CM OD FOR PRESS FIT INTO 304 – 1/8 HD STAINLESS STEEL CYLINDRICAL SHELL

0787-038

Section 5

THERMAL VACUUM TESTING OF THE ORIGINAL LIQUID BLOCKAGE (ORIFICE) CRYOGENIC THERMAL DIODE, ENGINEERING MODEL (MOD 11)

This section presents the results of a thermal vacuum test which was run to check previously measured data that had been obtained using an environmental cold box. The details of the earlier test evaluation are contained in References 2 and 4. The thermal vacuum tests confirmed that the performance was similar to the earlier test (November 1975 and March 1976) and close to theoretical predictions.

The engineering model liquid blockage diode consists of four sections: an evaporator, a transport section, a condenser and an excess fluid reservoir, which is attached to the end of the condenser. A blocking orifice is positioned in the transport section about 10.16 cm from the entrance to the evaporator. The liquid reservoir has a larger diameter than the rest of the heat pipe (1.588 cm vs 0.635 cm) and contains a matrix of laminated aluminum channels which retain the excess liquid. There is no capillary communication between the reservoir insert and the piral artery heat pipe wick. Design details are summarized in Table 5-1 and the overall layout, including thermocouple locations, is shown in Figure 5-1.

For this retest, the engineering model cryodiode was configured and instrumented in the same manner as in previous tests (see Reference 4), with one notable exception - the charge valve was removed and replaced with an intermediate pinch-off charge tube that was joined to the main charge tube by a swageloc fitting. This minimized the evaporator end-effects introduced with a large mass (the charge valve) and eliminated the need for guard heating and cooling. The heat pipe was charged with 4.8 grams of processed ethane fluid, which corresponds to about a 7% overfill at 200 K.

As before, three aluminum masses were attached to the pipe: at the evaporator, a 0.197 Kg mass to simulate a detector block; a condenser mass of 0.765 Kg for ease of mounting the pipe assembly to an LN_2 sink; and a reservoir mass of 0.205 Kg, also for maintaining the reservoir in contact with the LN_2 sink. The reservoir and condenser blocks were mounted to an LN_2 sink which was designed to capture the blocks in a compression-type arrangement. Rod heaters integral to the compression block were used to control the forward mode temperature and also provide an alternate means for diode reversal. Strip heaters were attached to the evaporator block for forward mode heat loads

Table 5-1 Engineering Model Liquid Blockage Thermal Diode Design Data

LENGTH, CM	
EVAPORATOR	10.160
TRANSPORT–BLOCKED	10.160
TRANSPORT–UNBLOCKED	24.130
CONDENSER	21.273
RESERVOIR	6.033
TRANSITION	1.524
CHARGE TUBE	4.445
INACTIVE SECTIONS	2.540
EFFECTIVE	50.010
DIAMETER, CM	
PIPE OD	0.635
PIPE ID	0.493
ARTERY OD	0.300
SOLID TUNNEL OD	0.051
RESERVOIR OD	1.588
CHARGE TUBE OD	0.318

OTHER PERTINENT DESIGN INFORMATION INCLUDES:

PIPE:	304 – 1/8 HD STAINLESS STEEL
SCREENING:	250–MESH 304 STAINLESS STEEL
CIRCUMFERENTIAL GROOVES:	63/CM (160/IN)
RESERVOIR:	6061 ALUMINUM LAMINATES 0.239 CM THICK WITH 0.127 CM DEEP AXIAL MACHINED GROOVES. CORE MACHINED TO 1.448 CM OD FOR PRESS FIT INTO 304 – 1/8 HD STAINLESS STEEL CYLINDRICAL SHELL
ORIFICE	
HEIGHT:	.076 CM (.030 IN)
OD:	.483 CM (.190 IN)
LOCATION:	10.16 CM FROM EVAPORATOR ENTRANCE

0787-039

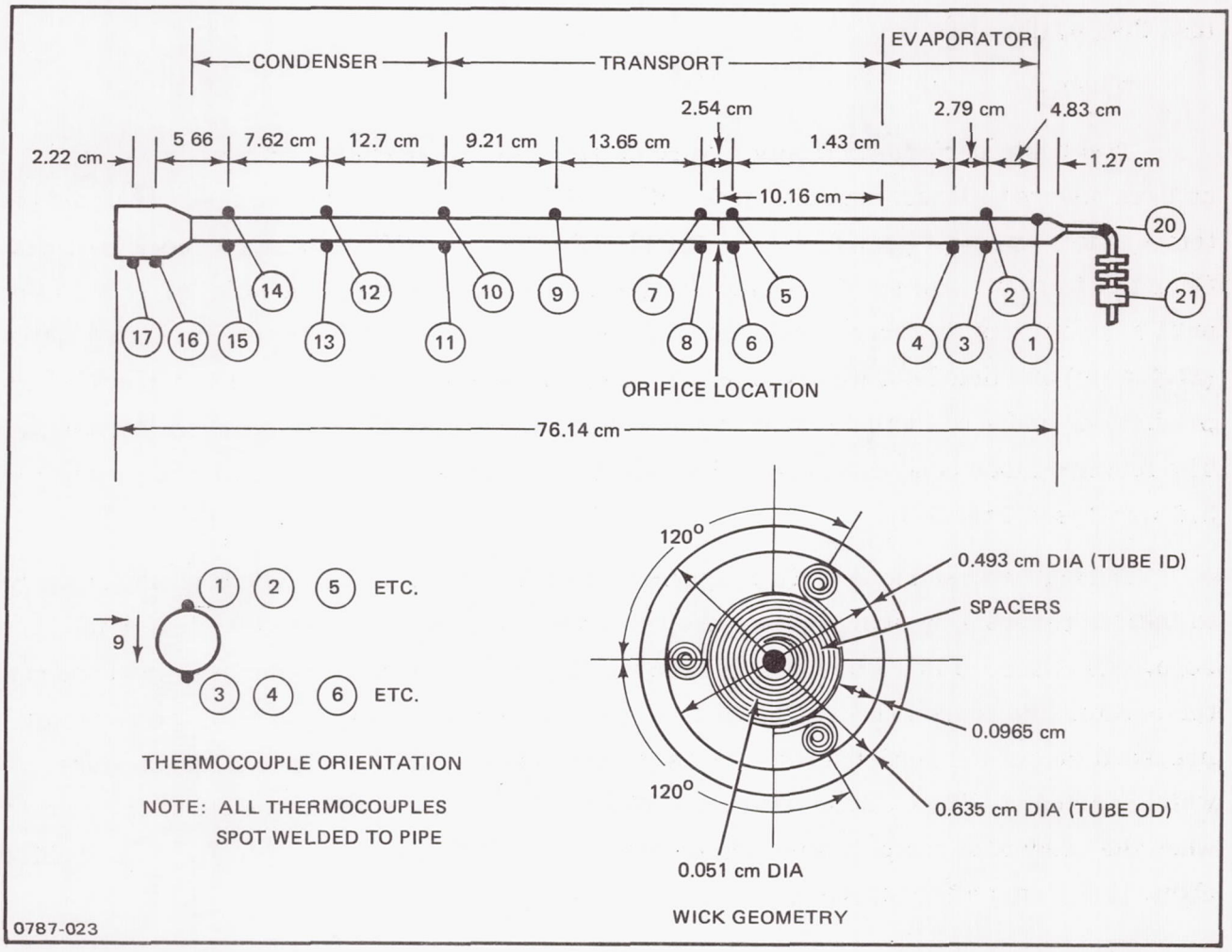

Fig. 5-1 Liquid Blockage Thermal Diode, Engineering Model Overall Layout and Instrumentation

and also to the reservoir block as the primary means to initiate diode reversal. All thermocouples were copper/constantan and were welded to the stainless steel pipe envelope. They were monitored with a Bristol strip chart recorder.

The entire assembly was insulated with 25 layers of aluminized mylar super-insulation (MLI) and installed in the thermal lab thermal vacuum chamber. During the tests, the cold wall was not filled and the vacuum was held to at least 10^{-5} torr. Thus the cold wall was warmer than the operating pipe, which promoted a conservative heat gain estimated at less than 0.15 watt.

Results:

Two basic performance points were obtained for comparison: forward mode Q_{max} at 1 cm adverse tilt and reverse mode with no tilt. During the forward mode runs the pipe temperature was kept near 200 K by suitable adjustments to the condenser block heaters. Once the 1 cm tilt was set the evaporator power was incremented and held for 15 minutes, until a dryout was achieved. As seen in Figure 5-2, the heat pipe transported 22.4 watts (11.2 w-m) and dried out when the power was increased to 27 watts. This agrees well with predictions and also indicates that performance had not degraded from the earlier tests. The forward mode conductance as calculated from the measured thermal profiles was 3.6 w/° C (see Fig. 5-3).

During reverse mode testing, the reservoir heater burned out and it was necessary to initiate reversal by overpowering the condenser block heater. The evaporator load was zero. As observed in Figure 5-4, a transient plot of average temperatures, the condenser temperature increased at a rate of 1.4° C/min and the temperature rise of the reservoir preceded that of the condenser due to its smaller mass. The evaporator temperature, which started at -79° C, held virtually constant and reached -76° C at the end of 30 minutes when the condenser temperature registered -51° C. Full evaporator blockage was achieved about 10 minutes after starting.

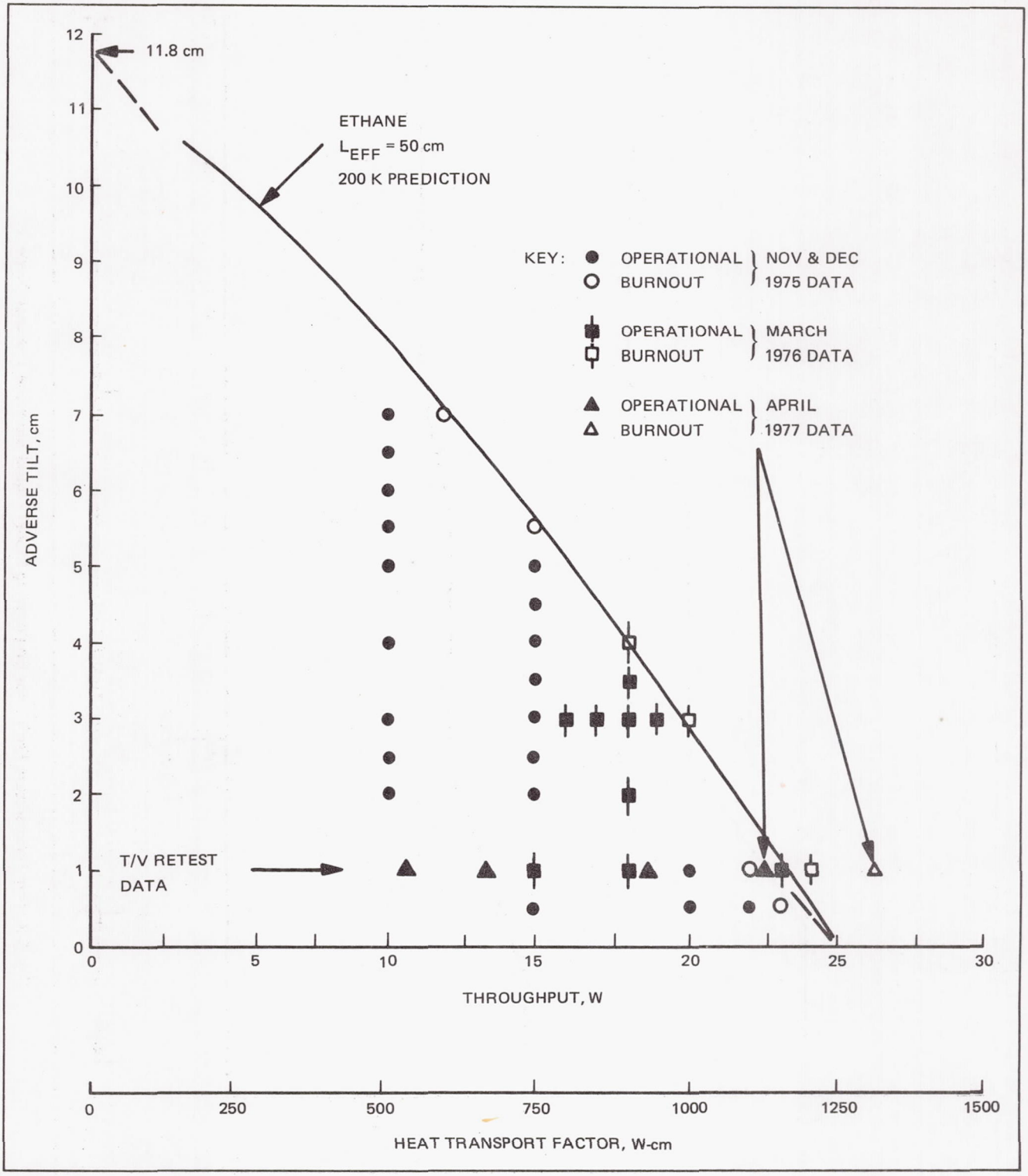

0787-024

Fig. 5-2 Cryodiode Test Points

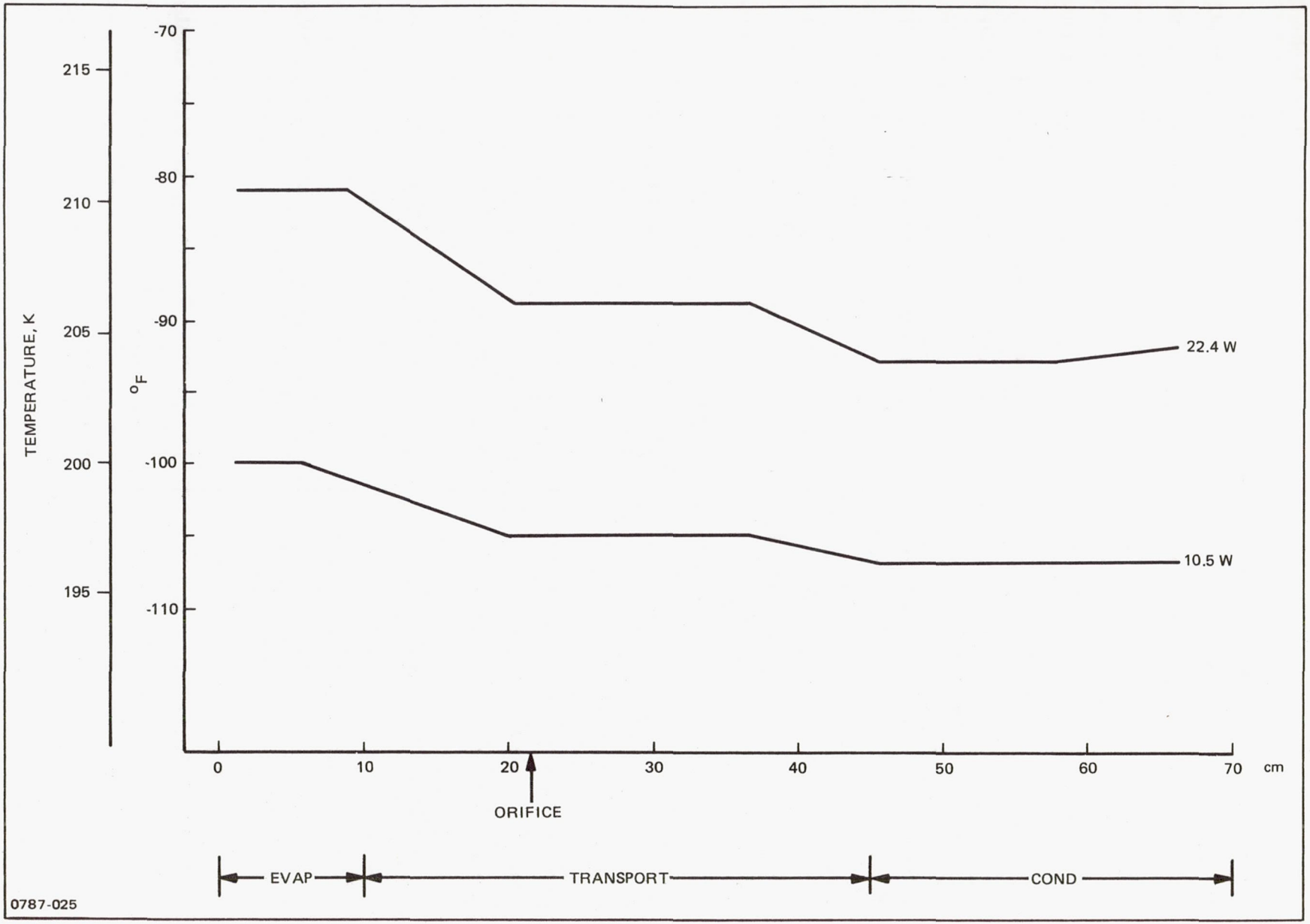

Fig. 5-3 Test Temperature Profile for Engineering Model Liquid Blockage Thermal Diode

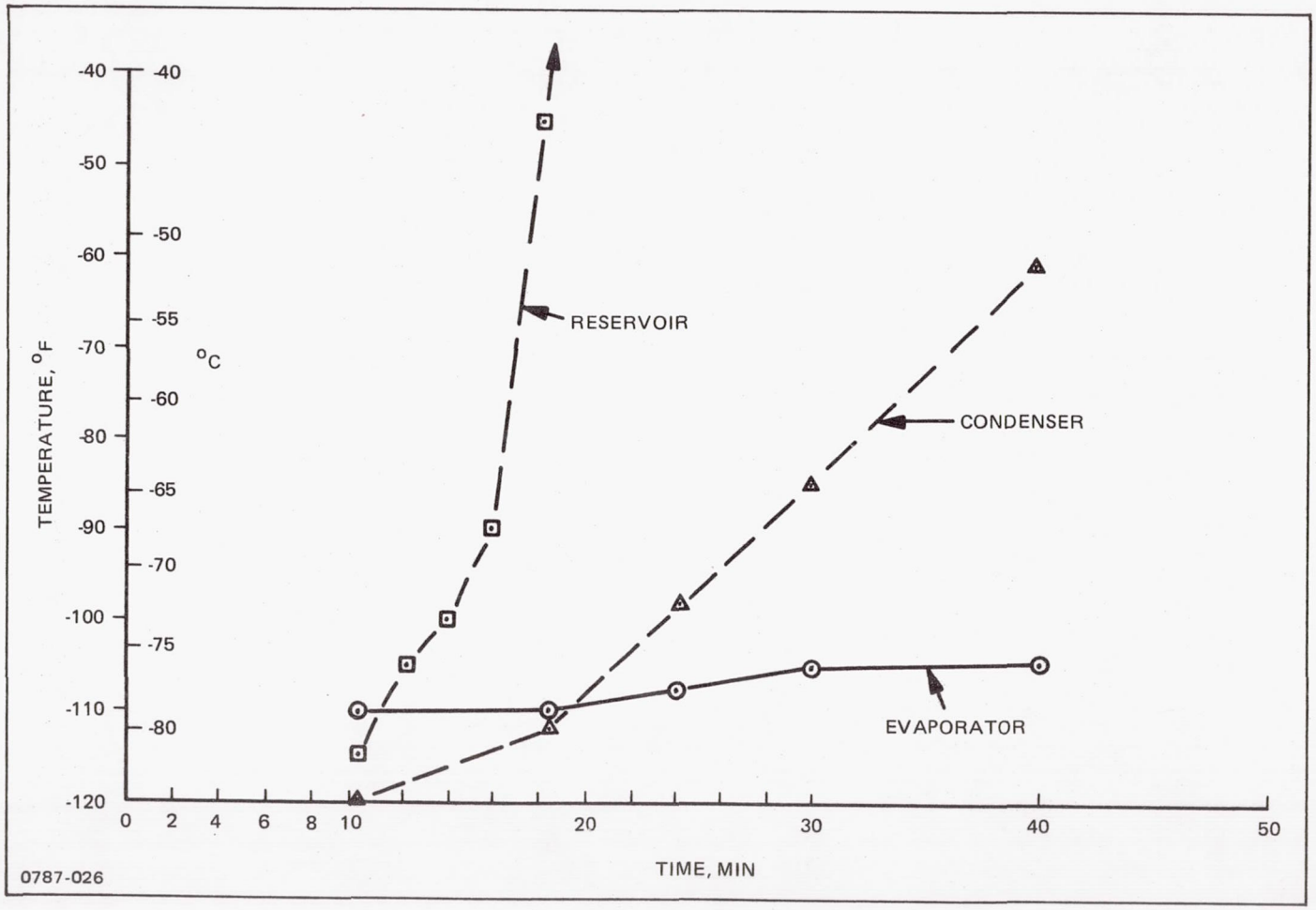

Fig. 5-4 Temperature During Reverse Mode

Section 6

AN INVESTIGATION OF THE START-UP DYNAMICS OF SPIRAL ARTERY CRYOGENIC THERMAL DIODE HEAT PIPES (MOD 12)

The previously reported test results for the cryogenic thermal diodes were good except for one persistent problem. The only way they could be reliably started from a dried out condition was to heat the condenser, which flooded the evaporator section with ethane fluid, followed by a gradual transition to a forward mode thermal gradient (evaporator temperature above condenser temperature). This start-up technique proved necessary for both the liquid trap and liquid blockage designs. Attempts to start the pipes directly from a room temperature cooldown or from an adiabatic condition after a hard dry-out usually failed, although a few successes were witnessed, usually after an initial cooldown.

Presuming a similar characteristic in zero g, this means that if a cryogenic thermal diode is used as a piece of flight hardware there would have to be operational constraints imposed which would involve preconditioning the heat pipe by flooding the evaporator. Within the present state-of-the-art, as far as a flight application is concerned, this means that only one preconditioning reversal mode is necessary as long as the imposed thermal loads are below the dry-out limit. In actuality, this might be acceptable for most cases since design safety margins of 2 to 4 are typically used. However, in some cases even the one preconditioning sequence might not be acceptable. Also, there is no reason to believe that this start-up problem is peculiar to diode-artery pipes, it probably exists in any cryogenic artery-type pipes made with the same materials and fluids. Since there are many useful spacecraft and sensor applications for cryogenic heat pipes and thermal diodes, it is important that they can be used without imposing any operational constraints upon the mission.

The specific reason for the start-up problem is not clear, but there are two prime candidates: surface wetting and artery priming. A surface wetting problem could exist between the 304 stainless steel surfaces and the ethane fluid. In a dried out condition, the existing surface chemistry (possible as a result of contaminants) could cause a non-wetting situation which can only be overcome by forcibly flooding and hence conditioning the surfaces. Once the surfaces have been wet, they tend to remain wet until a dryout condition is experienced. The "harder" the dry-out, the more surface area becomes dried out and non-wetting. Thus, on a subsequent start-up attempt the active evaporator surface area is

severely restricted which results in much lower throughput capability. There is strong evidence to support this wetting theory, since once a heat pipe has been started it can be repeatedly cycled from no load to high load as long as a dry-out situation is not encountered. In fact, it appears that, once started, it can remain in an adiabatic state indefinitely before a load is applied.

The other theory explaining the difficult start-up is that an artery priming problem exists. This would most probably be caused by the entrapment and subsequent growth of vapor bubbles within the arterial voids, thereby interrupting the liquid flow. Consider a cool-down from room temperature. Initially, the entire system (vapor and liquid) is isothermal and in an adiabatic condition. The screen artery is partially saturated by virtue of the screen-wicking capability. During the cool-down, heat is being pulled out of the condenser and the vapor pressure can drop below the saturation pressure of the liquid in the artery. The warmer liquid within the artery then tends to flash, which results in the formation of internal vapor bubbles. At this time the evaporator is dried out because it cannot draw enough fluid from the vapor-blocked artery. Gradually as the artery liquid cools, the saturation pressure drops and liquid capillary forces tend to collapse the arterial vapor bubbles. In theory, a partially primed artery can be fully primed by permitting continual fluid circulation at low heat loads and the introduction of cooler liquid from the condenser to the other parts of the artery. After a time, the cool liquid advances to the evaporator where the last remants of vapor bubbles collapse under the capillary forces. This sequence can be accomplished by operating the deprimed heat pipe at a load which is less than the maximum capacity of the partially primed artery and keeping it operating long enough to collapse all of the vapor bubbles.

Priming problems that come after a hard dryout at operating temperature can be described as follows. Once the capillary pumping limit is exceeded, the amount of fluid vaporized decreases which subsequently causes the vapor pressure to drop. This results in a pressure imbalance across the liquid in the artery which causes liquid flashing and vapor bubble formation within the artery. The displaced liquid ends up in the heat pipe as free liquid and the deprimed artery has a much reduced load capacity. Once again, in theory, the artery can be primed if operated long enough at a low load within the capability of the deprimed wick. As before, this is accomplished by the cool condenser liquid causing progressive collapsing of the vapor bubbles as it advances toward the evaporator.

For both the depriming sequences cited, the artery can be forcibly reprimed by heating the condenser. This raises the vapor pressure which then forces free liquid to enter the artery and displace or collapse the entrapped vapor bubbles.

The actual reason for the start-up difficulties encountered with the ethane artery cryodiode heat pipe could well be a combination of both wetting and priming problems. However, it was felt that the greatest insight could be obtained by separate investigations. Surface wetting characteristics were studied by experimental means, and an analytical investigation of the priming phenomenon consisted of predicting detailed temperature distributions and their influence on bubble growth.

6.1 ANALYTIC STUDIES OF PRIMING

Introduction

The 1/4" (6.35 mm) OD cryogenic diode with spiral artery wick has been made in several versions and tested with a variety of working fluids. Many of the diodes experienced difficulty in priming and/or required special priming procedures, such as diode reversal, prior to successful forward mode operation. To provide a better understanding of the artery priming problem, an analysis was performed which takes into account the detailed internal structure of the artery. The gap regions of the artery are assumed to be initially filled with vapor. The artery is divided longitudinally into sections, and calculations are performed to determine if each section, starting at the condenser end of the pipe, can fill. If all sections fill, the artery is said to be primed.

The discussion of the analysis covers the following areas:

1) Heat pipe geometry being studied
2) Priming criterion
3) Nodal model
4) Calculation of thermal couplings used in nodal model
5) Computer program
6) Analytic results
7) Conclusions and recommendations.

While only one pipe configuration was evaluated in this study, the method of analysis is easily adapted to other geometries and working fluids.

Diode Heat Pipe Geometry

The diode geometry modeled in this analysis is shown schematically in Figure 6-1. The pipe has a 1/4 inch (6.35 mm) OD and, exclusive of reservoirs, is 27 inch (0.68 m) long. For purposes of this study the reservoir is neglected. A liquid blockage reservoir would be the first region to fill on cooldown, and would be inactive during the priming process. A liquid trap reservoir would be dry during initial cooldown, and also be inactive during the priming process.

The pipe has a 4 inch (10.16 cm) evaporator, 15 inch (38.1 cm) adiabatic section, and 8 inch (20.32 cm) condenser. The evaporator uses electrical strip heaters for heat source and the condenser is clamped to a liquid nitrogen cooled block. Evaporator and condenser are wrapped in multilayer insulation (MLI) and the complete assembly is assumed to operate in a vacuum environment.

Priming Criterion

The priming criterion used in this analysis is that a vapor bubble in the gap region of the artery must collapse when subject to a temperature distribution within the pipe which is characteristic of steady state heat transfer conditions.

In equation form, this requires

$$Pv,g < Pl,g + \Delta Pc,g$$

where Pv,g is the saturated vapor pressure characteristic of a bubble within the artery, Pl,g is the liquid pressure adjacent to the bubble at the point on the bubble closest to the condenser and highest in elevation in a 1-g field, and $\Delta Pc,g$ is the pressure difference across the meniscus (surface tension divided by half the gap width) at the condenser end of the vapor bubble in the artery. The vapor bubble is assumed to be in thermal equilibrium with the liquid filled gap and screen regions which surround it. This implies some transport of heat (as vapor flow) within the bubble. There will also be an associated (extremely small) temperature variation over the surface of the bubble, which is neglected in this analysis. The bubble is treated as isothermal.

At the onset of this priming study, some thought was given to performing a transient calculation, modeling the pipe in detail as cooldown proceeded, starting from an initial isothermal room temperature condition. There were several difficulties with this approach:

1) Some fluids (e.g. methane) would initially be above critical temperature, presenting modeling problems for heat transfer within the pipe. Below critical temperature, there would be a problem in handling the filling of the porous regions with liquid consistant with the structure of a nodal thermal analysis model, and computational stability problems associated with the vapor nodes (small thermal capacitance and large thermal couplings).

2) Transient cooldown curves can vary considerably, so that a number of curves would have to be evaluated.

3) Programming and computation time would be considerable compared with a steady state approach.

Difficulties aside, however, it was recognized that in most cases where priming problems were encountered, the experimentalist would let the pipe remain (soak) at cold conditions for several hours. Hence, the ability of the pipe to prime under cold steady state condition is, in a sense, a more important aspect to assess analytically. A pipe which failed to prime under these conditions would not be likely to prime during a monotonic cooldown.

Nodal Model

The nodal model is shown schematically in Figure 6-2. The pipe is divided longitudinally into seven sections (2 in the evaporator, 3 in the adiabatic section, and 2 in the condenser). Multilayer Insulation (MLI) surrounds the evaporator and adiabatic sections. The condenser is coupled directly to a cooling block. In the radial direction, the MLI (which is subject to large temperature differences) is divided into 2 nodes, and the pipe itself into 4 nodes - the pipe wall, the vapor space, the porous wicking (artery screening and webs) and the gap region within the artery. A description of the nodes follows:

1) Nodes 1-5 - outer layers of MLI (nodes 1 and 2 cover the evaporator and nodes 3-5 cover the adiabatic section)

2) Nodes 6-10 - inner layers of MLI

3) Nodes 11-17 - pipe wall

4) Nodes 18-24 - pipe vapor space

5) Nodes 25-31 - porous wicking consisting of three cylindrical webs and the screening used to make the artery

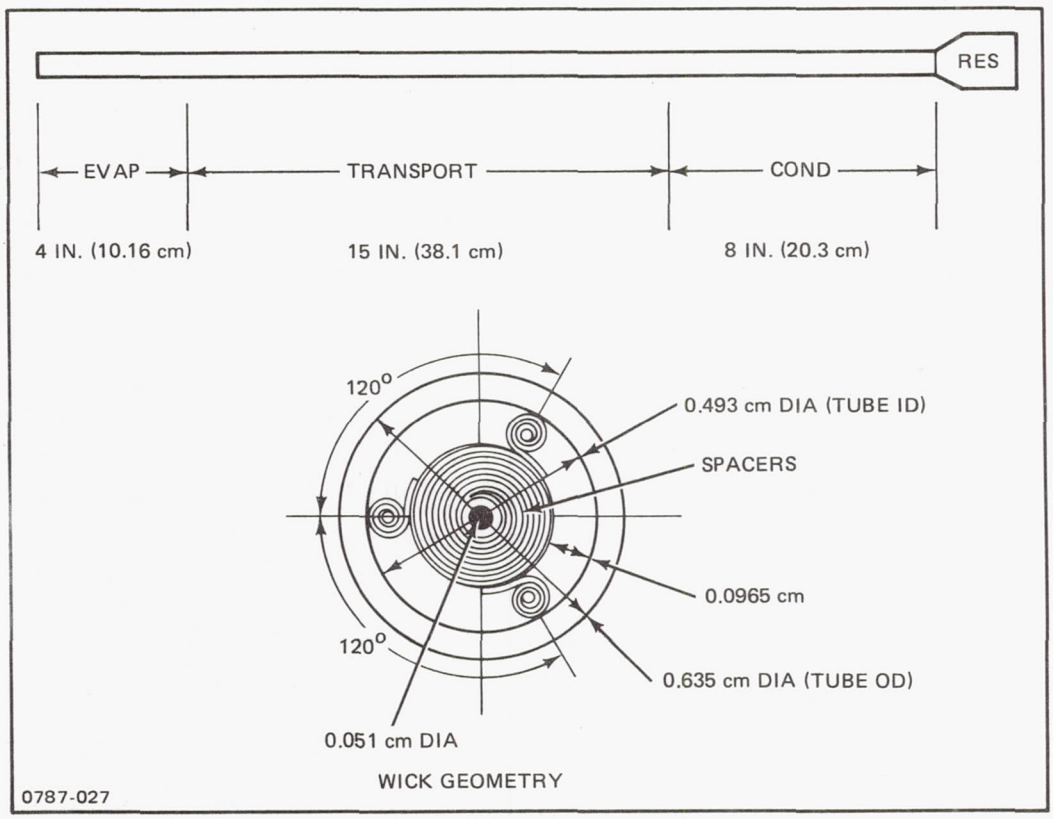

Fig. 6-1 Diode Heat Pipe Geometry

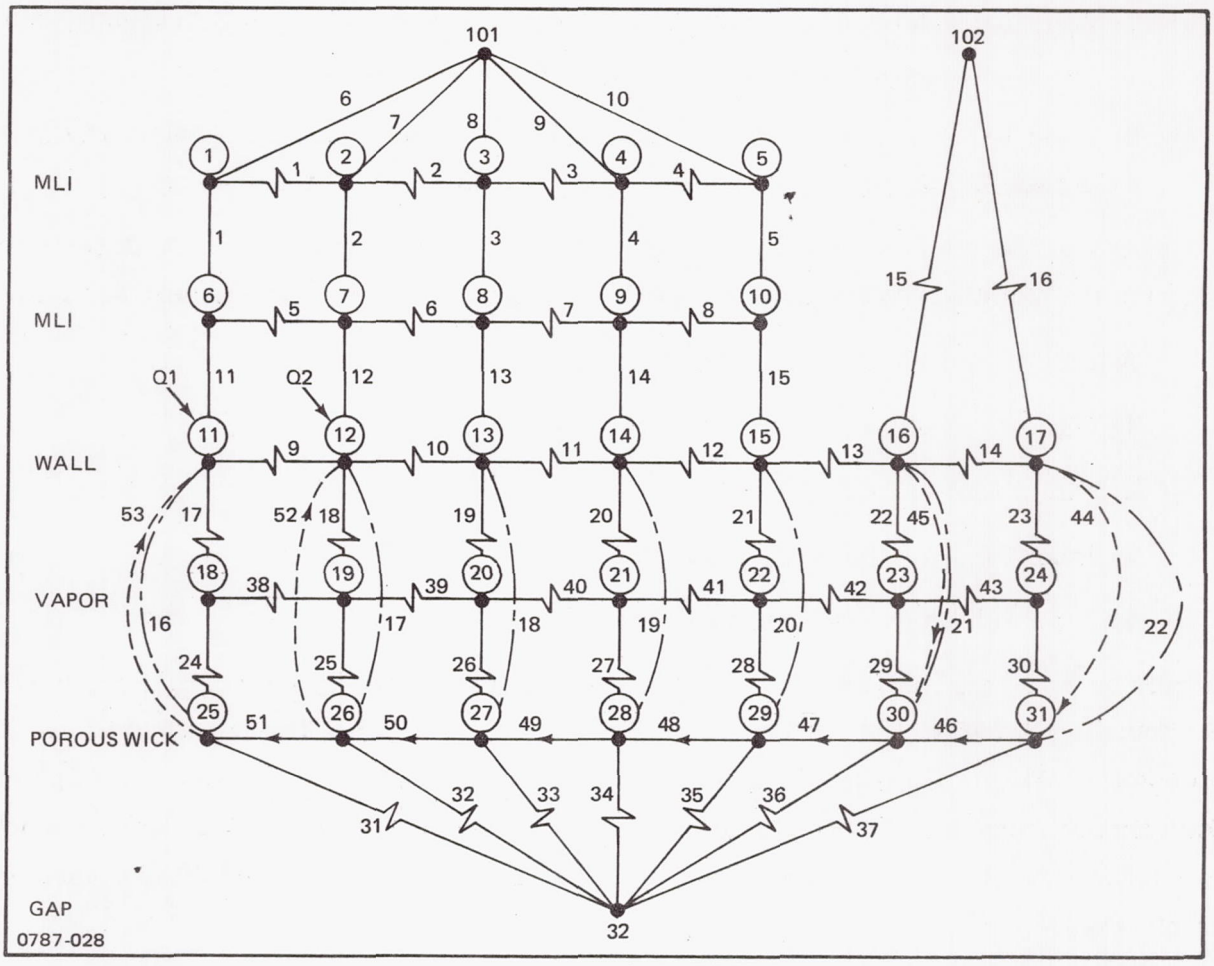

Fig. 6-2 Nodal Model for Priming Analysis

6) Node 32 - the vapor filled gap region within the artery. Initially, node 32 extends the full length of the artery and is thermally coupled to all the surrounding porous nodes. Priming is then tested for a meniscus across the gap at the condenser end (node 31). If priming can succeed, the gap region within node 31 is assumed filled with liquid, and the coupling between nodes 32 and 31 is set equal to zero. This is equivalent to having the vapor region of the gap extending from nodes 25 to 30. A new steady state temperature distribution is then obtained, and priming tested for filling node 30. The process is repeated until either priming fails or the last node (node 25)is filled

7) Node 101 - A boundary node representing the inside wall of the vacuum chamber, assumed kept at a constant temp (90° F) (27° C) in this analysis.

8) Node 102 - A boundary node representing the liquid nitrogen coolant in the condenser block, assumed to be at -136° F (-93° C) in this analysis.

A brief description of the couplings is given below. A more detailed description showing the quantitative evaluation of each coupling is presented in the next section.

A total of 22 radiation couplings are provided:

1) Vacuum chamber to outer MLI (5 couplings)

2) Outer MLI to inner MLI (5 couplings)

3) Inner MLI to pipe wall (5 couplings)

4) Pipe wall to porous material (7 couplings)

It may be noted that no radiant couplings have been provided in the longitudinal direction. Surrounding the MLI, the vacuum chamber is considered a relatively large high emittance enclosure. Within the MLI, longitudinal radiant heat transport is included in the couplings for conduction parallel to the laminations. Within the heat pipe, radiant flux is generally small because of the low temperatures and the view factors for longitudinal transport are fairly small.

A total of 43 ordinary conduction couplings are provided:

1) Parallel conductance within MLI (8 couplings)

2) Heat pipe wall (6 couplings)

3) Condenser wall to LN_2 (2 couplings)

4) Evaporator wall to vapor (2 couplings)

5) Adiabatic wall to vapor (3 couplings)

6) Condenser wall to vapor (2 couplings)

7) Vapor to porous wicking (7 couplings)

8) Porous wicking to gap region (7 couplings)

9) Between vapor space nodes (6 couplings)

A total of ten fluid conductors (one-way couplings) are provided:

1) Condenser wall to porous wicking (2 conductors)

2) Within porous wicking (6 conductors)

3) Porous wicking to evaporator wall (2 conductors)

It may be noted that fluid conductors are provided for the liquid flow path, whereas ordinary conductors are provided for the vapor flow path. The use of ordinary conductors for the vapor flow is related to the computational procedure used to calculate the vapor flow. For each vapor node, the vapor is assumed to be at saturation pressure, and the vapor flow between nodes is a consequence of the node to node pressure differences.

Thermal Coupling Calculations (Engineering Units used for convenience)

Nodal Geometry

A schematic of the nodal geometry, showing lengths and radii, is presented in Figure 6-3. Nodes are taken as centered within the boundaries.

Radiation Couplings (22)

1) MLI Blanket

The MLI blanket is assumed to consist of a total of 25 layers of crinkled, single aluminized mylar. This is divided into inner and outer blankets, each having an effective emittance of 0.015. Then

$$R_{i,j} = \epsilon_{eff} A_{i,j} - \epsilon_{eff} 2\pi \bar{r}_{i,j} l_i$$

For example

$$R_{1,6} = 0.015 \times 2\pi \left(\frac{0.3125}{12}\right)\frac{2}{12} = 4.091\ (10^{-4})\ ft^2$$

The coupling between the outer MLI nodes and the vacuum chamber, $R_{101,1}$ increased to 6.545×10^{-4} to reflect only half as many layers, and this value was also used between the inner MLI node and pipe outer wall, $R_{6,11}$. The corresponding blanket effective emittance values, allowing for the change in mean radius, are 0.0166 and 0.0436, respectively. Some runs were made with both of these values taken as 0.024. Results were similar.

2) Pipe Inner Wall to Artery Surface

The coupling between the pipe inner wall and the artery outer surface is based on an effective emittance for both surfaces of 1.0 and an area based on a mean radius of 0.153 inch less the thickness of the three webs (3 x .041 inch) which support the artery.

Table 6-1 is a list of the radiator couplings, showing nodes coupled and the coupling values.

Conduction Couplings - (Ordinary)

1) Longitudinal Conductance in MLI (Parallel to the Laminations)

Thermal conductance within the MLI parallel to the laminations is a complicated radiation and conduction phenomena which does not lend itself to treatment as a pure radiation or pure conduction coupling. Experimental data is available (Ref. 5) for crinkled single side aluminized mylar expressed in terms of effective conductivity, K_{eff}, at layer densities of 1850 and 3230 layers/meter. The data is shown plotted in Figure 6-4, from which it can be seen that K_{eff} is a strong function of temperature (taken here as a fourth power mean temperature).

We have 25 layers of MLI in a 3/8 inch thick annulus surrounding the pipe, corresponding to a layer density of 2625 layers/meter. An estimated curve for this layer density is also shown in Figure 6-4. The curve is a straight line on the semi-log plot with the form

$$K_{eff} = a\,\bar{T}^{b}$$

where $$\bar{T}_{i,j} = \left[\frac{T_i^4 + T_j^4}{2}\right]^{1/4}$$

$$a = 1.329\ (10^{-6})\ \text{w/(m-k)}$$

$$b = 1.972$$

the conductance coupling is then

$$K_{i,j} = K_{eff}\,\frac{A_x}{l_{i,j}}$$

where A_x is the cross-sectional area for parallel conductance

$$A_x = \pi\,(r_o^2 - r_i^2)$$

Table 6-1 Radiation Couplings

NO.	NODES COUPLED	R, (FT^2)
1	1, 6	4.091×10^{-4}
2	2, 7	4.09×10^{-4}
3	3, 8	10.23×10^{-4}
4	4, 9	10.23×10^{-4}
5	5, 10	10.23×10^{-4}
6	101, 1	6.545×10^{-4}
7	101, 2	6.545×10^{-4}
8	101, 3	16.36×10^{-4}
9	101, 4	16.36×10^{-4}
10	101, 5	16.36×10^{-4}
11	6, 11	6.545×10^{-4}
12	7, 12	6.545×10^{-4}
13	8, 13	16.36×10^{-4}
14	9, 14	16.36×10^{-4}
15	10, 15	16.36×10^{-4}
16	11, 25	$4,968 \times 10^{-3}$
17	12, 26	4.968×10^{-3}
18	13, 27	12.42×10^{-3}
19	14, 28	12.42×10^{-3}
20	15, 29	12.42×10^{-3}
21	16, 30	9.935×10^{-3}
22	17, 31	9.935×10^{-3}

0787-040

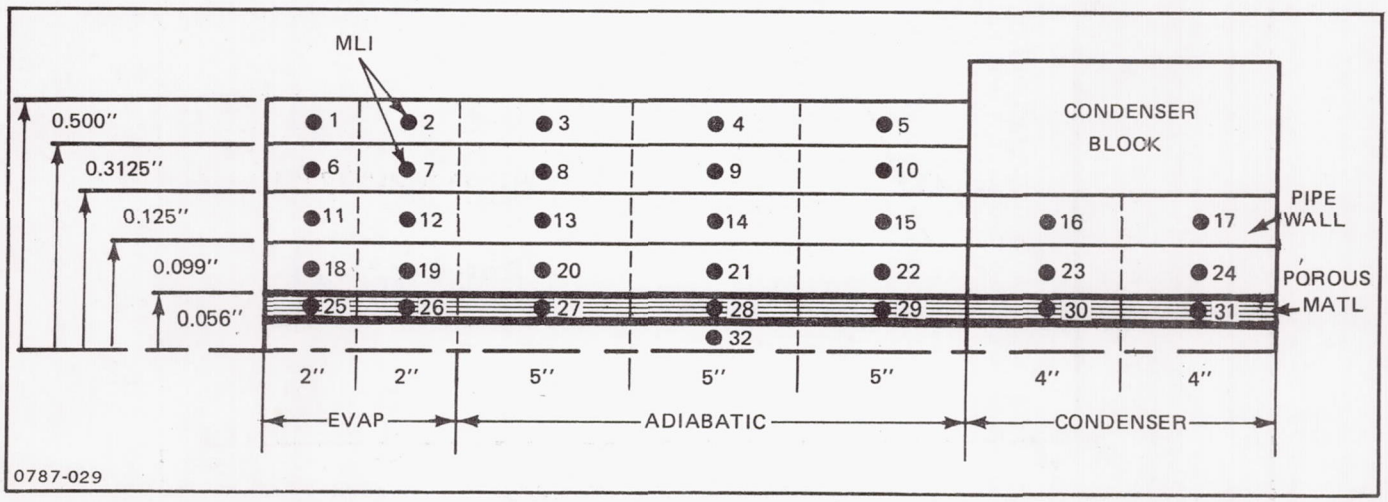

Fig. 6-3 Schematic for Nodal Geometry

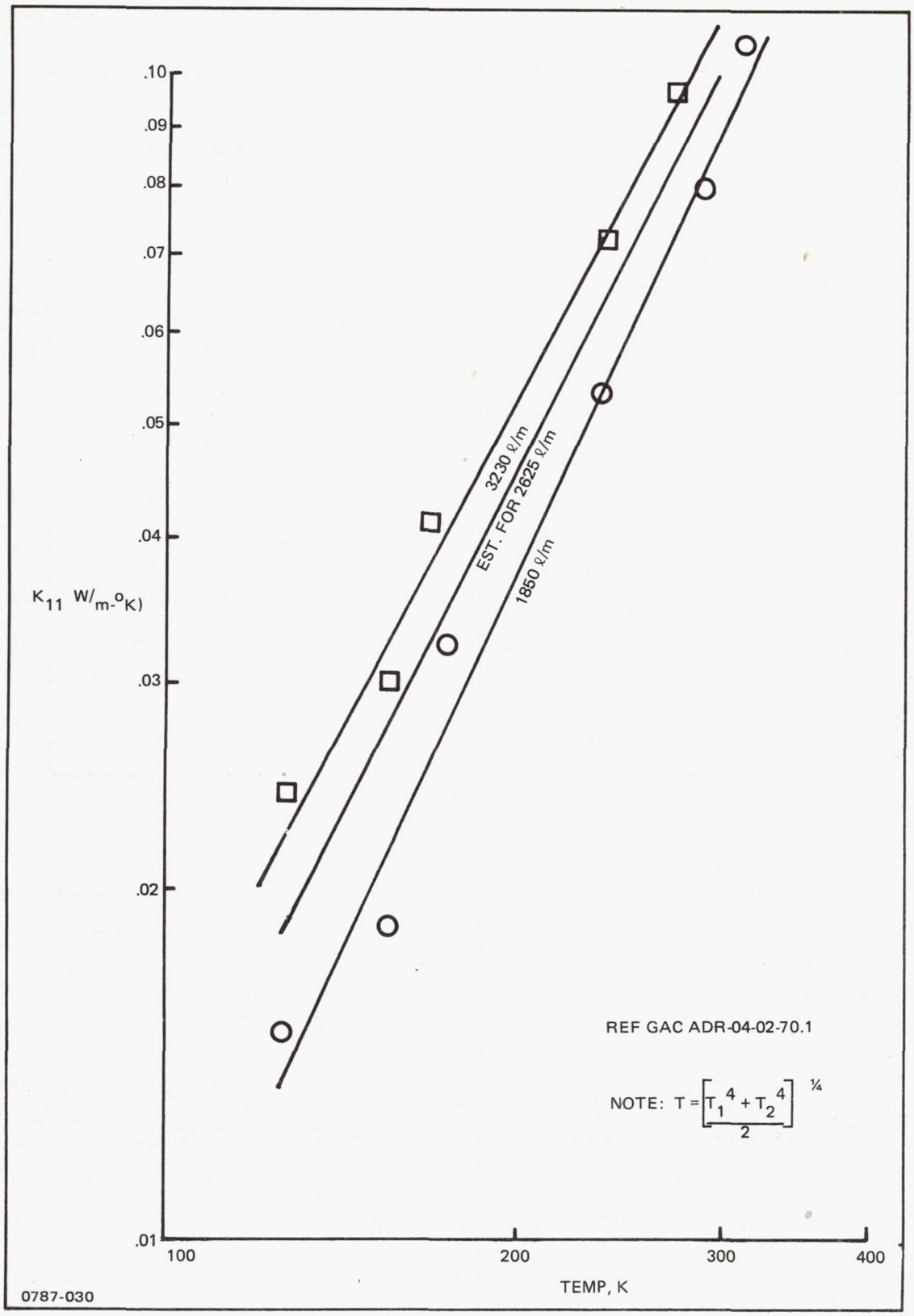

Fig. 6-4 K_{11} for Crinkled Aluminized Mylar

and $l_{i,j}$ is the distance between node centers. The A_x values for the outer and inner blankets are 3.32×10^{-3} ft^2 and 1.79×10^{-3} ft^2 respectively.

Because of the strong temperature dependence, the $K_{i,j}$ values must be computed based on nodal temperatures, making the solution interactive. The initial values loaded in are based on a mean temperature of 200°K (360°R). At 200°K, K_{eff} = .04583 w/m- °K (.0265 Btu/hr ft °R)

Then, in English units,

$$K_{i,j} = 0.0265 \left(\frac{\bar{T}_{i,j}}{360} \right)^b \frac{A_x}{L_{i,j}}$$

Values for $K_{i,j}$ are given in Table 6-2 for 360°R, for the 8 longitudinal MLI couplings.

2) Pipe Wall Conduction Couplings

The pipe wall is stainless steel with an assumed thermal conductivity, k - 10 Btu/(hr-ft - °F). The couplings are then

$$K_{i,j} = K \frac{A_x}{L_{i,j}} = \frac{K}{L_{i,j}} \frac{\pi}{4} (d_o^2 - d_i^2)$$

where d_o = 0.250 inch and d_i = 0.194 inch, and $L_{i,j}$ is the longitudinal distance between node centers.

Resulting $K_{i,j}$ values are given in Table 6-3.

3) Condenser Cooling Block Conduction Couplings

A schematic of the condenser cooling block geometry is shown in Figure 6-5. The total thermal resistance is made of of 5 parts - resistance between the node center and the pipe surface, contact resistance between pipe and V-Block, resistance across V-block, contact conductance between V-Block and LN_2 cooled block, and resistance across the LN_2 cooled block. Each node has a 4" longitudinal length. Then

$$\frac{1}{K_{i,j}} = \frac{1}{L} \left\{ \frac{t/2}{k_{ss} \pi \bar{D}} + \frac{1}{\pi D_o h_o} + \frac{1/2}{S_v K_{al}} + \frac{1/2}{y h_o} + \frac{1/2}{k_{al} \frac{y}{x}} \right\}$$

Table 6-2 MLI Parallel Conductance Couplings ($\bar{T}$ = 360°R)

NO.	NODES COUPLED	K_{ij} (at 360°R) BTU/HR °F
1	1, 2	5.285×10^{-4}
2	2, 3	3.020×10^{-4}
3	3, 4	2.114×10^{-4}
4	4, 5	2.114×10^{-4}
5	6, 7	2.846×10^{-4}
6	7, 8	1.626×10^{-4}
7	8, 9	1.138×10^{-4}
8	9, 10	1.138×10^{-4}

0787-040

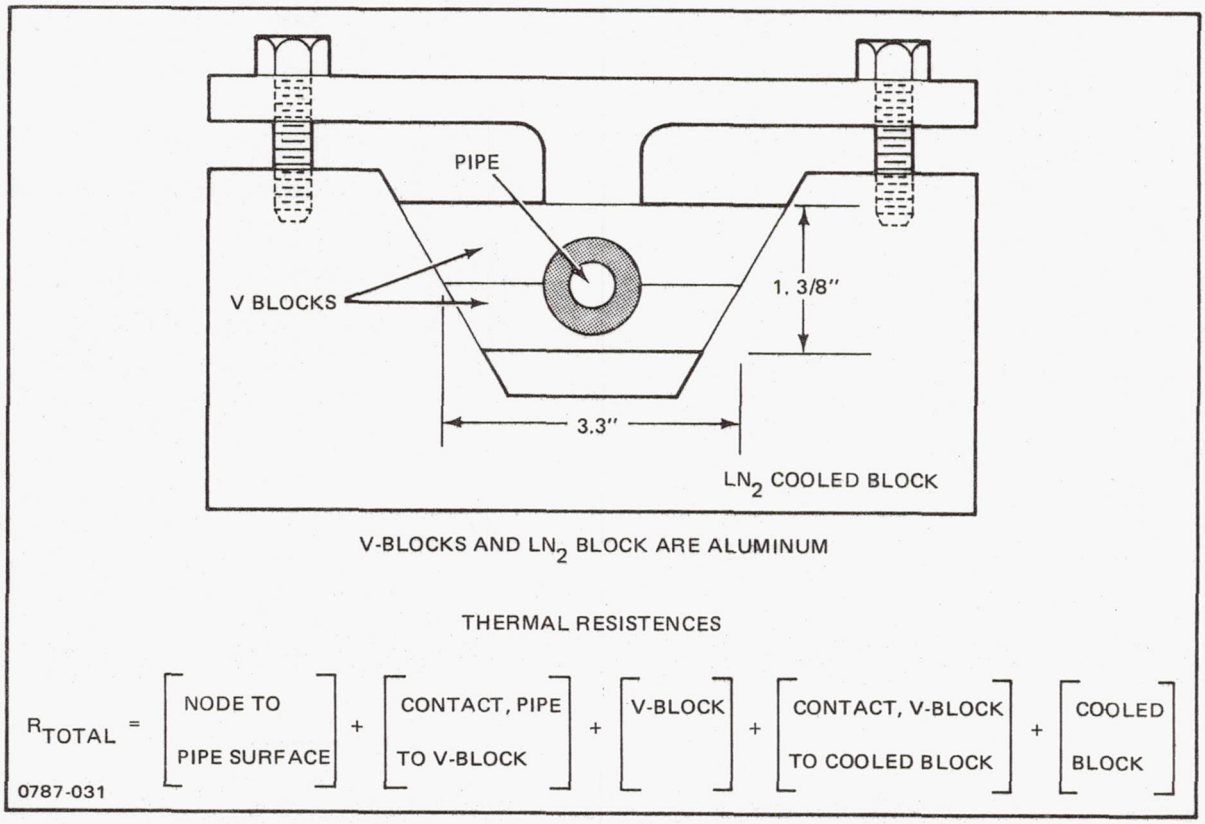

Fig. 6-5 Condenser Cooling Block Schematic

where

L = node longitudinal length - 4 inch

t = pipe wall thickness - .028 inch

D = pipe node to wall mean dia - 0.236 inch

k_{ss} = conductivity of stainless steel - 10 B/hr ft °F

D_o = pipe OD - 0.250 inch

h_o = contact conductance = 1000 B/hr ft^2 °F

S_v = shape factor, V Block = 0.9601

k_{al} = conductivity of aluminum = 100 B/hr ft °F

y = height of V-Block contact = 1.375 inch

x = heat transfer length in LN_2 block = 1 inch

Then, upon substitution of the appropriate values,

$$\frac{1}{K_{i,j}} = \frac{1}{11.0}$$

or

$$K_{i,j} = K_{102,16} = K_{102,17} = 11.0 \text{ B/hr °F}$$

These are conductors 15 and 16.

4) Pipe Wall to Vapor Couplings

The measured film coefficients for evaporation and condensation for ethane at 200 K are 1620 and 2890 Btu/hr ft^2 °F, respectively. The conductance values are then

$$K_{i,j} = h \pi \, d_i \, l_{i,j}$$

e.g.,

$$K_{11,18} = 1620 \times \pi \left(\frac{0.194}{12} \right) \frac{2}{12} = 13.7 \text{ Btu/hr °F}$$

For the adiabatic section, the wall will in general be hotter than the vapor, and dry, since there is no wicking between wall and artery in this region. For laminar vapor flow, the film coefficient is estimated to be 11 Btu/hr ft^2 °F.

The resulting wall to vapor couplings are given in Table 6-4.

5) Vapor Space to Artery Couplings

Evaporation or condensation may take place at the artery surface, with film coefficients representative of the thermal resistance of the liquid layer between the artery node and the artery surface. The conductance is then

$$K_{i,j} = K_l \frac{\pi D_{art} l_{i,j}}{t_l}$$

The thickness of the liquid layer is estimated as one layer of screening (since the outer sheath of the artery is 2 layers thick). Then, e.g.,

$$K_{18,25} = 0.0797 \frac{\pi(0.112)}{0.0026} \frac{2}{12} = 1.798 \text{ Btu/hr } ^\circ\text{F}$$

The set of resulting values is given in Table 6-5.

6) Artery Gap to Screen Couplings

Within the artery, the coupling between the vapor filled gap regions (node 32) and the spiral screening is based on the thermal resistance of one layer of screening. The area is based on a gap width inside the artery of 0.318 inch (assuming only the outer surface of the gap is effective for heat transfer), and the length of each porous screening node.

$$K_{i,j} = k_l \frac{w l_i}{t}$$

e.g.,

$$K_{25,32} = 0.0797 \times \frac{0.318\ (2)}{(.0026)\ (12)} = 1.635 \text{ B/hr } ^\circ\text{F}$$

The set of resulting values is given in Table 6-6.

7) Vapor Flow Couplings

For any vapor node, the vapor pressure is set equal to the saturation pressure corresponding to the temperature of the node. The flow rate of vapor between any two adjacent nodes, assuming laminar flow, is then

Table 6-3 Pipe Wall Conduction Couplings

NO.	NODES COUPLED	K_{ij} BTU/HR ^{o}F
9	11, 12	8.137×10^{-3}
10	12, 13	4.650×10^{-3}
11	13, 14	3.255×10^{-3}
12	14, 15	3.255×10^{-3}
13	15, 16	3.616×10^{-3}
14	16, 17	4.068×10^{-3}
0787-042		

Table 6-4 Wall to Vapor Couplings

NO.	NODES COUPLED	K_{ij} BTU/HR ^{o}F
17	11, 18	13.7
18	12, 19	13.7
19	13, 20	0.236
20	14, 21	0.236
21	15, 22	0.236
22	16, 23	48.9
23	17, 24	48.9
0787-043		

Table 6-5 Vapor to Artery Conductance Couplings

NO.	NODES COUPLED	K_{ij} BTU/HR ^{o}F
24	18, 25	1.798
25	19, 26	1.798
26	20, 27	4.494
27	21, 28	4.494
28	22, 29	4.494
29	23, 30	3.595
30	24, 31	3.595
0787-044		

$$m_{i,j} = \frac{A_v D_v^2}{2 (f N_R)} \left(\frac{\bar{\rho}_v G_c}{\mu_v} \right) \left(\frac{P_{v_i} - P_{v_j}}{L_{i,j}} \right)$$

where

A_v = vapor flow area

D_v = hydraulic diameter of vapor space

f = friction factor (shear stress/dynamic head)

N_R = Reynolds Number

$\bar{\rho}_v$ = Mean vapor density for nodes i, j

$\bar{\mu}_v$ = Mean vapor viscosity for nodes i,j

g_c = gravitational constant

P_{v_i}, P_{v_j} = vapor pressure for nodes i, j

L_{i_j} = distance between node centers for nodes i, j

As written, $m_{i,j}$ is positive for flow from i to j and negative for the reverse. The heat flux associated with this mass flux is

$$\dot{Q}_{i,j} = \bar{h}_{f_g} \dot{m}_{i,j}$$

where $\bar{h}_{f_g}$ = mean latent heat for nodes i,j

In terms of conductance, $K_{i,j}$

$$\dot{Q}_{i,j} = K_{i,j} (T_i - T_j)$$

The pressure and temperature differences are generally very small. To avoid numerical accuracy problems, the approximate form of the Clausius-Clapeyron relation is used:

$$\frac{P_{v_i} - P_{v_j}}{T_i - T_j} = \left(\frac{d P_v}{dT} \right)_{i,j} = \frac{\bar{\rho}_v \bar{h}_{fg}}{\bar{T}_{i,j}} J$$

where J = mechanical equivalent of heat (778 ft-lbs/Btu)

and $T_{ij} = (T_i + T_j)/2$

Also defining

$$k_{i,j} = \frac{A_v D_v^2}{2(fN_R)} \frac{g_c}{L_{i,j}}$$

we can write:

$$K_{i,j} = k_{i,j} \left(\frac{\rho_v \bar{h}_{fg}}{\mu_v} \right) \left(\frac{dP_v}{dT} \right)_{i,j}$$

Values for $k_{i,j}$ are input as initial values for the $K_{i,j}$ couplings. The CLC1 subroutine saves all the initial conductor coupling values, and recomputes new $K_{i,j}$ values for the latest set of temperatures in the nodal solution.

In evaluating the $k_{i,j}$, the vapor space area is the annullar area between wall and artery, less the web cross-sectional area, the hydraulic diameter is taken as twice the annulus area, and the fN_R product for laminar flow is taken as 23.8. Then evaluating, for example, $k_{18,19}$:

$$k_{18,19} = \frac{(.01575/144)\ (.082/12)^2}{2\ (23.8)} \frac{(4.18 \times 10^8)}{(2/12)} = 0.2691 \frac{lb_m - ft^4}{lb_f - hr^2}$$

Values for the $k_{i,j}$ are given in Table 6-7.

Liquid Flow Conduction Couplings

The liquid couplings are one-way conductors, identified in the nodal model by inserting a minus sign in front of the upstream node number. The heat conducted may be written

$$\dot{Q}_{-i,j} = K_{-i,j} (T_i - T_o) = \dot{m}_{-i,j} C_{P_l} (T_i - T_j)$$

whence $K_{-i,j} = \dot{m}_{-i,j} C_{P_l}$

Where C_{P_l} = liquid specific heat

The liquid mass flow is determined from the vapor mass flow, since the liquid inventory at each node is constant for steady state conditions. For example:

$$\dot{m}_{-25,11} = \dot{m}_{11,18}$$

That is, the liquid flow from the artery node 25 to evaporator node 18 must equal the evaporation at evaporator node 18.

Table 6-6 Artery Gap to Screen Couplings

NO.	NODES COUPLED	K_{ij} BTU/HR ^{o}F
31	25, 32	1.635
32	26, 32	1.635
33	27, 32	4.07
34	28, 32	4.07
35	29, 32	4.07
36	30, 32	3.27
37	31, 32	3.27
0787-045		

Table 6-7 Vapor Passage Couplings, $K_{i,j}$

CONDUCTOR NO.	NODES COUPLED	$K_{i,j}$ (LBM FT^4/LB HR^2)
38	18, 19	0.2691
39	19, 20	0.1538
40	20, 21	0.1076
41	21, 22	0.1076
42	22, 23	0.1196
43	23 24	0.1345
0787-046		

Then since

$$\dot{m}_{11,18} = \frac{\dot{Q}_{11,18}}{h_{f_g}} = \frac{K_{11,18}\ (T_{11} - T_{18})}{h_{f_g}}$$

$$K(53) = K_{-25,11} = C_2\ K_{11,18}\ (T_{11} - T_{18})$$

where $C_2 = C_{P_l}/h_{f_g}$

Similarly, conserving mass at 12,

$$K(52) = K_{-26,12} = C_2\ K_{12,19}\ (T_{12} - T_{19})$$

For flow along the artery from node 26 to node 25, conservation of mass at node 25 gives:

$$K(51) = K_{-26,25} = K_{-25,11} + C_2 \left[K(24)\ (T_{25} - T_{18}) + K(31)\ (T_{25} - T_{32}) \right]$$

where the extra terms account for evaporative flow to the vapor space and gap. Similar expressions conserving mass at nodes 26, 27, 28, and 29 (in sequence) are:

$$K(50) = K_{-27,26} = K(51) + K(52) + C_2 \left[K(25)\ (T_{26} - T_{19}) + K(32)\ (T_{25} - T_{32}) \right]$$

$$K(49) = K_{-28,27} = K(50) + C_2 \left[K(26)\ (T_{27} - T_{20}) + K(33)\ (T_{26} - T_{32}) \right]$$

$$K(48) = K_{-29,28} = K(49) + C_2 \left[K(27)\ (T_{28} - T_{21}) + K(34)\ (T_{27} - T_{32}) \right]$$

$$K(47) = K_{-30,29} = K(48) + C_2 \left[K(28)\ (T_{29} - T_{22}) + K(35)\ (T_{28} - T_{32}) \right]$$

The liquid flow from the condenser wall to the artery is assumed to be the same for each condenser node (since the condenser nodes could exchange liquid between themselves), giving

$$K(45) = K_{-16,30} = \frac{C_2}{2} \left[K(22)\ (T_{23} - T_{16}) + K(23)\ (T_{24} - T_{17}) \right]$$

and $K(44) = K_{-17,31} = K(45)$

Then a mass balance at node 30 gives

$$K(46) - K_{-31,30} = K(47) - K(45) + C_2 \left[K(29)\ (T_{30} - T_{23}) + K(36)\ (T_{30} - T_{32}) \right]$$

These couplings are recalculated with each iteration in the nodal model solution. Initial values of 1.0 are input for each liquid flow coupling for data handling purposes, but these are replaced by computed values during the first iteration.

Computer Program

The computer program used in this analysis is a large general purpose nodal program called T-15 - Transient Thermal Analyzer. T-15 contains a number of subroutines, including STEADY, which iteratively determines temperature distributions at steady state. T-15 also provides subroutine CLCI called during each iteration and subroutine CLC2, called after determination of a steady state solution. These subroutines can be used to update the nodal model or perform any auxiliary operations desired by the user.

For this artery priming study, the CLCI subroutine was used to perform the following operations:

1) Store the initial data set of conductance coupling values, for possible use later in the calculation

2) Modify couplings as required for parametric studies (vapor flow resistance, MLI conductance parallel to the lamination, and MLI effective emittance)

3) Calculate latest values for temperature dependent couplings (MLI parallel conductances, MLI normal emittance, vapor conductance, fluid conductors) during the iteration for the steady state temperature distribution

4) Calculate the priming head at the condenser end of the artery, with a statement "Artery primes in 1-G" printed out. This is not the real test of priming (which is made in subroutine CLC2), but it does provide evidence of each pass through CLCI during the calculation.

The operations performed by the CLC2 subroutine are:

1) Verification that priming can start at the condenser end of the artery

2) Determination of artery permeability for liquid pressure drop calculations

3) Modification of the nodal model to reflect filling of the artery node at the condenser end of the pipe (node 31) with liquid. This involves setting the coupling between this node and the gap (coupling 37) to zero, and reducing the coupling to the vapor space (coupling 30) to reflect the increased liquid thickness.

4) Recalculation of the steady state solution and printing the result

5) Calculation of the priming head in 1-g, allowing for the liquid pressure drop in the liquid filled artery node, and printing whether or not priming of node 30 can take place with node 31 filled

6) If priming can take place, the couplings between node 30 and the gap and vapor space are modified as in step (3) above to reflect node 30 filled with liquid, and the calculations of steps (4) and (5) are repeated. This process is similarly repeated in sequence for priming of nodes 29 down to 25. If node 25 can fill with liquid in 1-g, the entire artery is primed

7) If priming in 1-g cannot occur at any of the nodes from 31 to 25, the gravity head (liquid density times the gap height above the bottom of the pipe) is removed to see if priming can occur in o-g

8) If priming can occur in o-g, the node is assumed to fill with liquid, the couplings are adjusted as in step (3) above, a statement is printed out that priming in o-g can occur, and steps 4-7 are repeated. If node 25 can fill with liquid in o-g, the entire artery is primed

9) If priming cannot occur in 1-g, following the o-g priming caluclations, the evaporator heat flux is reduced (by an amount specified, in watts, as dummy conductor 127) and the entire sequence of steps (1) thru (8) is repeated.

Subroutines CLC1 and CLC2 are included in Appendix B.

Analytic Results

The computer nodal model previously described was run for off-design variations of three parameters; wick permeability C(124), MLI effective emittance C(123), and MLI parallel conductivity C(126). Wick permeability was found to have a direct influence on the ability of the artery to prime itself when under load. As seen in Figure 6-6, the maximum evaporator heat load under which the artery will still prime (i.e., maximum priming load) changes nearly linearly with wick permeability. The nominal artery design (normalized permeability = 1.0) has a maximum priming load of 5 watts, which decreases to under 3.5 watts at 75% of the design value. This type of performance is consistent with observed test results. Figure 6-6 indicates that higher priming loads can be obtained by suitable increases in wick permeability. For instance, doubling the permeability would increase the maximum priming load to about 10 watts. Another point of interest is that the o-g priming load is only 1/2 watt higher than the 1-g value. This means that any artery priming problems which exist in 1-g will not vanish in o-g.

The effect of degradation in MLI performance is to cause the wall temperature in the adiabatic (transport) section to become warmer than the evaporator wall temperature. This can be explained by the fact that the transport section is more poorly coupled to the

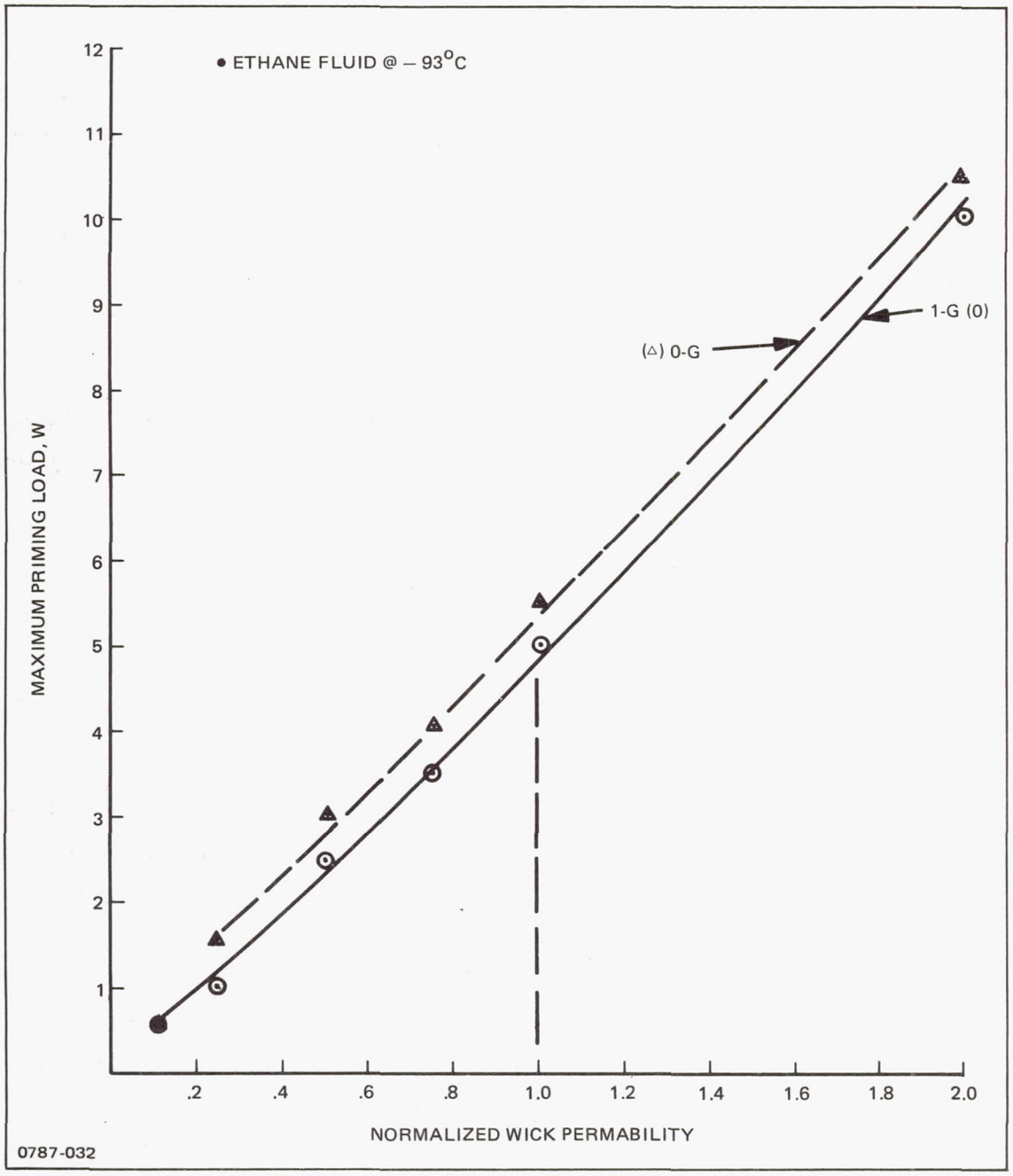

Fig. 6-6 Maximum Heat Pipe Priming Load vs Wick Permeability

condenser section and is therefore more sensitive to changes in MLI conductance which increase the coupling to the surrounding higher temperature ambient. Typical results are summarized below for degraded values of both effective emittance (ϵ_{eff}) and parallel conductivity (ϵ_{11}), using the nominal wick permeability. For these cases, the condenser temperature sink was -93°C.

Normalized MLI Parameter		(Tevaporator - Tadiabatic)° C
ϵ_{eff}	ϵ_{11}	
1.0	1.0	-.23
2.0	1.0	-.148
10.0	1.0	+.096
10.0	10.0	+.423

As seen, with nominal MLI parameters the evaporator is colder than the adiabatic section (ΔT is negative) as would be expected. However, as the MLI degrades the ΔT becomes more positive, which means the adiabatic section is warmer than the evaporator. This curious occurrence has actually been observed during some thermal vacuum tests, which correctly infers that these test articles were poorly insulated.

Conclusions and Recommendations

To permit higher maximum priming loads, the wick permeability must be increased. This can be accomplished by using composite artery wick designs with coarse interior mesh and large flow channels surrounded by the finer screen mesh needed to create the necessary capillary pressure rise. Also, it is recommended that permeability measurements be performed on each artery in addition to the normal capillary rise test which is used to check artery integrity.

6.2 EXPERIMENTAL INVESTIGATION OF SURFACE WETTING

Laboratory tests have been conducted to determine the wettability of ethane with various stainless steel wick samples. This data is considered necessary to help understand and explain priming and transport behavior recently obtained with the subject diode heat pipe.

Ethane wettability was determined by measuring its wicking height at cryogenic temperatures and comparing it with other fluids such as acetone and Freon-113 whose wetting characteristics are well known. The wicking height to which a particular fluid will rise with a square mesh screen wick is given by:

$$h = \frac{2\sigma \cos\theta}{r\rho} \qquad (1)$$

where h = measured wicking height

σ = surface tension

θ = contact angle

r = pore radius of screen opening, taken as one-half of opening

ρ = liquid density

A fluid which has perfect wettability will have a zero contact angle, and therefore, its ideal wicking height, h_i is

$$h_i = \frac{2\sigma}{r\rho}$$

Thus, a measure of wettability of a fluid with a particular wick is its actual wicking height versus its ideal wicking height, or

$$\text{wettability} = h/h_i = \frac{2\sigma \cos\theta / r\rho}{2\sigma/r\rho} = \cos\theta$$

A test rig was designed to allow visual observation of the wicking height (h) which, along with known fluid and wick properties (σ, ρ, r) was used to calculate wettability or $\cos\theta$ from equation (1). The wettability test apparatus is shown in Figure 6-7. It consists of a welded aluminum housing with three flanged ends that provide a leak tight enclosure using O-ring seals. The top flange has a see through glass port for viewing into the chamber. The test sample is held in position directly beneath the view port. One side flange has provision for evacuating the enclosure, introducing charge, and monitoring internal pressure. A cooling coil is wrapped around the chamber to enable it to reach cryogenic temperatures when testing with ethane. Thermocouples on the chamber wall monitor system temperature.

To determine the wicking height, a sample of screen wick about 1 inch (2.54 cm) by 4 inches (10.16 cm) is inserted into the chamber and held in place using a small spring clamp. The long side of the sample is notched every 1/2 inch (1.27 cm) to permit estimation of the wicking height attained. The chamber is then evacuated and cooled to the desired temperature. Next, the test fluid is introduced from a specially prepared charge bottle. The apparatus is tilted horizontally until the entire sample is wet with fluid and then set in the vertical position and allowed to stand until the wetted height reaches equilibrium (see Figure 6-8). The bottom of the wick is always in contact with fluid which will rise to a

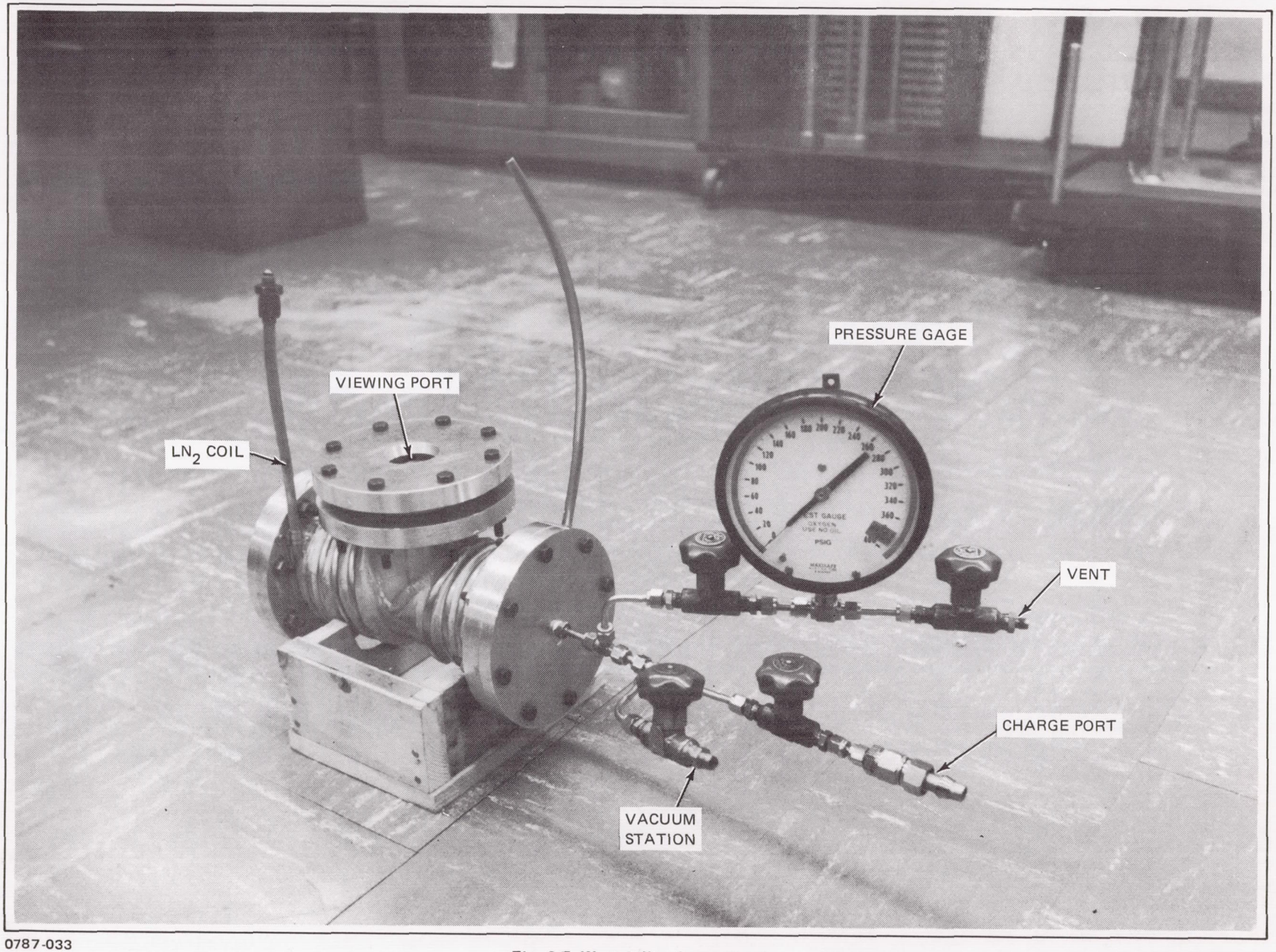

0787-033

Fig. 6-7 Wettability Apparatus

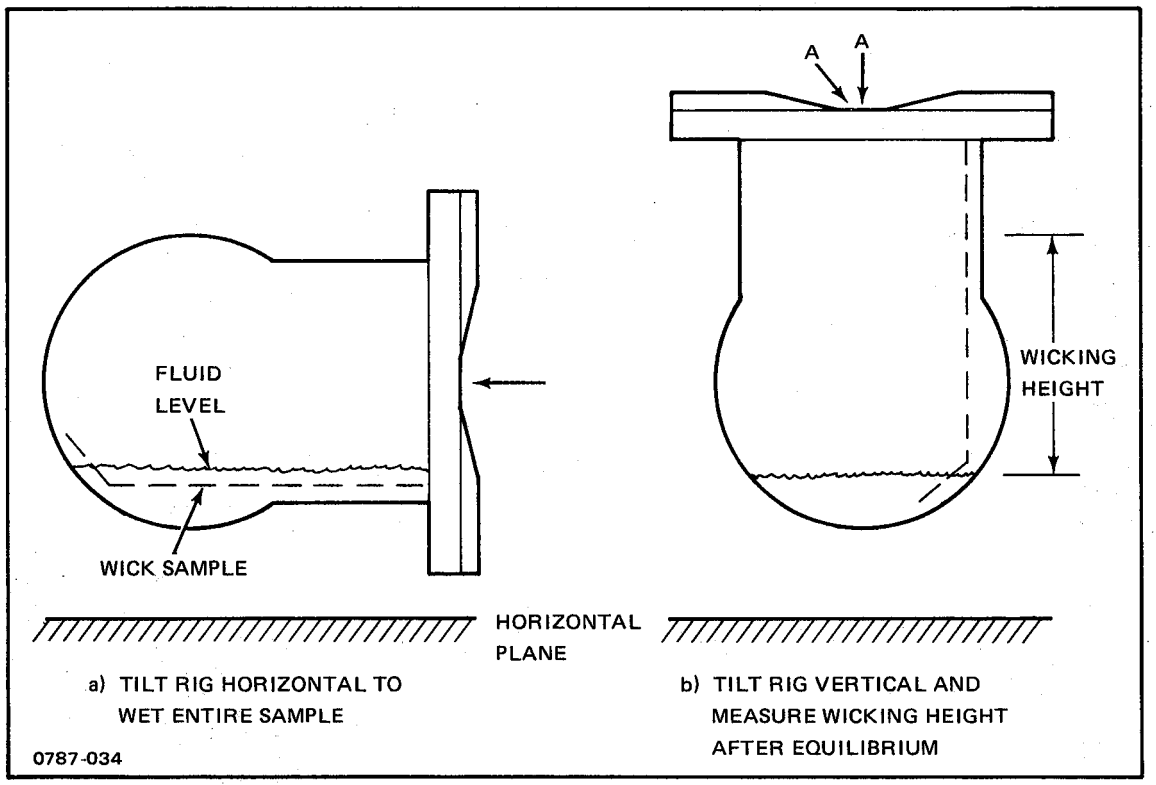

Fig. 6-8 Test Procedure

particular height on the wick according to its wettability. By shining a narrow beam of light through the viewing port, the darker wetted height can be discerned from the lighter unwetted region and its height gaged by the 1/2 inch (1.27 cm) marks along the sample.

A description of the wick sample used is given in Table 6-8. Applicable fluid properties are listed in Table 6-9 for the three fluids tested. Freon-113, acetone and ethane.

Test results showing observed wicking heights and calculated wettability, i.e., cos θ, are presented in Table 6-10. Because the test rig was designed to provide only an approximate measurement of wicking height the values shown in Table 6-10, which are accurate to ± 0.64 cm, should be treated as a qualitative comparison between the test fluids. From the results it is clear that ethane has the same wetting characteristics as Freon-113 and acetone with respect to stainless steel screen. A wicking height of 1.5 in. (3.81 cm) was observed for ethane, which indicates a wettability factor of about 0.5, comparable to that of Freon-113 and acetone.

It was observed during testing with all three fluids that the insertion of part of a dry sample of a single layer of screen into the fluid did not result in the fluid rising up along the wick. Rather it was found that the sample first had to be wet along its length then held vertically with one end in the fluid. In this way, drying would begin at the top of the wick and proceed to a certain point down the wick below which the wick continually remained wet.

The situation in the diode heat pipe is quite different since there are many layers of screen that make up the artery. The gaps formed between these layers promote capillary action that eventually wets the entire wick. Open air bench tests with a multiple layer screen wick dipped in acetone confirmed that the wick will draw fluid up along its length. This self-wetting property was also demonstrated with the multiple layer screen wick and ethane fluid using the test apparatus.

Table 6-8 Wick Sample Characteristics

TYPE	100 MESH STAINLESS STEEL
CONSTRUCTION	SINGLE LAYER 1 BY 4 INCH (2.54 cm BY 10.16 cm)
WIDTH OF OPENING, INCH (mm)	0.0055 (0.1397)
r, PORE RADIUS, INCH (mm)	0.00275 (0.0699)
CLEANING	PASSIVATED

0787-047

Table 6-9 Fluid Properties

FLUID	FREON-113	ACETONE	ETHANE
TEMP ^{o}F (K)	86^{o} (303 K)	70^{o}F (294 K)	-120^{o}F (189 K)
DENSITY, LB/FT^{3}	97	48.9	34
SURFACE TENSION LBF/FT	0.0013	0.00155	0.00106

0787-048

Table 6-10 Wettability Test Results

	TEMP ^{o}F (K)	WICK SAMPLE 100 MESH PASSIVATED
• WICKING HEIGHT, INCHES (cm)		
– FREON 113	70 (294)	0.75 (1.91)
– ACETONE	70 (294)	1.75 (4.45)
– ETHANE	-123 (187)	1.5 (3.81)
• WETTABILITY FACTOR COS θ		
– FREON 113	70 (294)	0.53
– ACETONE	70 (294)	0.53
– ETHANE	-123 (187)	0.46

0787-049

Section 7

CONCLUSIONS

The development of spiral artery cryogenic thermal diodes has been advanced to include the following accomplishments:

- A liquid blockage (blocking orifice) design was built and qualified for the HEPP spaceflight experiment
- A liquid trap engineering model was built and tested. Throughput (w-m) and forward mode conductance was similar to the liquid blockage design but reverse mode conductance and shutdown energy were higher
- An analytical and experimental investigation of the startup dynamics of steel/ethane heat pipes with spiral artery wicks revealed that wick permeability is an important influence on the maximum heat load permitted during startup. Higher initial heat load capability (priming load) can be obtained by increasing the wick permeability.

A modified composite artery wick should be built to evaluate design improvements aimed at increasing the priming heat load capability. It would include a coarse interior screen with relatively large and uniform gaps (for increased permeability), surrounded by a closure wrap of very fine pore screening (for maximum capillary pressure rise).

Section 8

REFERENCES

1. Kosson, R., Quadrini, J. and Kirkpatrick, J., "Development of a Blocking Orifice Thermal Diode Heat Pipe," AIAA Paper 74-754

2. Quadrini, J., and McCreight, C.R., "Development of a Thermal Diode Heat Pipe for Cryogenic Applications," AIAA Paper 77-192

3. Williams, R.J., "Parametric Performance of a Spiral-Artery Liquid Trap Diode Heat Pipe," NASA TM-78,448, October 1977

4. Quadrini, J., "Design and Performance of a Cryogenic Thermal Diode," Memo TLM-76-012, March 1976

5. Androulakis, J., Grumman Advanced Development Report ADR-04-02-70.1

Appendix A

HEPP Liquid Blockage Thermal Diode, Computer Model

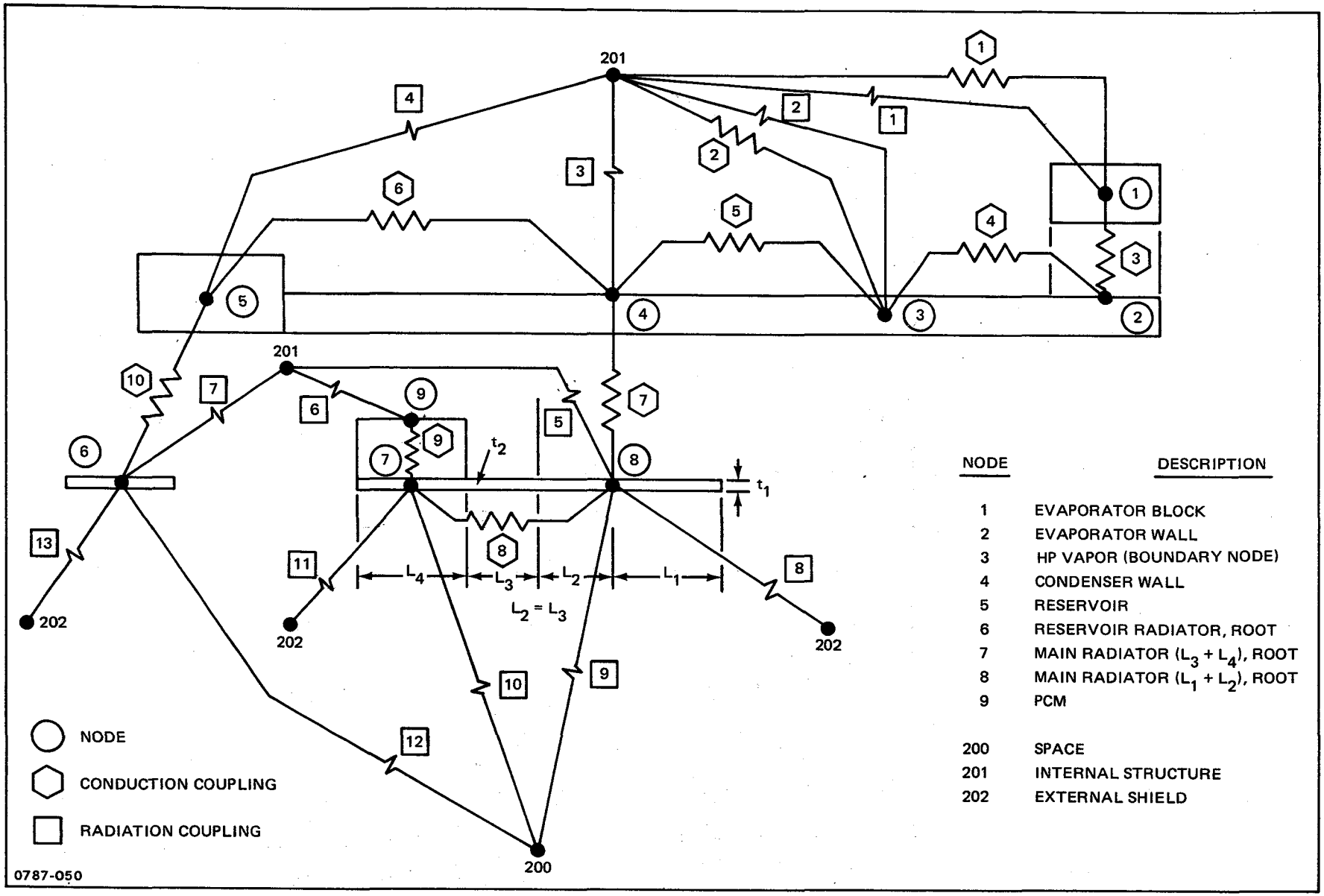

Figure A1. HEPP Cryo-Diode Network

MASS CAPACITANCE

NODE NUMBER	THERMAL MASS	
	(BTU/^{o}F)	(WATT-HR/^{o}C)
1	.0870	.0459
2	.00557	.00294
4	.0324	.0171
5	.0160	.00844
6	.0217	.0114
7	.078	.0411
8	.174	.918
9	.72 (SOLID)	.38
	108.6 (MELT)	57.26
	.956 (LIQUID)	.504

CONDUCTION			
COUPLING NUMBER	JOINING NODES	COUPLING VALUE	
		(BTU/HR ^{o}F)	(WATTS/^{o}C)
1	1-201	1.254×10^{-4}	6.614×10^{-5}
2	3-201	4.854×10^{-4}	2.560×10^{-4}
3	1-2	20.480	10.801
4	2-3	27.4	14.45
5	3-4	311.0	164.02
6	4-5	.773	.408
7	4-8	46.9	24.73
8	7-8	1.44	.759
9	9-7	10.000	5.274
10	5-6	2.75	1.45
RADIATION			
		(BTU/HR $^{o}R^{4}$)	(WATTS/$^{o}K^{4}$)
1	1-201	2.242×10^{-12}	6.89×10^{-12}
2	3-201	6.18×10^{-12}	1.9×10^{-12}
3	4-201	3.259×10^{-12}	10.02×10^{-12}
4	5-201	1.051×10^{-12}	3.233×10^{-12}
5	8-201	18.6×10^{-12}	57.2×10^{-12}
6	9-201	5.044×10^{-12}	15.51×10^{-12}
7	6-201	1.607×10^{-12}	4.943×10^{-12}
8	8-202	9.62×10^{-12}	2.96×10^{-12}
9	8-200	9.52×10^{-10}	29.3×10^{-10}
10	7-200	6.86×10^{-10}	21.1×10^{-10}
11	7-202	6.93×10^{-12}	21.3×10^{-12}
12	6-200	94.1×10^{-12}	2.89×10^{-10}
13	6-202	$.95 \times 10^{-12}$	2.92×10^{-12}

INPUT VARIABLE	DEFINITION
T(231)	RESERVOIR RADIATOR FIN LENGTH (IN)
T(232)	RESERVOIR RADIATOR SURFACE AREA (IN^2)
T(233)	RESERVOIR RADIATOR FIN THICKNESS (IN)
T(234)	PCM RADIATOR AREA (FOR L_4) (IN^2)
T(236)	PCM RADIATOR FIN LENGTH (L_3) (IN)
T(237)	PCM RADIATOR FIN THICKNESS (IN)
T(238)	PCM RADIATOR AREA (FOR L_3) (IN^2)
T(239)	DIODE RADIATOR AREA (FOR L_2) (IN^2)
T(241)	DIODE RADIATOR FIN LENGTH (L_2) (IN)
T(242)	DIODE RADIATOR THICKNESS (IN)
T(244)	DIODE RADIATOR FIN LENGTH (FOR L_1) (IN)
T(245)	DIODE RADIATOR AREA (FOR L_1) (IN^2)
T(246)	PCM RADIATOR FIN LENGTH (L_4) (IN)
T(247)	WIDTH OF PCM AND DIODE RADIATORS (IN)
T(248)	RESERVOIR RADIATOR EMITTANCE
T(249)	PCM AND DIODE RADIATOR EMITTANCE
T(250)	T1, LOWER LIMIT OF MELT RANGE (^oF)
T(251)	T2, UPPER LIMIT OF MELT RANGE (^oF)
T(252)	LATENT HEAT OF PCM (BTU/LBM)
T(253)	MASS OF PCM MATERIAL (LBM)
T(254)	CP (SOLID) (BTU/LB ^oF)
T(255)	$RAT1 = \frac{CP\ (LATENT)}{CP(SOLID)}$
T(256)	$RAT2 = \frac{CP\ (LATENT)}{CP\ (LIQUID)}$
T(257)	CHECK VALUE TO DETERMINE WHAT CP TO USE (CPMCK) (BTU/^oF)
T(260)	FRACTION OF PCM REMAINING
T(261)	WATT-HOURS REMAINING
T(263)	CAP(9) – INITIAL VALUE
T(262)	COUNTER (MUST INITIALIZE TO 0.0)
T(264	OPTION CODE FOR HEATER ROUTINES +1 ACCEPTS HEATER CYCLING ROUTINE 0 REJECTS BOTH OPTIONS -1 ACCEPTS DUTY CYCLE ROUTINE
T(271)	% DUTY CYCLE ON PCM
T(272)	TIME SPAN FOR PCM (SEC)
T(273)	% DUTY CYCLE ON RESERVOIR
T(274)	TIME SPAN FOR RESERVOIR (SEC)

OUTPUT VARIABLE	DEFINITION
T(205)	HEAT INPUT TO THE PCM (BTU/HR)
T(206)	HEAT INPUT TO THE RESERVOIR (BTU/HR)
T(208)	NET HEAT AT DIODE PIPE (BTU/HR)
T(209)	CURRENT MASS IN RESERVOIR (GMS)
T(210)	MASS IN BLOCKED SECTION (GMS)
T(211)	EVAPORATOR LENGTH (INCHES)
T(212)	BLOCKED LENGTH (INCHES)
T(214)	CONDUCTANCE BETWEEN EVAPORATOR & CONDENSER (BTU/HR^{o}F)
T(215)	LATENT HEAT OF WORKING FLUID (BTU/LBM)
T(216)	LIQUID DENSITY OF WORKING FLUID (LBM/FT^{3})
T(217)	δ MASS IN RESERVOIR (GMS)
T(220)	EVAPORATOR TEMPERATURE RATE OF CHANGE (^{o}F/HR)
T(221)	PCM TEMPERATURE RATE OF CHANGE (^{o}F/HR)
T(222)	CONDENSER TEMPERATURE RATE OF CHANGE (^{o}F/HR)
T(223)	RESERVOIR TEMPERATURE RATE OF CHANGE (^{o}F/HR)
T(226)	REVERSE MODE ENERGY (WATT-HRS)
T(227)	% RESERVOIR CHARGE REMAINING
T(228)	OUTPUT INTERVAL (HRS)
T(229)	PREVIOUS PRINTOUT TIME (SEC)
T(230)	FIN EFFECTIVENESS FOR RESERVOIR RADIATOR
T(235)	FIN EFFECTIVENESS FOR L_3 PORTION OF PCM RADIATOR
T(240)	FIN EFFECTIVENESS FOR DIODE RADIATOR FOR L_2
T(243)	FIN EFFECTIVENESS FOR DIODE RADIATOR FOR L_1

```
      SUBROUTINE CLC1                                                    TTA00010
C  THIS SUBROUTINE IS CALLED AT THE START OF EVERY ITERATION             TTA00020
      COMMON   STG(5000), NPOS(50), L1(50), L2(50), NLAST(50), FCT(50)   TTA00030
      COMMON KILL,NTABS,NMTRIC,METPR,IHEAT,SIG,XJ1,XJ2,XJ3               TTA00040
      COMMON   BUFF(20),T(1000),CAP(1000),COND(2000),RAD(2000),Q(100),   TTA00050
     1    NCOND(2,2000),NRAD(2,2000),NIN(1000),NBN(250),KEY(5),NQ(100),  TTA00060
     2    KAY(4),FLUX(1000)                                              TTA00070
      COMMON         TIME,     DTIME,    FTIME,    DUM,                  TTA00080
     1    KNIN,     KNBN,     N4,       N5,       KODE,     KNQ,        TTA00090
     2    KOUT,     KOUNT,    NOSRT                                      TTA00100
C REVISED TIROS-N CRYO EXPERIMENT NETWORK                                TTA00110
      IF(TIME.GT.0.0) GO TO 132                                          TTA00120
      SUMQ=1.0                                                           TTA00130
      BKL=0.0                                                            TTA00140
      HPCOND=25.18                                                       TTA00150
      XLAT=1.0                                                           TTA00160
      RHOL=1.0                                                           TTA00170
      AK=0.0                                                             TTA00180
  132 AX=TIME-AK*1.667                                                   TTA00190
      IF(AX.LT.1.667) GO TO 133                                          TTA00200
      AK=AK+1.0                                                          TTA00210
  133 IF(AX.LE.0.56335) GO TO 134                                        TTA00220
      Q(4)=0.0                                                           TTA00230
      Q(5)=0.0                                                           TTA00240
      GO TO 135                                                          TTA00250
  134 Q(4)=.417*T(232)*SIN(5.5738*AX)                                    TTA00260
      Q(5)=.417*(T(239)+T(245))*SIN(5.5738*AX)                           TTA00270
  135 T(230)=TANH(2.390E-06*T(231)*(T(248)*((T(6)+460.)**3)/T(233))**.5)TTA00280
     A/(2.390E-06*T(231)*(T(248)*((T(6)+460.)**3)/T(233))**.5)           TTA00290
      RAD(12)=1.061E-11*(T(232)*T(230))                                  TTA00300
      RAD(13)=1.071E-13*(T(232)*T(230))                                  TTA00310
      T(240)=TANH(2.390E-06*T(241)*(T(249)*((T(8)+460.)**3)/T(242))**.5)TTA00320
     C/(2.390E-06*T(241)*(T(249)*((T(8)+460.)**3)/T(242))**.5)           TTA00330
      T(243)=TANH(2.390E-06*T(244)*(T(249)*((T(8)+460.)**3)/T(242))**.5)TTA00340
     D/(2.390E-06*T(244)*(T(249)*((T(8)+460.)**3)/T(242))**.5)           TTA00350
      RAD(8)=9.522E-14*(T(239)*T(240)+T(243)*T(245))                     TTA00360
      RAD(9)=9.427E-12*(T(239)*T(240)+T(243)*T(245))                     TTA00370
      RAD(5)=1.785E-13*(T(245)+T(239))                                   TTA00380
      RAD(7)=1.735E-13*T(232)                                            TTA00390
      CAP(6)=.0214*(T(232)*T(233))                                       TTA00400
      CAP(8)=.0214*((T(245)+T(239))*T(242)+2.906)                        TTA00410
C     T(3)=(COND(4)*T(2)+COND(5)*T(4)+COND(2)*T(201)+RAD(2)*((T(201)+460TTA00420
C    A.)**4))/(COND(4)+COND(5)+COND(2)+(RAD(2)*((T(201)+460.)**3)))      TTA00430
      IF(T(264))401,400,402                                              TTA00440
  401 CYCLE=TIME*3600./T(272)                                            TTA00450
      ICYCLE=CYCLE                                                       TTA00460
      CYTIME=CYCLE-ICYCLE                                                TTA00470
      IF(CYTIME-T(271))403,403,404                                       TTA00480
  403 Q(1)=T(269)                                                        TTA00490
      GO TO 405                                                          TTA00500
  404 Q(1)=0.0                                                           TTA00510
  405 RYCLE=TIME*3600./T(274)                                            TTA00520
      IRYCLE=RYCLE                                                       TTA00530
      RYTIME=RYCLE-IRYCLE                                                TTA00540
      IF(RYTIME-T(273))406,406,407                                       TTA00550
```

```
  406 Q(2)=T(270)                                                          TTA00560
      GO TO 400                                                            TTA00570
  407 Q(2)=0.0                                                             TTA00580
      GO TO 400                                                            TTA00590
  402 IF(T(4).LT.T(265)) Q(1)=T(269)                                       TTA00600
      IF(T(4).GE.T(265).AND.T(4).LE.(T(265)+T(266))) Q(1)=Q(1)             TTA00610
      IF(T(4).GT.(T(265)+T(266))) Q(1)=0.0                                 TTA00620
      IF(T(5).LT.T(267)) Q(2)=T(270)                                       TTA00630
      IF(T(5).GE.T(267).AND.T(5).LE.(T(267)+T(268))) Q(2)=Q(2)             TTA00640
      IF(T(5).GT.(T(267)+T(268))) Q(2)=0.0                                 TTA00650
  400 T(205)=Q(1)                                                          TTA00660
      T(206)=Q(2)                                                          TTA00670
      RES1=1.376/453.5924                                                  TTA00680
      EVPL=4./12.                                                          TTA00690
      IF(BKL.GT.0.0) GO TO 600                                             TTA00700
      COND(4)=27.4                                                         TTA00710
      COND(5)=311.0                                                        TTA00720
      HPCOND=1./((1./COND(4))+(1./COND(5)))                                TTA00730
  600 IF(TIME.GT.0.) GO TO 150                                             TTA00740
      T20=T(2)                                                             TTA00750
      T90=T(9)                                                             TTA00760
      T40=T(4)                                                             TTA00770
      T50=T(5)                                                             TTA00780
      QREV=0.                                                              TTA00790
  150 IF(T(3).GT.T(2)) GO TO 100                                           TTA00800
      BLKM=0.                                                              TTA00810
      BKL=0.                                                               TTA00820
      DREM=0.                                                              TTA00830
      RESM=RES1                                                            TTA00840
      GO TO 14                                                             TTA00850
  100 IF(RESM.GT.0.) GO TO 200                                             TTA00860
      DREM=0.                                                              TTA00870
      RESM=0.0                                                             TTA00880
      BLKM=RES1                                                            TTA00890
      IF(T(4).LT.T(2)) GO TO 14                                            TTA00900
      GO TO 8                                                              TTA00910
  200 T5R=460.+T(5)                                                        TTA00920
      T201R=460.+T(201)                                                    TTA00930
      SUMQ=Q(4)-RAD(4)*(T5R**4.-T201R**4.)-COND(10)*(T(5)-T(6))            TTA00940
      TT=T(5)                                                              TTA00950
      XLAT=PROP(6.6,TT)                                                    TTA00960
      RHOL=PROP(1.6,TT)                                                    TTA00970
      DREM=(SUMQ*DTIME-CAP(5)*(T(5)-T50))/XLAT                             TTA00980
      RESM=RESM-DREM                                                       TTA00990
      BLKM=BLKM+DREM                                                       TTA01000
    8 IF(BLKM.LT.0.0) BLKM=0.0                                             TTA01010
      BKL=BLKM/(RHOL*1.2566E-4)                                            TTA01020
      IF(BKL.LT.0.0) BKL=0.0                                               TTA01030
      IF(BKL.LT.EVPL) GO TO 300                                            TTA01040
      BKLT=BKL-EVPL                                                        TTA01050
      IF(T(4).LE.T(2)) GO TO 14                                            TTA01060
      COND(4)=9.155E-04                                                    TTA01070
      COND(5)=174.0                                                        TTA01080
      QREV=9.155E-04*(T(4)-T(2))+QREV                                      TTA01090
      GO TO 14                                                             TTA01100
```

```
  300 IF(T(4).LE.T(2)) GO TO 14                                          TTA01110
      HPCOND=27.40*(1.-12.*BKL/4.)+SQRT(.01276*BKL)*TANH(112.97*BKL)     TTA01120
      COND(4)=HPCOND                                                     TTA01130
      COND(5)=174.0                                                      TTA01140
      QREV=HPCOND*(T(4)-T(2))+QREV                                       TTA01150
   14 CONTINUE                                                           TTA01160
C PCM CALCULATIONS, T1=LOWER MELT TEMP, T2=UPPER MELT TEMP, XLAT=LAT HT  TTA01170
C SLDST= WT PCM, CPSLD= CP SOLID, RAT1= CP(MELT)  /CP SOLID, RAT2=CP(LQ)TTA01180
C /CP(MELT)  , CPMCK= CP CHECK VALUE, MCP SOLID,MCP(LQ).LT.MCP(MELT)     TTA01190
      COMMON/PCM/ RAT1,T1,T2,CPMCK                                       TTA01200
      CPMCK=T(257)                                                       TTA01210
      T1=T(250)                                                          TTA01220
      T2=T(251)                                                          TTA01230
      RAT1=T(255)                                                        TTA01240
      RAT2=T(256)                                                        TTA01250
      TMID=T1/2. + T2/2.                                                 TTA01260
C T(9)=PCM NODE                                                          TTA01270
      IF(T(9).LT.T1) GO TO 10                                            TTA01280
      IF(T(9).LT.TMID) GO TO 20                                          TTA01290
      IF(T(9).LT.T2) GO TO 30                                            TTA01300
      IF(CAP(9) .GT. CPMCK) CAP(9)=CAP(9)*RAT2                           TTA01310
      GO TO 98                                                           TTA01320
   10 IF(CAP(9) .GT. CPMCK) CAP(9)=CAP(9)/RAT1                           TTA01330
      GO TO 98                                                           TTA01340
   20 IF(CAP(9) .LT. CPMCK) CAP(9)=CAP(9)*RAT1                           TTA01350
      GO TO 98                                                           TTA01360
   30 IF(CAP(9) .LT. CPMCK) CAP(9)=CAP(9)/RAT2                           TTA01370
   98 CONTINUE                                                           TTA01380
    4 T(208)=SUMQ                                                        TTA01390
      T(209)=RESM*453.5924                                               TTA01400
      T(210)=BLKM*453.5924                                               TTA01410
      T(211)=COND(4)                                                     TTA01420
      T(212)=BKL*12.                                                     TTA01430
      T(214)=COND(5)                                                     TTA01440
      T(215)=XLAT                                                        TTA01450
      T(216)=RHOL                                                        TTA01460
      T(217)=DREM*453.5924                                               TTA01470
      T(220)=(T(2)-T20)/DTIME                                            TTA01480
      T(221)=(T(9)-T90)/DTIME                                            TTA01490
      T(222)=(T(4)-T40)/DTIME                                            TTA01500
      T(223)=(T(5)-T50)/DTIME                                            TTA01510
      T(226)=QREV*DTIME/3.413                                            TTA01520
      T(227)=T(209)/(RES1*453.5924)                                      TTA01530
      T(228)=KOUT                                                        TTA01540
      T(229)=TIME*3600.                                                  TTA01550
      T20=T(2)                                                           TTA01560
      T90=T(9)                                                           TTA01570
      T40=T(4)                                                           TTA01580
      T50=T(5)                                                           TTA01590
      T(263)=CAP(9)                                                      TTA01600
      T(234)=Q(4)/3.413                                                  TTA01610
      T(235)=Q(5)/3.413                                                  TTA01620
      RETURN                                                             TTA01630
      END                                                                TTA01640
```

```
FILE0 TCASE1   DATA     P1                    G R U M M A N   D A T A   S Y S T E M S

1. REVISED TRANSIENT MODEL FOR TIROS-N CRYO EXPERIMENT
2.
3.
4.BYBRAZE AT RESERVOIR SADDLE
5. NODE 3 ITERATED
    0    0    1    0
    0 0.0        5.000E-05 5.000E-05
    0     1-9.000E 01     0     0
    0     2-9.000E 01     0     0
    0     3-9.400E 01     0     0
    0     4-9.800E 01     0     0
    0     5-9.800E 01     0     0
    0     6-9.800E 01     0     0
    0     8-9.800E 01     0     0
    0     9-8.000E 01     0     0
11100     0 0.0           0     0
    0   200-4.600E 02     0     0
    0   201 7.000E 01     0     0
    0   202-2.000E 02     0     0
    0   205 0.0           0     0
    0   206 0.0           0     0
    0   208 0.0           0     0
    0   209 0.0           0     0
    0   210 0.0           0     0
    0   211 0.0           0     0
    0   212 0.0           0     0
    0   214 0.0           0     0
    0   215 0.0           0     0
    0   216 0.0           0     0
    0   217 0.0           0     0
    0   220 0.0           0     0
    0   221 0.0           0     0
    0   222 0.0           0     0
    0   223 0.0           0     0
    0   226 0.0           0     0
    0   227 0.0           0     0
    0   228 0.0           0     0
    0   229 0.0           0     0
    0   230 8.000E-01     0     0
    0   231 4.690E 00     0     0
    0   232 22.00E 00     0     0
    0   233 2.000E-02     0     0
    0   234 0.000E 00     0     0
    0   235 0.000E 00     0     0
    0   239 15.00E 01     0     0
    0   240 8.000E-01     0     0
    0   241 8.660E 00     0     0
    0   242 2.000E-02     0     0
    0   243 8.000E-01     0     0
    0   244 8.660E 00     0     0
    0   245 15.00E 01     0     0
    0   248 9.000E-01     0     0
    0   249 9.000E-01     0     0
    0   250-1.315E 02     0     0
    0   251-1.305E 02     0     0
```

```
    0  252 6.030E 01     0     0
    0  253 3.000E 00     0     0
    0  254 4.000E-01     0     0
    0  255 1.508E 02     0     0
    0  256 8.800E-03     0     0
    0  257 1.000E 02     0     0
    0  260 1.000E 00     0     0
    0  261 1.000E 00     0     0
    0  262 0.0           0     0
    0  263 0.0           0     0
    0  264-1.0           0     0
    0  265-9.400E 01     0     0
    0  266 1.800E 01     0     0
    0  267-8.500E 01     0     0
    0  268 1.800E 01     0     0
    0  269 0.000E 02     0     0
    0  270 0.000E 00     0     0
    0  271 4.000E-01     0     0
    0  272 1.000E 01     0     0
    0  273 1.000E 00     0     0
    0  274 1.000E 01     0     0
11100    0 0.0           0     0
    0    1 8.700E-02     0     0
    0    2 5.570E-03     0     0
    0    3 6.150E-02     0     0
    0    4 3.240E-02     0     0
    0    5 5.000E-03     0     0
    0    6 1.000E 00     0     0
    0    8 1.000E 00     0     0
    0    9 1.593E 00     0     0
11100    0 0.0           0     0
    0    1    1  201 1.254E-04     0     0
    0    2    3  201 4.854E-04     0     0
    0    3    1    2 2.048E 01     0     0
    0    4    2    3 27.40E 00     0     0
    0    5    3    4 31.10E 01     0     0
    0    6    4    5 7.730E-01     0     0
    0    7    4    8 4.690E 01     0     0
    0   10    5    6 2.750E 00     0     0
    0   11    8  201 0.0           0     0
    0   13    6  201 0.0           0     0
11100    0    0    0 0.0           0     0
    0    1    1  201 2.242E-12     0     0
    0    2    3  201 6.180E-12     0     0
    0    3    4  201 3.259E-12     0     0
    0    4    5  201 1.051E-12     0     0
    0    5    8  201 1.000E-09     0     0
    0    6    9  201 5.044E-12     0     0
    0    7    6  201 1.000E-09     0     0
    0    8    8  202 1.000E-09     0     0
    0    9    8  200 1.000E-09     0     0
    0   12    6  200 1.000E-09     0     0
    0   13    6  202 1.000E-09     0     0
11100    0    0    0 0.0           0     0
    0    1    9 0.000E 02
```

```
FILE0 TCASE1   DATA      P1                    G R U M M A N   D A T A   S Y S T E M S

    0     2     5 0.000E 00
    0     3     1 0.000E 00
    0     4     6 0.0
    0     5     8 0.0
11100     0     0 0.0
11100     0     0
    0
1.
2.
3.
4.
5.
    0     0 2000     0
    0 0.0         5.000E-05 2.400E 01
    0     1 7.700E 01     0     0
    0     2 7.700E 01     0     0
    0     4 7.700E 01     0     0
    0     5 7.700E 01     0     0
    0     6 7.700E 01     0     0
    0     8 7.700E 01     0     0
    0     9 7.700E 01     0     0
    0     3 7.700E 01     0     0
    0   200-4.600E 02     0     0
    0   201 7.000E 01     0     0
    0   202-2.000E 02     0     0
    0   262 0.0           0     0
11100     0 0.0           0     0
11100     0 0.0           0     0
11100     0     0     0 0.0           0     0
11100     0     0     0 0.0           0     0
11100     0     0 0.0
11100     0     0
11100
```

Appendix B

Subroutines CLC1 and CLC2 for T15 Computer Code (Priming Analysis)

```
      SUBROUTINE CLC1                                                    T1500010
C  THIS SUBROUTINE IS CALLED AT THE START OF EVERY ITERATION             T1500020
      COMMON   STG(5000), NPOS(50), L1(50), L2(50), NLAST(50), FCT(50)   T1500030
      COMMON KILL,NTABS,NMTRIC,METPB,IHEAT,SIG,XJ1,XJ2,XJ3               T1500040
      COMMON   BUFF(20),T(1000),CAP(1000),COND(2000),RAD(2000),Q(100),   T1500050
     1    NCOND(2,2000),NRAD(2,2000),NIN(1000),NBN(250),KEY(5),NQ(100),  T1500060
     2    KAY(4),FLUX(1000),DIS1(2000),DIS2(2000),ISC1(2000),ISC2(2000)  T1500070
      COMMON        TIME,     DTIME,    PTIME,    DUM,                   T1500080
     1    KNIN,     KNBN,     N4,       N5,       KODE,     KNQ,         T1500090
     2    KOUT,     KOUNT,    NOSRT                                      T1500100
      DIMENSION A(43),TB(8),P(10),RHOV(10),XMUV(10),HFG(10)              T1500110
C     COND(54)=PV, SAT. PRESSURE FOR T(24), PSF                          T1500120
C     COND(55)=DELPP, PRESSURE DIFF. AVAILABLE FOR GAP PRIMING, PSF      T1500130
C     COND(56)=RHOL, LIQUID DENSITY OF NODE 28, PCF                      T1500140
C     COND(57)=PGAP, GAP PRESSURE,PSF                                    T1500150
C     COND(58)=PCGAP, CAPILLARY PRESSURE OF GAP, PSF                     T1500160
C     COND(59)= KVAP, FLUID IDENTIFICATION FOR PROP SUBROUTINE           T1500170
C     COND(60)= B, EXPONENT FOR MLI PARALLEL CONDUCTANCE CALC            T1500180
C     COND(61)= CPV, VAPOR SPECIFIC HEAT                                 T1500190
C     COND(62)= CPL, LIQUID SPECIFIC HEAT                                T1500200
C     COND(63)= TGAP, GAP THICKNESS, INCHES                              T1500210
C     COND(64)= HGAP, GAP HEIGHT ABOVE LOW POINT OF CONDENSER            T1500220
C     COND(65)-COND(107)= INITIAL VALUES OF COND 1-43 RESPECTIVELY       T1500230
C     COND(108)=1.01 SKIPS INITIAL BOOKKEEPING                           T1500240
C     COND(109)=T(24)                                                    T1500250
C     COND(110)=T(32)                                                    T1500260
C     COND(118)=DPL, LIQUID PRESSURE DROP, PSF                           T1500270
C     COND(119)=DART, ARTERY O.D., INCHES                                T1500280
C     COND(120)=APOR, POROUS AREA, SQ. IN.                               T1500290
C     COND(121)=DPOR, POROUS MATL. HYD. DIA., INCHES                     T1500300
C     COND(122)=DI, INSIDE DIA. OF PIPE, INCHES                          T1500310
C     KVAP= 6 FOR ETHANE                                                 T1500320
C     COND(123)=XMLI, COR. FACTOR FOR MLI RADIAL RAD. LINKS              T1500330
C     COND(124)=CORRECTION FACTOR(FRACTION) TO ARTERY PERMEABILITY*AREA  T1500340
C     COND(125)=ARTERY PERMEABILITY*AREA,FT**4                           T1500350
C     COND(126)=CORRECTION FACTOR FOR MLI PARALLEL CONDUCTANCE           T1500360
C     COND(127)=TOTAL HEAT DECREMENT IN WATTS TO FIND PRIMING LIMIT      T1500370
      N1=COND(108)                                                       T1500380
      IF(N1.EQ.1) GO TO 2                                                T1500390
      KVAP= COND(59)                                                     T1500400
      B = COND(60)                                                       T1500410
      CPV= COND(61)                                                      T1500420
      CPL= COND(62)                                                      T1500430
      TGAP=COND(63)/12.                                                  T1500440
      HGAP=COND(64)/12.                                                  T1500450
C   STORE INITIAL  CONDUCTANCE VALUES FOR ALL REGULAR CONDUCTORS         T1500460
      DO 1 I=1,43                                                        T1500470
    1 COND(I+64)=COND(I)                                                 T1500480
```

```
      COND(108)=1.01                                                    T1500490
C  ALTER VAPOR PRESSURE DROP BY FACTOR INPUT AS COND(111)               T1500500
      PFAC=COND(111)                                                    T1500510
      DO 7 I=38,43                                                      T1500520
    7 COND(I)=COND(I)/PFAC                                              T1500530
C  ALTER MLI EFF EMITTANCE BY FACTOR INPUT AS COND(123)                 T1500540
      XMLI=COND(123)                                                    T1500550
      DO 9 I=1,5                                                        T1500560
      RAD(I)=XMLI*RAD(I)                                                T1500570
    9 RAD(I+10)=XMLI*RAD(I+10)                                          T1500580
C     RECOMPUTE CONDUCTORS 1 THRU 8                                     T1500590
    2 DO 5 I=1,43                                                       T1500600
    5 A(I)=COND(I+64)                                                   T1500610
      DO 12 I=1,8                                                       T1500620
   12 A(I)=COND(126)*A(I)                                               T1500630
      DO 3 I=1,4                                                        T1500640
      TB(I)=(((T(I)+459.6)**4+(T(I+1)+459.6)**4)/2.)**.25               T1500650
    3 COND(I)= A(I)*(TB(I)/360.)**B                                     T1500660
      DO 4 I=5,8                                                        T1500670
      TB(I)=(((T(I+1)+459.6)**4+(T(I+2)+459.6)**4)/2.)**.25             T1500680
    4 COND(I)= A(I)*(TB(I)/360.)**B                                     T1500690
C RECOMPUTE FLUID CONDUCTORS 38 THRU 53                                 T1500700
      TV=T(24)                                                          T1500710
      HFGV=PROP(6,KVAP,TV)                                              T1500720
C TEMP TV MUST BE IN DEGREES F FOR PROP SUBROUTINE                      T1500730
      C2=CPL/HFGV                                                       T1500740
      DO 6 I=1,7                                                        T1500750
      J=I+17                                                            T1500760
      P(I)=PROP(8,KVAP,T(J))                                            T1500770
      HFG(I)=PROP(6,KVAP,T(J))                                          T1500780
      RHOV(I)=PROP(3,KVAP,T(J))                                         T1500790
    6 XMUV(I)=PROP(4,KVAP,T(J))                                         T1500800
      DO 8 I=1,6                                                        T1500810
      J=I+37                                                            T1500820
      HFGB=(HFG(I)+HFG(I+1))/2.                                         T1500830
      RHOVB=(RHOV(I)+RHOV(I+1))/2.                                      T1500840
      XMUVB=(XMUV(I)+XMUV(I+1))/2.                                      T1500850
      DPVDT=RHOVB*HFGB/(T(I+17)+459.6)*778.                             T1500860
    8 COND(J)=A(J)*DPVDT*HFGB*RHOVB/XMUVB                               T1500870
      COND(53)=C2*COND(17)*(T(11)-T(18))                                T1500880
      COND(52)=C2*COND(18)*(T(12)-T(19))                                T1500890
      COND(51)=C2*(COND(24)*(T(25)-T(18))+COND(31)*(T(25)-T(32)))+COND  T1500900
     1(53)                                                              T1500910
      COND(50)=C2*(COND(25)*(T(26)-T(19))+COND(32)*(T(26)-T(32)))+COND  T1500920
     1(52)+COND(51)                                                     T1500930
      COND(49)=C2*(COND(26)*(T(27)-T(20))+COND(33)*(T(27)-T(32)))+COND  T1500940
     1(50)                                                              T1500950
      COND(48)=C2*(COND(27)*(T(28)-T(21))+COND(34)*(T(28)-T(32)))+COND  T1500960
```

```
     1(49)                                                                    T1500970
      COND(47)=C2*(COND(28)*(T(29)-T(22))+COND(35)*(T(29)-T(32)))+COND        T1500980
     1(48)                                                                    T1500990
      COND(45)=C2*(COND(22)*(T(23)-T(16))+COND(23)*(T(24)-T(17)))/2.          T1501000
      COND(44)=COND(45)                                                       T1501010
      COND(46)=C2*(COND(29)*(T(30)-T(23))+COND(36)*(T(30)-T(32)))+COND        T1501020
     1(47)-COND(45)                                                           T1501030
      PV=PROP(8,KVAP,TV)                                                      T1501040
      RHOL=PROP(1,KVAP,T(31))                                                 T1501050
      STEN=PROP(5,KVAP,T(32))                                                 T1501060
      DART=COND(119)                                                          T1501070
      DI=COND(122)                                                            T1501080
      WVAP=(DI-DART)/24.                                                      T1501090
      STENV=PROP(5,KVAP,TV)                                                   T1501100
      PL=PV-RHOL*HGAP-2.*STENV/WVAP                                           T1501110
      PCGAP=STEN*2./TGAP                                                      T1501120
      RHV=PROP(3,KVAP,T(24))                                                  T1501130
      HG=PROP(6,KVAP,T(24))                                                   T1501140
      DPVDT=RHV*HG*778./(T(24)+459.6)                                         T1501150
      PGAP=PV+DPVDT*(T(32)-T(24))                                             T1501160
      COND(54)=PV                                                             T1501170
      COND(56)=RHOL                                                           T1501180
      COND(57)=PGAP                                                           T1501190
      COND(58)=PCGAP                                                          T1501200
      DELPP=PL+PCGAP-PGAP                                                     T1501210
      COND(55)=DELPP                                                          T1501220
      IF(COND(43).EQ.0.)GO TO 11                                              T1501230
      IF(DELPP.GT.0.) GO TO 10                                                T1501240
      DELH= -DELPP/RHOL*12.                                                   T1501250
      WRITE (6,100)DELH                                                       T1501260
      IF(DELH.LE.HGAP) WRITE(6,102)                                           T1501270
      TG1=24.*STEN/(PGAP-PL)                                                  T1501280
      TG0=24.*STEN/(PGAP-PV)                                                  T1501290
      WRITE(6,103)TG1                                                         T1501300
      WRITE(6,104)TG0                                                         T1501310
      GO TO 11                                                                T1501320
   10 WRITE (6,101)                                                           T1501330
   11 CONTINUE                                                                T1501340
  100 FORMAT(' ARTERY WILL NOT PRIME IN 1-G, EXTRA HEAD REQ. = ',F9.5,'       T1501350
     1INCHES')                                                                T1501360
  101 FORMAT(' ARTERY PRIMES IN 1-G')                                         T1501370
  102 FORMAT(' ARTERY PRIMES IN 0-G')                                         T1501380
  103 FORMAT(' MAX GAP WIDTH FOR 1-G PRIMING = ',F6.5,' INCHES')              T1501390
  104 FORMAT(' MAX GAP WIDTH FOR 0-G PRIMING = ',F6.5,' INCHES')              T1501400
      RETURN                                                                  T1501410
C     DEBUG INIT, SUBCHK                                                      T1501420
      END                                                                     T1501430
```

```
      SUBROUTINE CIC2                                                    T1500010
C     THIS SUBROUTINE IS CALLED AT THE END OF EVERY                      T1500020
C     ITERATION BEFORE TIME IS INCREMENTED                               T1500030
      COMMON   STG(5000), NPOS(50), L1(50), L2(50), NLAST(50), FCT(50)   T1500040
      COMMON KILL,NTABS,NETRIC,METPR,IHEAT,SIG,XJ1,XJ2,XJ3               T1500050
      COMMON   BUFF(20),T(1000),CAP(1000),COND(2000),RAD(2000),Q(100),   T1500060
     1    NCOND(2,2000),NEAD(2,2000),NIN(1000),NBN(250),KEY(5),NQ(100),  T1500070
     2    KAY(4),FLUX(1000),DIS1(2000),DIS2(2000),ISC1(2000),ISC2(2000)  T1500080
      COMMON        TIME,     DTIME,    FTIME,    DUM,                   T1500090
     1    KNIN,     KNBN,     N4,       N5,       KODE,     KNQ,         T1500100
     2    KOUT,     KOUNT,    NOSRT                                      T1500110
      DIMENSION A(43)                                                    T1500120
C     THIS SUBROUTINE PERMITS PARTIAL ARTERY PRIMING                     T1500130
      DELPP=COND(55)                                                     T1500140
      IF(DELPP.LE.0.)GO TO 10                                            T1500150
      DPOR=COND(121)                                                     T1500160
      PI=3.141596                                                        T1500170
      DART=COND(119)                                                     T1500180
      APOR=COND(120)                                                     T1500190
      AGAP=PI*DART**2./4.-APOR-.75*PI*(.016)**2                          T1500200
      TGAP=COND(63)                                                      T1500210
      C1=AGAP*TGAP**2./248832.                                           T1500220
      C2=APOR*DPOR**2./1658880.                                          T1500230
      CLF=(C1+C2)*12.                                                    T1500240
      CIF=CIF*COND(124)                                                  T1500250
      COND(125)=CLF/12.                                                  T1500260
      N=37                                                               T1500270
    2 IF(COND(N).LT..0001)GO TO 1                                        T1500280
      COND(N)=0.                                                         T1500290
C     COND(N-7)=COND(N-7)*.0821                                          T1500300
      GO TO 9                                                            T1500310
    1 N=N-1                                                              T1500320
      IF(N.LE.31)GO TO 10                                                T1500330
      GO TO 2                                                            T1500340
   11 Q(1)=Q(1)-COND(127)*3.413/2.                                       T1500350
      Q(2)=Q(1)                                                          T1500360
      N=37                                                               T1500370
      IF(Q(1).LE.0.)GO TO 10                                             T1500380
      DO 12 I=31,37                                                      T1500390
   12 COND(I)=COND(I+64)                                                 T1500400
      QEVAP=(Q(1)+Q(2))/3.413                                            T1500410
      WRITE(6,204)QEVAP                                                  T1500420
    9 CALL STEADY                                                        T1500430
      KVAP=COND(59)                                                      T1500440
      HGAP=COND(64)/12.                                                  T1500450
      TGAP=COND(63)/12.                                                  T1500460
      PV=PROP(8,KVAP,T(24))                                              T1500470
      BHOL=PROP(1,KVAP,T(31))                                            T1500480
```

```
      STEN=PROP(5,KVAP,T(32))                                          T1500490
C     PGAP=PROP(8,KVAP,T(32))                                          T1500500
      RHOV=PROP(3,KVAP,T(24))                                          T1500510
      HFG =PROP(6,KVAP,T(24))                                          T1500520
      DPVDT=RHOV*HFG*778./(T(24)+459.6)                                T1500530
      PGAP=PV+DPVDT*(T(32)-T(24))                                      T1500540
      PCGAP=STEN*2./TGAP                                               T1500550
      DPL=0.                                                           T1500560
      XMUL=PROP(2,KVAP,T(31))                                          T1500570
      C3=XMUL/RHCL/COND(62)/CLF/4.18E08                                T1500580
      J=38-N                                                           T1500590
      DO 4 I=1,J                                                       T1500600
    4 DPL=C3*COND(45+I)*COND(111+I)+DPL                                T1500610
      COND(118)=DPL                                                    T1500620
      WVAP=(COND(122)-DART)/24.                                        T1500630
      STENV=PROP(5,KVAP,T(24))                                         T1500640
      PI=PV-RHOL*HGAP-2.*STENV/WVAP-DPL                                T1500650
      DELPP=PL+PCGAP-PGAP                                              T1500660
      COND(54)=PV                                                      T1500670
      COND(55)=DELPP                                                   T1500680
      COND(56)=RHCL                                                    T1500690
      COND(57)=PGAP                                                    T1500700
      COND(58)=PCGAP                                                   T1500710
      COND(109)=T(24)                                                  T1500720
      COND(110)=T(32)                                                  T1500730
      CALL RITE                                                        T1500740
      N=N-6                                                            T1500750
      IF(DELPP.LT.0.)GO TO 3                                           T1500760
      WRITE(6,200)N,DELPP                                              T1500770
      GO TO 1                                                          T1500780
    3 WRITE(6,201)N,DELPP                                              T1500790
C     DPPZG=PRESSURE DIFF FOR PRIMING IN ZERO-G                        T1500800
      DPPZG=DELPP+RHOL*HGAP                                            T1500810
      IF(DPPZG.LT.0.)GO TO 5                                           T1500820
      WRITE(6,202)N,DPPZG                                              T1500830
      GO TO 1                                                          T1500840
    5 WRITE(6,203)N,DPPZG                                              T1500850
      IF(DELPP.LT.0.)GO TO 11                                          T1500860
  200 FORMAT(' ARTERY PRIMES IN 1-G WITH NODE',I3,' FILLED, PRESSURE DIFT1500870
     1F=',F9.5,' PSF')                                                 T1500880
  201 FORMAT(' ARTERY WILL NOT PRIME IN 1-G WITH NODE',I3,' FILLED, PREST1500890
     1SURE DIFF =',F9.5,' PSF')                                        T1500900
  202 FORMAT('ARTERY PRIMES IN 0-G WITH NODE ',I3,'FILLED, PRESSURE    T1500910
     1DIFFERENCE = ',F9.5,' PSF')                                      T1500920
  203 FORMAT('ARTERY WILL NOT PRIME IN 0-G WITH NODE ',I3,' FILLED, PREST1500930
     1SURE DIFF = ',F9.5,' PSF')                                       T1500940
  204 FORMAT(//,' EVAPORATOR POWER CHANGED TO',F9.5,' WATTS')          T1500950
   10 IF(DELPP.LT.0..AND.Q(1).GT.0.)GO TO 11                           T1500960
```

```
      CALL BITE                                                    T1500970
      RETURN                                                       T1500980
      END                                                          T1500990
```